Assessment of empirically-derived parameters and their transferability in mountain glacier modeling and application for regional melt projections under climate change scenarios

by

Amanda Kotila

A thesis submitted in partial fulfillment of the requirements for the degree of

Master of Science

Department of Earth and Atmospheric Sciences
University of Alberta

ABSTRACT

Mountain glaciers, key sources of freshwater to downstream ecosystems and users, are responsive and vulnerable to changes in climate. Understanding their current influence, their potential future changes, and consequences of those changes are all important research goals, so many modeling approaches have been developed to address these questions. However, modeling at the regional scale can be difficult since input data from field measurements is limited and there is high spatiotemporal variability. High uncertainty in model predictions can come from empirical modeling parameters, often based on limited observations which are then applied to other glaciers in potentially very different topographic settings. In this study, we aim to assess parameter uncertainty and transferability by revisiting empirical parameters that are commonly used in glacier modeling and explore potential future glacier behaviours by utilizing a range of values for each glacier modeling parameter. This approach allows us to quantify uncertainty bands due to both projected future climate uncertainty and predicted model uncertainty.

First, rather than using a set of single parameter values we explore a range for the value of each parameter based on their physically meaningful maximum and minimum values. We set up a modeling framework by coupling glacier melt, surface mass balance, and spline-based volume-area scaling (called evolution hereafter), denoted as CGME model for Coupled Glacier Mass-balance Evolution model, to predict glacier melt runoff. Within the CGME model, we evaluate two temperature-index melt modeling approaches: the Classical Temperature Index Model (CTIM), which uses a degree-day approach, and the Pellicciotti Temperature-Index Model (PTIM), which incorporates radiative melt factors. Our study area is the Athabasca River Basin in Alberta, Canada, which contains 258 glaciers.

After calibration and optimization, we find that both of the melt models used in our CGME model predicted similar ranges of uncertainty (i.e., 95 Percent Prediction Uncertainty, 95PPU) in melt runoff, but the CTIM-based model reproduced more observed data points within its prediction uncertainty range (71% of observed data were captured within the predicted 95PPU) whereas the PTIM-based model reproduced 31% of the observed data.

Second, we applied these optimized parameter ranges at the regional scale for the period 1984-2007. Approximately 63% of the glaciers in the region had a normalized uncertainty value of greater than 0.5 for melt runoff, indicating that the parameter range transferability is not appropriate for the majority of glaciers in the region and that small glaciers are especially sensitive to input parameter variability. The framework developed here assesses the parameter transferability issue, especially in catchments where small-sized glaciers are dominant contributors to downstream water-ways that may have a cumulative ecological impact.

Further, we explore the impact of potential future change. The glacier model is forced using 4 CMIP6 GCMs under two shared socioeconomic pathways scenarios (SSP126 and SSP585) for the 258 glaciers for the period 1980-2100. From the maximum physically meaningful range for each parameter, 100 sets of model input parameters are sampled using Latin Hypercube Sampling technique. The 100 sets of sampled parameters are used with the future projected and downscaled climate data to force 100 simulations using CGME model for each glacier. This allows us to assess the projections' ranges of uncertainty (using the 95PPU) stemming from input parameterization.

Glacier changes are assessed based on two categorizations: glacier initial area and glacier initial elevation. Our results, based on size, show that glaciers are predicted to decrease in volume 75-80%, decrease in area 72-78%, and discharge 70-80% of their potential melt runoff in the first forty years of the simulation period (1980-2019, the historical period). Monthly predicted flow

regimes not only indicate greatly reduced melt runoff as the century progresses, but also the loss of late spring and early fall melt runoff. Assessing potential changes by glacier initial elevation indicated similar trends, though low elevation glaciers are predicted to be especially responsive, discharging ~95% of their melt runoff during the historical period. Monthly melt runoff reflects similar trends to those found during size analysis, though low elevation glaciers have the most extreme response. These assessments show the potential range of glacier changes under various future climate scenarios and the uncertainty stemming from model parameterizations. This can assist with freshwater resource management as well as adaptation and mitigation planning and implementation.

PREFACE

This master's research is original work by Amanda J. Kotila. It is a paper-based Master's Thesis. Chapter 2 is currently under peer review with the Journal of Hydrology and Chapter 3 is in the final stages of preparation before submission.

Amanda J. Kotila is the primary author of all the research presented here. For the publication under review (Chapter 2), the co-authors are Dr. Quan Cui, previously a post-doctoral researcher at the University of Alberta, Gunjan Silwal, Dr. Andrew B.G. Bush, and Dr. Monireh Faramarzi, an Associate Professor in the Department of Earth and Atmospheric Sciences who led the project and supervised this study. The second manuscript (Chapter 3) is in the final stages of preparations for submission. Amanda J. Kotila is the primary author. The co-authors are Dr. Edward Bam, a post-doctoral researcher at the University of Saskatchewan, Dr. Andrew B.G. Bush, and Dr. Monireh Faramarzi. Dr. Bush is a climate modeller and a Professor in the Department of Earth and Atmospheric Sciences who provided feedback on project development, methodology, and both manuscripts.

DEDICATION

My sincerest gratitude is extended to my supervisor, Dr. Faramarzi. She gave me a chance to pursue research, trusted, equipped, and encouraged me the whole time during the research project. She increased my skills and confidence in my research, made me a better scientist, and I will always be grateful.

Many thanks also to my fellow lab members, who have been incredibly welcoming and helpful since I came to the lab. Your generosity with your knowledge and expertise have assisted me in countless ways. Quan Cui has been an invaluable collaborator in this research, with her superior technical abilities and willingness to teach and demonstrate clean, correct scientific methods. Gunjan Silwal's model development and willingness to clarify technical details and theoretical reasoning has been amazingly helpful. Edward Bam made substantial contributions by compiling data, collaborating on study objectives, and being a co-author on the second manuscript. Many thanks to Dr. Andrew Bush, who provided suggestions, feedbacks, and encouragement during the project and on the thesis draft. I would also like to acknowledge Dr. Jeff Kavanaugh for agreeing to chair my master's thesis defense.

Finally, I would like to thank my parents, without whom I would not have had the spark to begin and the flame to continue in science. This work is dedicated to them. Endless thanks to my sister, family, and friends, both in Edmonton and back home, for their interest and continued emotional and intellectual support. They gifted me love, support advice, knowledge, and ideas. Amor auget.

TABLE OF CONTENTS

LIST OF TABLES

LIST OF FIGURES

CHAPTER I – INTRODUCTION

1.1 Overview

Mountain glaciers act as natural "water towers," storing and discharging water to downstream ecosystems and societies (Viviroli et al., 2007). Nearly a quarter of the people across the globe live directly downstream of mountainous areas and receive water from these water towers, yet these are some of the most vulnerable and irreplaceable sources of freshwater (IPCC, 2019; Immerzeel et al., 2019). This is due to the fact that unlike renewable water resources, glaciers are regarded as paleo waters, which are ancient bodies of water that have been created over millennia (Gleick & Palaniappan, 2010). Moreover, the water is stored as ice and snowpack, which are both sensitive to changes in climate. Understanding the changes in dynamics of glaciers, their accumulation, ablation, and melt runoff is crucial for downstream users and for aquatic ecosystems not only globally, but at the regional and local scales (Clarke et al., 2015).

Western Canada contains many watersheds that are fed by glaciers (Marshall et al., 2011) and they rely on glacier runoff for anthropogenic use during low flow season (such as irrigation, hydropower generation, and municipal use) as well as for freshwater ecosystems and processes (Payne et al., 2004). The province of Alberta is one such area; its western boundary lies along the eastern slope of the Canadian Rocky Mountains (CRM) and has five main watersheds with glaciers at the headwaters. It contains approximately 700 glaciers that collectively cover an area of ~787.14 km^2 and contain an ice volume of ~55±15 km^3 (Bolch et al., 2010; Marshall et al., 2011). These glaciers contribute to seasonal river discharge during the summer melt season; this contribution

ranges from ~10% (Bash & Marshall, 2014) to up to 80% (Comeau et al., 2009) in some stream systems. Bolch et al. (2010) and Marshall et al. (2011) estimate that the glaciers on the eastern slope of the CRM lost more than 20% of their area during 1985-2005. While the majority of the glaciers are small, there are some that are quite large and contribute significantly to downstream systems. One of these is a part of the larger Columbia Icefield that lies completely within Alberta, known as the Athabasca Glacier (~14km^2), which directly feeds some of the upper tributaries of the Athabasca River basin. This watershed allows the province to thrive, by providing water for both its natural and socioeconomic resources.

Glaciers are dynamic systems with energy, water, and debris in constant flux in and out of their mass. One way to study glaciers and how they change is to model the mass of water in the glacier. Glaciers gain mass via accumulation (precipitation onto the glacier), lose mass via ablation (primarily through melt in mountain glaciers), and the difference between accumulation and ablation is the glacier mass balance (GMB). Snow and ice melt on the surface of the glacier is a factor of air temperature, incoming solar radiation, and albedo (Hock, 1999; Pellicciotti et al., 2005). By tracking the GMB (net mass loss or gain) through time, trends in the glacier's mass content can be determined. Historical trends not only lend insight into a glacier's dynamics, but can also be used to understand the glacier's response to changes in climate and for future projections (Intergovernmental Panel on Climate Change's Fifth Assessment Report, IPCC AR5).

Hydrological models are among the best means to study dynamics of glacier runoff and their evolution over time at a regional scale. A variety of glacier melt models have been developed to study such dynamics, yet a full understanding of the processes involved in glacier melt is subject to uncertainty due to various reasons. The availability of observations and input data is a major concern that limits the application of the most comprehensive process-based models in glacier melt

and mass balance simulations. Energy balance models are among the most robust process-based models to simulate energy fluxes. One example of such a model is that developed by Brock and Arnold (2000), which calculated the net shortwave and longwave radiation fluxes, the turbulent sensible and latent heat fluxes, and the surface melt rate of snow or ice. It required hourly inputs of incoming shortwave radiation, water vapour pressure, air temperature, and wind speed data, as well as details about the study site (the latitude, longitude, slope angle, aspect, elevation, local temperature lapse rate, albedo and aerodynamic roughness of the study site, and the elevation of the meteorological station) in order to calculate the fluxes. Clarke et al. (2015) employed similar calculations to determine mass balance, and their model also incorporated an ice flow/dynamics model, which required a DEM of subglacial bed topography, initial ice thickness, and a sliding coefficient. While these models are capable of simulating many processes involved in representing melt and dynamics, they require extensive measurements as inputs which are not often available for large spatial or temporal ranges. This limits their applicability for regional assessments at high spatiotemporal resolution for current management and future planning.

On the other hand, temperature Index models (TIMs) have been developed in the past few decades, requiring fewer data to simulate glacier melt, mass balance, and evolution. TIMs are empirically-derived approaches that relate the air temperature to the accumulation or ablation of individual glaciers through several empirical parameters. Various TIM formulations (e.g., Braithwaite, 1995; Hock, 1999; Pellicciotti et al., 2005) have been developed, and their performance has been enhanced to represent spatiotemporal variability of melt processes across selected glaciers. While these models have been used extensively in glacier hydrologic modeling at a regional scale, often the parameters required by these models are kept constant and have been derived based on empirical studies from a limited number of glaciers across the world.

Climatological parameters, such as temperature lapse rate, precipitation gradient, and radiation factors vary widely among observational sites (e. g. Hock, 2003; Rabatel et al., 2011; Heynen et al., 2013) and this variability cannot be accounted for in specifically chosen global parameters. Moreover, in TIMs several physical processes are represented by a few empirical parameters, in their process simulations, which demonstrate considerable sensitivity to local hydro-climate and topographical conditions. Such limitations related to empirical TIMs, can produce high uncertainty in model predictions especially when parameters, which are often based on limited observations, are applied to other glaciers in potentially very different topographic settings. Therefore, it is crucial to assess parameter uncertainty and transferability in empirical parameters of TIMs that are commonly used in glacier modeling and applied for studying future glacier behaviours.

1.2 Research Objectives

This Master of Science thesis aims to revisit commonly used mountain glacier melt and mass balance simulation approaches to improve understanding of their simulation capacity at a regional scale. The overarching goal of this study is to address the parameters' transferability and quantify their uncertainty by developing and examining a coupled glacier melt, mass balance, and evolution model (CGME) using the common empirical approaches. We hypothesize that using a single set of parameter values based on empirical studies that had application to a regionally large number of melting glaciers in mountain environment setting is subject to uncertainty. The specific objectives listed below are developed to examine our hypothesis using the glaciers of the upper Athabasca watershed in western Canada as a study region:

1. Calibrate and validate a coupled glacier melt-mass balance-evolution (CGME) model, using two temperature-index model (TIM) melt modeling approaches including the Classical TIM (CTIM, Braithwaite, 1995) and the Pellicciotti TIM (PTIM, Pellicciotti et al., 2005), a surface mass balance calculation approach (Huss et al., 2010), a volume-area change approach (after Bahr et al., 1997; and Kraainjenbrink et al., 2017), to determine an optimal range of values for each model input parameter.
2. Compare the glacier melt runoff results of CTIM and PTIM to study the most important physical processes affecting melt runoff, mass balance, and volume-area changes and to assess parameter sensitivity of the model.
3. Assess historical changes in the glacier melt runoff of 258 glaciers across the study region to assess parameter transferability and associated uncertainty.
4. Utilize optimized parameter uncertainty range and various future climate scenarios to assess the potential regional glacier responses in melt runoff, area and volume change for the period 1980-2100. Explore how glacier size and elevation affect glacier dynamics and uncertainty throughout the study period.

1.3 Thesis Structure

Chapter 2 introduces the CGME model and data used to setup the model. Model details, as well as an optimized parametrization, calibration and validation of melt runoff, and sensitivity analysis are described. Then the model is applied to 258 glaciers in a study area in the Canadian Rocky Mountains to evaluate parameter transferability issue via quantification of parameter uncertainty range.

Chapter 3 utilizes the glacier model and the optimized parameter ranges forced with future climate scenarios to assess glacier change and associated uncertainty at the regional scale for the period 1980-2100. Glaciers are categorized by initial area and initial elevation and changes in melt runoff, glacier area, and volume are assessed at various time scales.

Chapter 4 summarizes the findings of the previous chapters and draws conclusions about the future of glaciers in the face of a changing environment. Finally, the applicability of these parametrization, uncertainty assessment, and scenario analysis are linked with the importance of glacio-hydrological studies, and their implications for adaptation and mitigation measures in the face of a changing world are discussed.

CHAPTER II – MANUSCRIPT 1

Uncertainty assessment of empirically-derived parameters and parameter transferability in mountain glacier modeling at the regional scale

Amanda J. Kotila[1], Quan Cui[1], Gunjan Silwal[1], Andrew B.G. Bush[2], Monireh Faramarzi[1]

[1] Watershed Science & Modeling Laboratory, Department of Earth and Atmospheric Sciences, Faculty of Science, University of Alberta, Edmonton, AB T6G 2R3, Canada

[2] Department of Earth and Atmospheric Sciences, Faculty of Science, University of Alberta, Edmonton

Graphical Abstract

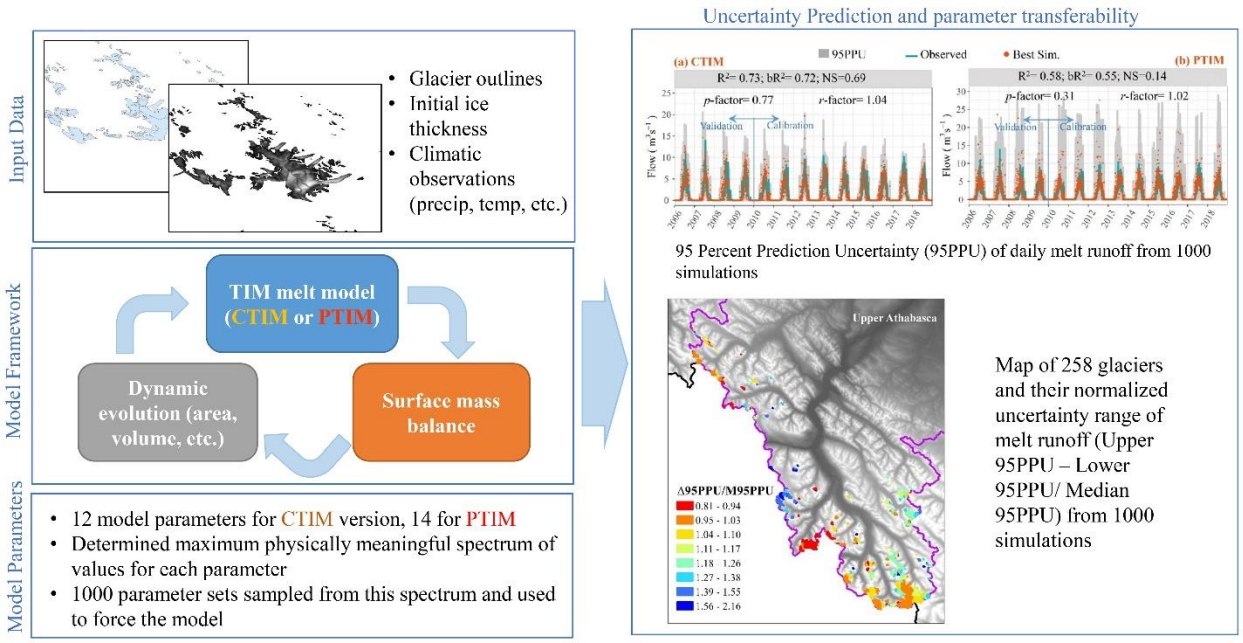

Highlights

- Widely used glacier melt runoff, mass balance, and evolution models were coupled
- Classical temperature index and enhanced melt modeling approaches were examined
- Model forced to assess parameter uncertainty and transferability in 258 mountain glaciers
- Transferability of parameters deemed not appropriate for most glaciers in the region
- Small glaciers are especially sensitive to input parameter variability and transferability

2.1 Abtract

Mountain glaciers are key sources of freshwater to surrounding ecosystems and downstream users. Understanding their current impact and potential changes is important, and many modeling approaches have been developed to this end. However, modeling at the regional scale can be difficult, where input data is limited and there is high spatiotemporal variability. High uncertainty in model predictions can come from empirical modeling parameters, often based on limited observations which are then applied to other glaciers. In this study, we aim to assess parameter uncertainty and transferability revisiting empirical parameters that are commonly used in glacier melt, mass balance, and evolution modeling by examining them in 258 glaciers in the Upper Athabasca Watershed in Alberta, Canada.

First, rather than using a set of single parameter values we explore a range for each parameter value based on their physically meaningful maximum and minimum spectrum. We set up a modeling framework by coupling melt, surface mass balance, and spline-based volume-area scaling models to evaluate glacier melt runoff simulations using two temperature-index model approaches including the Classical Temperature Index Model (CTIM), which uses a degree-day approach, and the Pellicciotti Temperature-Index Model (PTIM), which incorporates radiative melt factors. We found that both model results predicted similar ranges of uncertainty (i.e., 95 Percent Prediction Uncertainty, 95PPU), but the CTIM-based model reproduced more observed data points within its prediction uncertainty range (71% of observed data were captured within the predicted 95PPU as opposed to the PTIM-based model, which reproduced only 31% of observed data).

Second, we applied these optimized parameter ranges at the regional scale. Approximately 63% of the glaciers in the region had a normalized uncertainty value of greater than 0.5 for melt

runoff, indicating that the parameter range transferability is not appropriate for the majority of glaciers in the region and that small glaciers are especially sensitive to input parameter variability. The framework developed in this study facilitates assessment of the parameter transferability issue, and conveys an important message for regional glacier melt modeling, especially in catchments where small-sized glaciers are dominant contributors to downstream water ways that may have a cumulative ecological impact.

Keywords: melt runoff modeling, temperature index, mass balance modeling, evolution modeling, glacier size

2.2 Introduction

Mountain glaciers act as natural water towers, storing and discharging water to downstream ecosystems and societies (Viviroli et al., 2007). Nearly two billion people across the globe live directly downstream of mountainous areas and benefit from these water towers. These towers, however, are vulnerable yet irreplaceable sources of freshwater (IPCC, 2019; Immerzeel et al., 2019). Glaciers are created over millennia and their demise would mean it would take millennia for them to reform (Gleick & Palaniappan, 2010). Moreover, most of the annually-sourced water is stored as young ice and snowpack, which are sensitive to changes in climate. Understanding the changes in dynamics of glaciers in terms of their accumulation, ablation, and melt runoff is crucial for downstream users and aquatic ecosystems from the global to the regional and local scales (Clarke et al., 2015).

Hydro-glacial models are ideal tools to study the meltwater and important processes driving their mass and melt runoff changes over time. Furthermore, coupled glacier melt, mass balance, and evolution models are critical for studying the transient and long-term changes in glacier area, extent, volume, and thickness with hydrological implications at basin- to local-scales (Jost et al., 2012; Naz et al., 2014; Clarke et al., 2015; Kraaijenbrink et al., 2017; Marzeion et al., 2012; Radić et al. 2014; Huss & Hock, 2018). However, a full understanding of the processes involved in glacier dynamics is subject to uncertainty due to various reasons. The paucity of observations and input data is a significant concern that limits the application of the most comprehensive process-based models in glacier melt and mass balance simulations. Energy balance models are among the most robust process-based models to simulate energy fluxes. These models calculate the net shortwave and longwave radiation fluxes, the turbulent sensible and latent heat fluxes, and the surface melt rate of snow or ice. They require hourly input data including incoming shortwave

radiation, vapour pressure, air temperature, and wind speed at a high spatial resolution, as well as details about the study site (e.g., the latitude, longitude, slope angle, aspect, elevation, local temperature lapse rate, albedo and aerodynamic roughness of the study site, and the elevation of the meteorological station), to calculate the energy fluxes. More advanced models employ similar calculations to determine mass balance, which are coupled with an ice flow dynamics model that require a DEM of subglacial bed topography, initial ice thickness, and a sliding coefficient (e.g., Clarke et al., 2015). In these models the net shortwave and longwave radiation fluxes, the turbulent sensible and latent heat fluxes, and the surface melt rate of snow or ice are calculated. For such energy flux calculations, a comprehensive set of hourly input data and details about the study site are required. Clarke et al. (2015) employed similar calculations to determine mass balance, which was coupled with an ice flow dynamics model that required a DEM of subglacial bed topography, initial ice thickness, and a sliding coefficient. While these models are capable of simulating many processes involved in representing glacier melt and dynamics, they require extensive measurements at a high spatiotemporal resolution at each glacier site as inputs, which are not often available for large spatial or temporal ranges. This limits their applicability for regional assessments at high resolution for management and planning.

In contrast to energy balance models, several temperature Index models (TIMs) have been developed in the past few decades, requiring fewer data to simulate glacier melt, mass balance, and evolution. TIMs are empirically-derived approaches that relate the air temperature to the accumulation or ablation of individual glaciers through several empirical parameters. Various TIM formulations (e.g., Braithwaite, 1995; Hock, 1999; Pellicciotti et al., 2005) have been developed, and their performance has been enhanced to represent spatiotemporal variability of melt processes across selected glaciers. TIMs have been used extensively in glacier hydrologic modeling because

they can model a number of dynamical processes with a small number of glacial and meteorological inputs that are readily available (e.g., temperature and precipitation data; Hock, 1999). The Classical Temperature-Index Model (CTIM) was initially developed by Finsterwalder and Schunk in 1887 for use on Alpine glaciers and has since evolved for use in various studies (e.g., Braithwaite, 1995; Braun et al., 1993; Fuchs et al., 2016; Réveillet et al., 2017; Chen et al., 2019). The CTIM uses empirical parameters such as the Degree Day Factor related to snow and ice (i.e., DDF_{snow} and DDF_{ice}), as well as a threshold temperature (i.e., the temperature above which snow and/or ice melt can occur, T_{thres}), to correlate air temperature to snow and ice melt. To further refine the simulation of glacier melt using this method, some studies use an elevation band approach, in which a glacier is delineated into bands of equal mean elevation based on glacier size and area (e.g., Huss & Hock, 2015). Such refined approaches account for changes in temperature due to elevation (Hock, 2003; Ohmura, 2001) and changes in precipitation due to orographic lifting (Shea et al., 2015). However, these refinements are not adequate to account for the simplifications and uncertainties inherent in the application of the CTIM approach. A more refined approach relates the snow and ice-melt factors, which alter throughout the melt season and observation periods (Rango & Martinec, 2008), and they vary spatially due to changes in albedo, insolation, and the relative contributions of surface energy balance fluxes (Shea et al., 2009). However, in most regional studies the parameters required by these models are kept constant and have been derived based on empirical studies from a limited number of glaciers across the world. Climatological parameters, such as temperature lapse rate, precipitation gradient, and radiation factors vary widely among observational sites (e. g. Hock, 2003; Rabatel et al., 2011; Heynen et al., 2013) and this variability cannot be accounted for in specifically chosen global parameters.

Tsai and Ruan (2018) demonstrated that the Braithwaite TIM approach consistently overestimates early season melt, which occurs above 0°C. These overestimations are partially because of constant DDF_{snow}, DDF_{ice}, and T_{thres} values, which are empirically derived but can vary widely across different spatiotemporal scales. On the other hand, Pellicciotti (2005) and Hock (1999) showed that by not accounting for melt due to incoming radiation, the CTIM cannot capture the spatiotemporal variability of DDFs and the resulting effects on melt, due to the surrounding topography and the changes in the melt and discharge cyclicity due to diurnal and seasonal changes. It has been suggested, therefore, that the CTIM has relatively poor predictive capability (Hock, 1999). To overcome the shortcomings of the CTIM approach, Pellicciotti et al. (2005) developed an enhanced TIM that incorporates radiation melt, hereafter referred to as the Pellicciotti Temperature-Index Model (PTIM). Using the PTIM approach, Bash and Marshall (2014) found that an average of 80% of summer melt could be attributed to absorbed radiation in Haig Glacier, which is a relatively small glacier feeding the upper tributaries of the Bow river basin in the Canadian Rocky Mountains. However, it is unknown whether this improved approach can be applied to large regional–scale studies.

In another study Braithwaite and Olesen (1985) show that while DDFs have high temporal stability across a range of climatic regimes, differentiation of the DDF for ice and snow can account for some of these variations due to local surface conditions (Arendt & Sharp, 1999). According to their study, the DDF of snow can be less than half of that for ice because snow can have a wider range of albedos than ice and thus its energy absorption can vary more. These refinements to the TIM approach have been shown to assist surface mass balance (SMB) models to reproduce historical observations and to be a component of models that suitably simulate a glacier's SMB responses to climate change, although these studies are limited by the fact that they

are local rather than regional or global in spatial scale (Jóhannesson, et al., 1995; Hock, 2003; Pellicciotti et al., 2005; Haslinger et al., 2014).

The coupling of melt and SMB models with a dynamic glacier evolution model has been used in various studies to understand glacier mass balance sensitivity and response to climate change (e.g., by Jóhannesson, 1997; Khadka et al., 2020). While fully distributed physically process-based models are the best means to simulate ice flow dynamics and their evolution, they are often suitable only in areas for which high resolution data are available. As an alternative for data-poor areas, incomplex approaches have been developed and coupled with improved TIM and SMB models to simulate glacier dynamics that require only a minimal amount of input data. As an example, the volume-area scaling (VAS) approach (Bahr, 1997; Radić et al., 2007) allows for recalculation of glacier area and volume in response to changes in mass, making it suitable for simulating the evolution of glaciers over time. This approach has been used widely at the regional scale (for example, see Radić & Hock, 2010; Farrinotti et al., 2009). However, Bahr et al. (2015) point out that while the theoretical basis of the VAS equation has been validated for glaciers of a wide range of sizes, it is best applied to estimate aggregate volume of ensembles of glaciers and cannot be used on individual branches of a glacier. Moreover, the VAS is generally an empirically-based approach; the physical parameters that identify spatiotemporal relationships are not explicitly simulated. Most of the recent VAS-based model studies hold the V-A parameters constant in space and time while simulating glacier evolution which may not represent V-A relationships accurately. To minimize these limitations, some studies suggest using a smoothing spline interpolation that finds a relationship between volume and area, in the first year based on initial glacier area, volume, and ice thickness observations and changing at each time step as the glacier evolves (Kraaijenbrink et al., 2017; Shekar et al., 2021; Brenning et al., 2007; Tarasov et

al., 2003). This relation between volume and area is used to predict the change in area (after Kraaijenbrink et al., 2017) in response to the SMB and to estimate the volume of melt runoff per year. The smoothing spline method is completed at an annual time step when, after annual SMB and mass redistribution are estimated, the volume is sampled at different ice thicknesses. A predictive spline model is fitted through these samples to determine the volume-area relation per glacier per year (further details in section 2.3.2.3). This allows for a determination of the volume-area relation for each glacier in the study area, in contrast to the VAS approach which uses an empirically-derived scaling parameter which may not be appropriate for all glaciers in the region at any given time. By estimating volume-area changes for each glacier individually, a higher spatial resolution and more heterogeneity in glacier topography (elevation, aspect, etc.) is simulated.

The overarching goal of this study is to revisit empirical models that are commonly used in glacier melt, mass balance, and evolution modeling and address those areas of uncertainty when these models are applied at a regional scale for planning and management. We hypothesize that using a single set of parameter values based on empirical studies that had application to a regionally large number of melting glaciers is subject to uncertainty. To achieve our goal we have setup a modeling framework by coupling melt, SMB, and spline-based VAS models in order to evaluate glacier melt simulations using both the CTIM and PTIM approaches. Our objective is to examine the response of glacier melt, SMB, and evolution (e.g. changes in volume, area, and depth) to physical parameters that are driven based on their maximum physically meaningful spectrum. This allows a comparison of the performance and predictive capability of PTIM, CTIM, SMB, and spline-based VAS models at the regional scale and also when measurements for critical parameters are poor or totally lacking.

Our model is applied to the Canadian Rocky Mountains (CRM) at the upstream, western portion of the Athabasca River basin (ARB) that drains melt water from approximately 258 glaciers. The region is characterized by heterogeneous hydro-climate and geospatial conditions, as well as a diverse range of glacier sizes, each with their own specific hydro-climatic settings. Moreover, there is a unique conglomerate glacier called the Columbia Icefield, which gives rise to the Athabasca Glacier (~14 km^2) that has long-term runoff observations at its outlet, altogether making the upper ARB a suitable study region for our model application and uncertainty analyses.

2.3. Material and methods

2.3.1 Study area

The ARB has a drainage area of ~ 150,000 km^2 (24% of the area of the province of Alberta, Canada) and is a key source of water for both natural ecosystems and downstream human consumption. Bawden et al. (2014) in their basin-wide, multi-decadal analysis found a strong decreasing trend in summer flows which were more prominent in the ARB than in the surrounding river basins during the same period. Numerous glaciers exist at elevations ranging from ~2,200 m to ~3,500 m, within the region 117-120°W to 52-54°N (Fig. 1). According to climate observations available from the Jasper Warden climate station (Environment and Climate Change Canada), the annual mean temperature and precipitation are, respectively, 3.5 ˚C and 352 mm. Autumn and winter have average air temperatures below freezing, denoting the accumulation seasons. Spring and summer are the ablation seasons, despite higher average precipitation. The Athabasca River begins at the outlet of the Athabasca glacier and flows more than 1500 km to where it empties into Lake Athabasca. Along its extent, it crosses forests, agricultural lands, oil sands and notable amounts of water are abstracted for use in these industries (Peters et al., 2013). At its delta in north-

eastern Alberta, the river becomes a part of the Peace-Athabasca Delta, a deltaic lake and wetland ecosystem of international significance recognized by the Ramsar Convention to be susceptible to climate change (Peters et al., 2013; Rokaya et al., 2020).

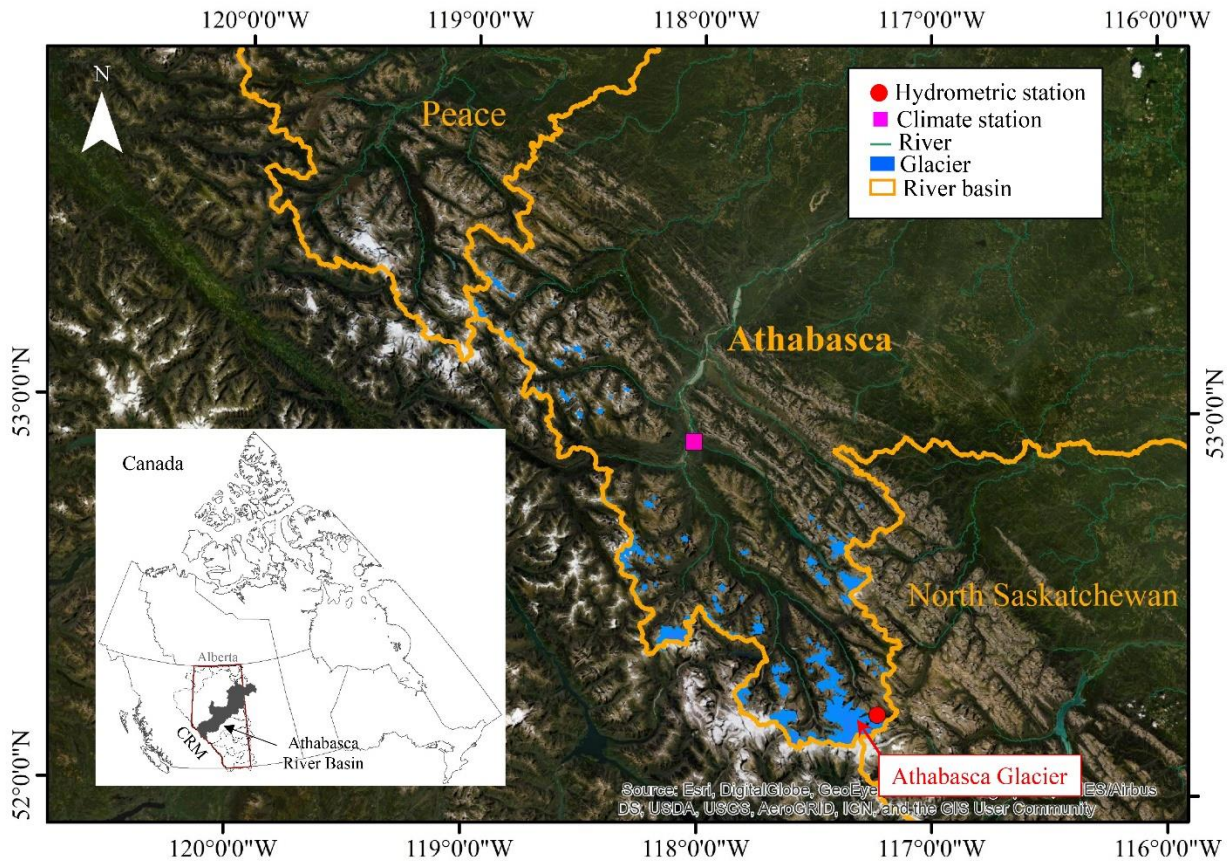

Figure 1. Study area, showing the upper (glacierized) end of the Athabasca river basin in western Alberta, Canada. Watershed boundaries, glaciers, and climate and hydrometric stations are highlighted. The 258 glaciers are illustrated in blue, with the Athabasca Glacier and the Albertan extents of the Columbia Icefield in the lower right of the watershed; the hydrometric station used for calibration is indicated in red.

There are 258 glaciers in the Athabasca river basin, which are the focus of this study. They lie on the eastern slope of the CRM. The Athabasca Glacier (part of the Columbia Icefield) feeds one of the main tributaries in the Athabasca River basin; there are other tributaries fed by smaller mountain glaciers present in the upper Athabasca region which are also affected by the decrease in their extent. Negative changes in glacier extent have been reported for other glaciers in the

region, including other portions of the Columbia Icefield (Clarke et al., 2013; Intsiful & Ambinakudige, 2020) that run off to the North Saskatchewan River basin (Alberta) and the Columbia River basin (British Columbia). Figure 1 shows the glaciers, as well as the location of the climate station and hydrometric stations, used in this study.

2.3.2 Model Description

We developed a coupled glacier mass balance-dynamic evolution model (CGME) in the

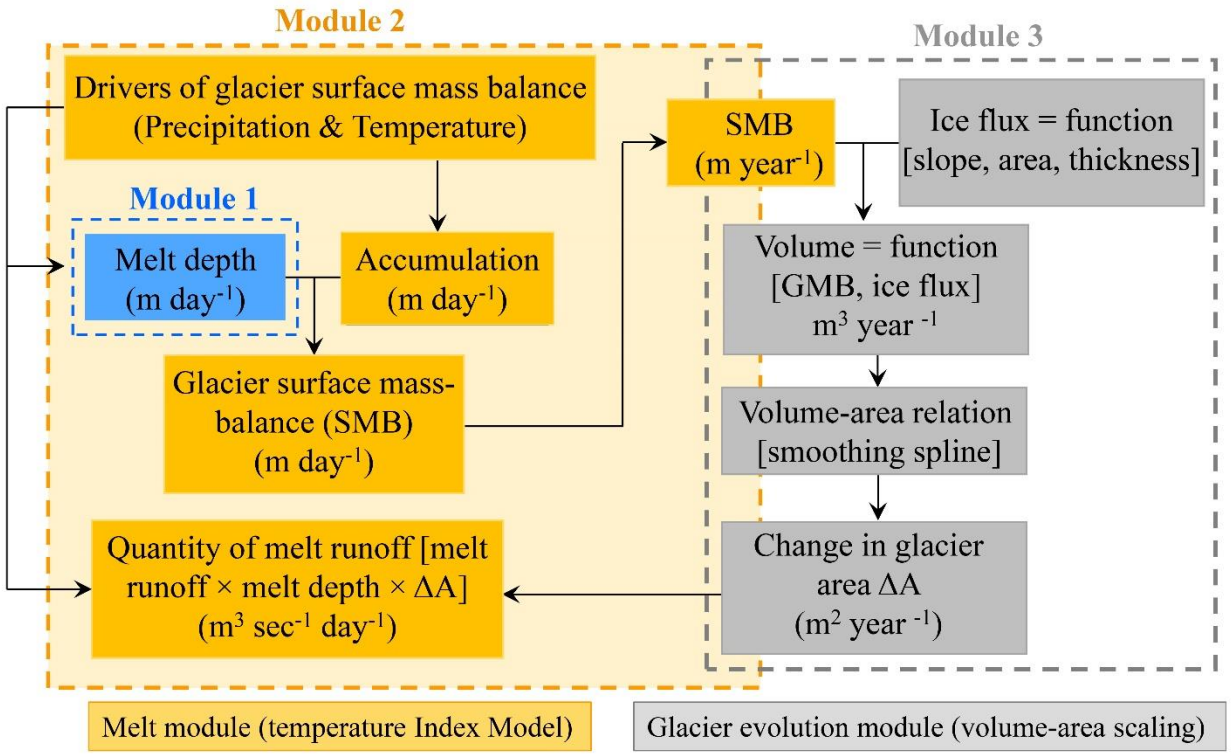

Figure 2. Flow chart, illustrating the coupled glacier melt mass balance dynamic-evolution model (CGME). Module 1 (blue) is the Temperature Index Model that calculates daily melt depth. Module 2 (orange) calculates the daily surface mass balance and daily melt runoff. Module 3 (gray) calculates the annual change in glacier geometry using a volume-area smoothing spline relation and initial glacier hypsometry (Farinotti et al., 2019). Further details can be found in Appendix figure A3.

R programming environment (Fig. 2). Our model is composed of three modules: Module 1, which calculates daily melt from a glacier (m day^{-1}) based on a temperature index model (TIM) that will

be explained in section 2.3.2.1. In Module 2 and Module 3, annual volumetric melt and surface area change are calculated. Module 2 calculates the daily surface mass balance of the glacier (m day^{-1}), which is summed to an annual mass balance (m $year^{-1}$). The simulated SMB in Module 2 is an input into Module 3, which calculates the change in glacier surface area (m^2 $year^{-1}$) in response to this change in mass. Module 3 also performs calculations per elevation band and sums to find the total change for the entire glacier. A new glacier volume (m^3) is then computed using surface area and changes in glacier elevation (ice thickness). Changes in ice thickness per elevation band are calculated using the ice-flux divergence (see section 2.3.2.3). This approach enables analysis of not only mass loss due to volume-area decrease but also changes in the discharge regime downstream (Huss & Hock, 2015) and is appropriate at the basin or regional scale (Immerzeel et al., 2012) and in multi-decade to multi-century timescales (Radić et al., 2007). It is noteworthy that the elevation band approach used in our model framework allows each glacier to be delineated into bands of equal mean elevation based on glacier area. The glaciers are divided into a minimum of 6 elevation bands (for the smallest glaciers) and up to 16 elevation bands (for the largest glaciers). In the initial year, glacier area (based on input glacier outlines and DEM) and minimum and maximum elevation is determined, with elevation being equally distributed across the glacier surface; e.g., if a glacier's area determines that it falls into a 10-band size class, the maximum – minimum elevation will be divided by 10 and each band will be assigned an equal elevation difference ("band width"). This will be held constant through time as the simulation progresses; as volume, area, ice thickness, and mean elevation of each band are updated at each time step (in this study, daily), band width will stay the same. This is assigned and held constant per glacier; band width will vary glacier to glacier based on overall initial glacier elevation difference. The simulation of melt, mass balance, and evolution for each band individually, allows

for a more refined model of the entire glacier's mass flux and geometry changes through time because it accounts for changes in temperature due to elevation (Hock, 2003; Ohmura, 2001) and changes in precipitation due to orographic lifting (Shea et al., 2015). The elevation band approach also allows for intra-band mass exchange via ice-flux divergence (described further in 2.2.3.1), as well as for complete meltdown (i.e., when the volume becomes negligible) of bands while still modeling the further melt, SMB, and volume-area change of the remaining bands.

2.3.2.1 Temperature Index Model (TIM)

In this study, we employed two widely used TIM approaches in Module 1 (cf., Fig. 2): the Classical Temperature Index model (CTIM), and the Pellicciotti Temperature Index model (PTIM). The Classical Temperature-Index Model (CTIM) was initially developed by Finsterwalder and Schunk in 1887 for use on Alpine glaciers and has since evolved over time for use in various studies (e.g., Braithwaite, 1995; Braun et al., 1993; Fuchs et al., 2016; Chen et al., 2019). CTIM is an empirically-derived approach that relates the air temperature to accumulation or ablation using two degree day factors (DDFs, sometimes called melt coefficients) and based on a threshold temperature (T_{thres}) above which snow/ice melt can occur. The two DDFs used in this approach are related to snow (DDF_{snow}) and ice (DDF_{ice}), both in mm day^{-1} $^{o}C^{-1}$, which are computed from statistical relationships between positive degree-days (Ohmura, 2001) and surface melt and crudely account for the effect of local surface conditions such as surface albedo and turbulence (Arendt & Sharp, 1999). This approach statistically relates ablation to the sum of positive degree days (days with an average temperature above 0°C) and allows for the calculation of the amount of melt that occurs per degree above freezing (the DDF). The maximum physically meaningful ranges, based on an extensive literature review, are reported to be 0.38-14 mm day^{-1} $^{o}C^{-1}$ for DDF_{snow} and 4.5-10.6 mm day^{-1} $^{o}C^{-1}$ for DDF_{ice} (Silwal et al., 2022; Du et al., 2022). We

have examined the effects of parameter variation on melt simulations using such physically meaningful ranges. All parameters and the ranges used in this study are listed in Table 1.

To overcome the shortcomings of the CTIM approach in process representation, Pellicciotti et al. (2005) developed an enhanced TIM that incorporates radiation melt into the TIM approach, hereafter referred to as the Pellicciotti Temperature-Index Model (PTIM). The PTIM simulates snow and ice melt based on a temperature melt factor (TF), shortwave radiation factors (SRFs) for snow and ice, daily incoming shortwave radiation, and the albedos for snow and ice. Daily incoming shortwave radiation is considered a model input; daily observations are not available for the full study region, so it is estimated after Walter et al. (2005) and modified due to atmospheric conditions (e.g. thickness, aerosols) after Follum et al. (2015). The albedo for ice, TF, and SRFs for ice and snow are considered input parameters to melt modeling. TF and SRF are empirical coefficients, which account for the effects of temperature and shortwave radiation on surface melt (Pellicciotti et al., 2005). In most regional analyses, the albedo for ice, TF, and SRFs for snow and ice are either assigned from a limited number of glaciers (Tawde et al., 2016; Kienholz et al., 2020) or they are manually calibrated based on a limited amount of measurements (Gardner & Sharp, 2009; Wortmann et al., 2019). In this study we evaluate how varying parameters generated through a parameter sampling technique from their physically meaningful minima and maxima can impact melt simulations (see section 2.3.4.1, Table 1).

While spatial and temporal variability in albedo introduces challenges and uncertainty in glacier melt modeling (Hock, 2005), by separating albedo into that of snow and ice we are able to better simulate the changes in melt runoff due to seasonal changes in surface albedo (Arnold et al., 1996). Snow albedo, due to its ability to reflect radiation and thus affect the glacier surface energy budget, greatly influences melt runoff (Hock, 2005). In this study, daily snow albedo was a model

input, approximated using a logarithmic function of accumulated daily maximum positive temperature adapted by Pellicciotti et al. (2005) from Brock et al. (2001a). Ice albedo has been the focus of only a few studies and is often held as a spatiotemporal constant (Brock et al., 2001a; Hock, 2005). Instead of a using a fixed value for the albedo of ice from an empirical survey of the literature, we included it as a melt model parameter of interest and used Latin Hypercube Sampling (LHS) to sample and test values from a range suggested for mountain glaciers in the Rocky Mountains (see Table 1). The modeled melt depth using CTIM and PTIM is later converted to a volumetric melt runoff (the output of Module 1), which is based on the combined melt runoff due to rainfall on the glacier surface, snowmelt on the glacier surface, and melting of glacier ice (see Eq. 1).

$$Q_{melt} = [\text{Icemelt} \times \text{GlacC} + s\text{nowmelt} \times \text{SnowC} + \text{P}_{\text{rain}} \times \text{RainC}] \times \text{A} \quad \text{[Eq. 1]}$$

Where, Q_{melt} is the total runoff (m^3s^{-1}) from the elevation band; GlacC, SnowC, and RainC are coefficients of, respectively, glacier ice melt (m), snowmelt (m), and liquid precipitation (rainfall, m) that convert melt depth into melt runoff considering the glacier surface area (m^2) and using the storage-discharge relationship, after Martinec et al. (2008). In this study, GlacC, SnowC, and RainC were considered as input parameters and were estimated using calibration and uncertainty analyses explained in section 2.3.4.3 P_{rain} is the liquid precipitation (mm) for each elevation band, determined by temperature thresholds that convert daily precipitation into rain (Quick & Pipes, 1977). Each type of runoff (rain, snowmelt, and glacier ice melt) is calculated per band, then the bands are summed to determine the total melt runoff for the glacier per day. This is used by Module 2 to calculate the daily SMB.

Because air temperature is essential to the TIM calculation and since mountain glacier models are highly sensitive to temperature lapse rates, two temperature lapse rates (Ragettli & Pellicciotti, 2011) are used in our model in the melt calculation. Using a singular temperature lapse rate has been found to overestimate the number of positive degree days (PDDs; Gardner et al., 2009), especially at higher elevations (Shea et al., 2009). The lapse rate along a glacier surface can be vastly different from an assumed free air lapse rate (Arendt & Sharp, 1999; Gardner & Sharp, 2009; Gardner et al., 2009). While lapse rate can be estimated using a linear regression of measured temperature, such a lapse rate introduces high uncertainty both spatially and temporally because of sample size, dataset noise, domain selection, and estimation methods (Lute & Abatzoglou, 2021) and will likely be a poor approximation at the regional level (Gardner & Sharp, 2009). In addition, the presence of a glacier can strongly affect local climate conditions (Arendt & Sharp, 1999), and a lapse rate estimated from observed climate data can overestimate the lapse rate near the surface of the glacier (Arendt & Sharp, 1999). This is because such estimation does not account for the cooling presence of the glacier (Gardner et al., 2009). Lapse rate can also have great seasonal variability due to fluctuations in temperature (Arendt & Sharp, 1999) and thus some studies, such as that by Schaefli and Huss (2011), use seasonal lapse rates. While this was not feasible in our study, we did use two distinct lapse rates. The altitudinal temperature lapse rate (LR) is used to calculate the change in air temperature between the temperature measured at the elevation of the climate station and the elevation at the base of the glacier (lowest elevation of the glacier surface). Then the temperature lapse rate along the glacier surface (LRGlacier) is used to calculate the temperature from the base of the glacier up to each elevation band of the glacier. Both LR and LRGlacier are not calculated individually for each glacier, but are treated as input parameters and are sampled from within the range utilized by similar studies in the region.

2.3.2.2 Surface Mass Balance (SMB)

Surface mass balance (SMB) was modelled by taking the difference between modelled accumulation and ablation. Though this is a simplified mass balance relation, it has been used by numerous glacier modeling studies, including temperature-indexed studies (Stahl et al., 2008; Hock, 2003), studies in the CRM (Marshall et al., 2011), and studies of coupled models used for glacier melt runoff projections (Khadka et al., 2020). In our modeling framework (Fig. 2), Module 2 calculates SMB by using estimates of the accumulation (snowfall) and the ablation (total melt runoff) calculated in Module 1 (CTIM or PTIM). The SMB is calculated based on daily total solid precipitation or accumulation for each elevation band and the daily total ice and snow melt from Module 1. The temperatures that are extrapolated and assigned to each elevation band in Module 1 are used to determine the amount of accumulation and ablation. The simulated daily net SMB for each elevation band is then summed to calculate the net annual SMB for the glacier. This is used to find the mass balance gradient (MBG) of the glacier for the simulation year by fitting a linear regression between the net SMB and the mean elevation of different elevation bands in each year. The annual net SMB and MBG compared to the previous time step are used in Module 3 to determine the annual evolution in the glacier's geometry (see section 2.3.2.3).

2.3.2.3 Evolution

Though this is a regional study, because our model simulates glacier melt and SMB for an individual glacier (and further divides into elevation bands), the simplistic VAS approach would not be an appropriate approach due to its limitations (Bahr et al., 2015; Frey et al., 2014; Stahl et al., 2008). Instead, we used a smoothing spline that fits a cubic polynomial line (Green & Silverman, 1994) to find a relationship between volume and area. The relation between volume and area is used to estimate the volume of melt runoff per band per year based on the predicted

change in area of the elevation band (Kraaijenbrink et al., 2017) in response to the SMB. In the following paragraphs we provide more details.

Module 3 uses the elevation bands defined in Module 1, and the SMB and glacier surface gradient are calculated in Module 2 to compute the change in glacier area per elevation band per year. Module 3 translates glacier mass changes, as represented by surface glacier mass balance, into area and volume changes (i.e., evolution) in each elevation band. The coupling of a TIM-SMB simulation to a dynamic glacier evolution model has been used in various studies to understand glacier mass balance sensitivity and response to climate change (e.g., by Jóhannesson, 1997; Kraaijenbrink et al., 2017; Khadka et al., 2020). By using the elevation bands in Module 3, ice flux at the sub-glacial scale is simulated (i.e., mass flux to/from one elevation band to another) before being summed and used in conjunction with the net annual SMB rate to determine the annual change in glacier mass.

The rate of change of ice thickness, $\frac{\partial \mathrm{H_i}}{\partial \mathrm{t}}$, (at the *i*th elevation band) is calculated as the difference between the net annual SMB rate and the ice flux:

$$\frac{\partial H_i}{\partial t} = SMB_i - \nabla . q_i \qquad \text{[Eq. 2]}$$

Where $\nabla.q_i$, the ice flux, is calculated per elevation band after Kraaijenbrink et al. (2017):

$$\nabla . q_i = rhe \times A_i \times H_i^5 \times \nabla z_i{}^3 \qquad \text{[Eq. 3]}$$

where, rhe is the rheology parameter. In our study it was specified through sampling from a physically meaningful range (see next section). A_i (m^2) is the area of the glacier in *i*th elevation band. H_i (m) is the average ice-thickness of *i*th elevation band. ∇z_i the gradient of the glacier surface at elevation band *i*. The initial ice thickness for the first time step (initial year) is from

Farinotti et al. (2019; see section 2.3.4.1) and is updated with Eq. 2 for each subsequent time step (the next year in our simulation). After the ice flux is calculated, it, the glacier surface gradient, and the net annual surface mass balance are used to determine the new volume of each elevation band (net change in mass per band and the corresponding change in ice thickness and volume. Ice thickness is simulated for the grid cells per band, based on the initial DEM raster input, and the new volume is distributed across the ice thickness grid cells). Both ice thickness H_i and mean elevation of band *i* are updated at each time step, while "band width" of the *i*th elevation band is fixed (see section 2.3.2.1). Then the volume-area dynamic model, which is a smoothing spline approach, begins by sampling the volume for different ice thickness grid cells across the band and determining the sample's area from the sample's volume and length. It then fits a smoothing spline (a cubic polynomial) to these volume-area samples to find the unique volume-area relation for the entire band, and uses this volume-area relation to predict the new area of this band. If a band is not large enough to fit the spline (which may happen if a band becomes small enough that it does not have enough unique volume-area combinations), the model instead uses a linear regression to determine the volume-area relation. In contrast, when a glacier grows beyond its initial volume, a volume-area relation is applied to simulate the glacier's advance. Once the surface area for the elevation bands are calculated, they are then summed to determine the annual change in surface area and ice thickness for the entire glacier. The annual change in glacier area from Module 3, together with the melt depth calculated from the TIM of Module 1, are then used to calculate the total melt runoff (m^3) of the glacier for that simulation year. This is one cycle of the CGME model (Module 1 and Module 2 at the daily time step to calculate annual melt depth and SMB; then Module 3 at the yearly time step to calculate annual surface area and volume change, and annual total melt runoff calculation. An enhanced workflow is provided in Appendix figure A3). Further,

the new glacier geometry (i.e. glacier area, volume, and depth) is used as input into the CGME to calculate the melt, SMB, volume-area, and runoff for the next year and it cycles thus through the number of years set for the simulation. When simulating multiple glaciers, the model cycles through all the simulation years for an individual glacier before looping to the next glacier. For a cost effective simulation, we developed a parallel processing framework using a multicore computer and performed 1000 simulations for each of the 258 glaciers to test the effect of parameter transferability on the prediction uncertainty across our study region.

2.3.4 Data Description

The data required for this study includes: 1) the input data required to setup the simulation models; and 2) the observed historical data required for model calibration, validation, and uncertainty assessments.

2.3.4.1 Input data

The modeling framework used in this study (cf., Fig. 2) requires two types of input data to initiate a simulation: input modeling parameters and spatiotemporal data required to run the model.

The input parameters include the meteorological modeling parameters that can vary spatiotemporally (e.g., temperature lapse rate and precipitation gradient), glacier characteristics (e.g., albedo of glacier ice, rheology parameter), and TIM parameters (e.g., degree day factor for ice, coefficient of ice melt), as detailed in section 2.3.2. These input parameters can fall within a physically meaningful range, described by previous empirical studies for glaciers with similar climate regimes (e.g., Gardner & Sharp, 2009; Shea et al., 2009; and Stahl et al., 2008); the maximum physically meaningful range for each parameter are listed in Table 1. To examine the effects of parameter transferability on model prediction uncertainty for regional-scale studies, a

total of 1000 samples from each parameter were created via the Latin Hypercube Sampling technique (Krause et al., 2005). The samples were generated from the parameters' physically meaningful minima and maxima based on a literature review. This process is detailed further in section 2.3.2.

Aside from the model input parameters, the model simulations also require geospatial and time series data. These data include observations of initial glacier geometry (i.e., DEM), initial surface area of the glaciers, initial ice thickness, aspect, hill slope, and a time series of climate for the simulation period (i.e., daily maximum, minimum, mean, and difference between maximum and minimum temperature; daily precipitation; and daily incoming solar radiation at the glacier surface). The data used in this study and their sources are detailed in Table 2. The initial glacier surface area and aspect are used to initiate Module 2, which calculates the daily SMB. Initial ice thickness, slope, and extent (outline) for the glaciers are required as inputs for Module 3 to calculate initial volume (for the first year of the simulation); later years use the ice volume calculated at the end of the previous simulated year (see section 2.3.2). Initial glacier outlines were obtained from the Randolph Glacier Inventory version 6 (RGI Consortium, Pfeffer et al., 2017). Glacier hypsometry was derived from a digital elevation model (DEM), with a grid resolution of 10 m ×10 m, sourced from maps Canada (http://maps.canada.ca/) based on Shuttle Radar Topography Mission (SRTM) DEM version 4 (Jarvis et al., 2008).

Table 1. The studied meteorological and glacier melt, runoff, and evolution parameters that are considered for examination of their response to different scenarios using CGME in this study. The maximum physically-meaningful initial ranges are set based on literature review (see Silwal et al., 2023).

Parameter	Description	Unit	Initial range	CTIM calibrated range	PTIM calibrated range
	Melt model parameters				
DDF_{snow}	Degree day factor for snow melt	$mmd^{-1}{}^{\circ}C^{-1}$	2.0-4.5	3.0-4.5	--

DDF_{ice}	Degree day factor for ice melt	$mmd^{-1}\,^{\circ}C^{-1}$	4.5-12.5	6.0-10.0	--
T_{thres}	Temperature threshold for melting	$^{\circ}C$	0.0-4.5	0.0-3.0	0.0-2.0
TF	Temperature melt factor	$mmd^{-1}{}^{\circ}C^{-1}$	0.0-1.5	--	0.0-1.5
SRF_{snow}	Shortwave radiation factor for snow	$m^2\ w^{-1}mmd^{-1}{}^{\circ}C^{-1}$	0.01-0.12	--	0.004-0.10
SRF_{ice}	Shortwave radiation factor for ice	--	0.011-0.14	--	0.004-0.4
Rexp	Exposition factor that modifies DDF_{snow} and DDF_{ice} with respect to aspect of glacier	--	0.02-0.2	0.1-0.2	0.05-0.2
α_{ice}	Albedo of glacier ice	--	0.2-0.4	--	0.2-0.43
	Parameters used in modeling surface meteorological variables				
LR	Temperature lapse rate (Altitudinal)	$^{\circ}Cm^{-1}$	0.006-0.0085	0.006-0.007	0.004-0.007
LRGlacier	Temperature lapse rate (along surface of glacier)	$^{\circ}Cm^{-1}$	0.0015-0.0055	0.0015-0.0040	0.0010-0.0025
Ppara	Precipitation parameter	--	1.05-1.85	1.2-1.7	1.5-3.0
Prate	Precipitation gradient	mm/m	0-0.25	0.1-0.2	0.02-0.1
	Melt runoff coefficients				
RainC	Coefficient of rainfall	--	0.1-0.2	0.1-0.15	0.2-0.3
SnowC	Coefficient of snowmelt	--	0.2-0.6	0.2-0.4	0.7-1.0
GlacC	Coefficient of glacier ice melt	--	0.2-0.9	0.4-0.7	0.9-1.5
	Volume-Area parameters				
rhe[1]	Rheology parameter	$m^{-4}\ yr^{-1}$	$0.6e^{-8}$ -$1.8e^{-8}$	$1.0\ e^{-8}$ -$1.8\ e^{-8}$	$1.2\ e^{-8}$ -$1.8\ e^{-8}$

Ice thickness used for model initiation in year 1 are from the estimates by Farinotti et al., 2019, who used glacier topography from SRTMv4, glacier outlines from RGIv6, and a combination of five ice thickness estimation models to provide an ensemble-based estimate for the ice thickness distribution (by inverting for local ice thickness using the principles of ice flow dynamics and the glacier's surface topography). Ice thickness data was resampled to 10m to match the DEM resolution. These geospatial data (initial area, thickness, slope, and aspect) for each glacier are

[1] Not calibrated in Silwal et al., 2023. Initial range suggested by Marshall and White, 2010; Adhikari and Marshall, 2013; and Wortmann et all 2019.

used for the initial year and updated annually in response to the geometry changes calculated by Module 3 for the following time steps.

Table 2. Data accessed or obtained for the purpose of this study.

Data type, description	Source	Resolution
Glacier Outlines, Randolph Glacier Inventory-RGI v6.0, 2017	Global Land Ice Measurements from Space (GLIMS) Randolph Glacier Inventory http://www.glims.org/RGI/randolph.html	Polygon
Digital elevation model of glacier hypsometry, 2017	Government of Canada https://maps.canada.ca/czs/index-en.html	10m×10m
Digital elevation model of glacier ice thickness, 2018	DEM processed with GlabTop2 https://glabtop2-py.readthedocs.io/en/latest/installation.html	10m×10m
Daily precipitation, 1994-2018 (station 3053536, Jasper Warden)	Environment and Climate Change Canada http://climate.weather.gc.ca/historical_data/search_historic_data_e.html	daily mm
Daily max, min, mean temperature, 1994-2018 (station 3053536, Jasper Warden)	Environment and Climate Change Canada http://climate.weather.gc.ca/historical_data/search_historic_data_e.html	daily ◦C
Daily seasonal streamflow data, 2006-2018 (station 07AA007, Sunwapta River)	Environment Canada Water Survey Data Explorer https://collaboration.cmc.ec.gc.ca/cmc/hydrometrics/www/	daily m^3/s

Both CTIM and PTIM versions of the melt module require precipitation, maximum temperature, minimum temperature, mean temperature, and difference between maximum and minimum temperature at the daily time step to calculate daily melt runoff. Similar to other regional-scale glacier melt modeling studies, the historical climate observations in our study area are sparse, limited by spatial and temporal discontinuity of data collection, the type of data collected, or both. For this study, historical climate data are from the Jasper Warden climate station (chosen for its proximity to the glaciers and the robustness of its records, Environment and Climate Change Canada). The PTIM also requires daily inputs for incoming shortwave radiation (SW) and

albedo for snow (α_{snow}). These are calculated from available observed climate data (see section 2.3.1). Estimations of SW and α_{snow} are based from the approach taken by Walter et al. (2005), where PET is estimated using the Hargreaves-Samani method for the continental interior regime, after Li et al. (2018).

2.3.4.2 Observed Data for Calibration and Validation

For validation and calibration of model performance, this study also requires time series measurements of melt runoff from the outlet of glacier lakes. The Sunwapta River hydrometric station is located near the terminus of the Athabasca Glacier where the meltwater flows downstream to feed the headwaters of the Sunwapta River. Athabasca Glacier is one of the largest glaciers in the study area, with an ice volume of approximately 1.84×10^8 m^3, several orders of magnitude larger than the majority of the glaciers in the study area. Due to the proximity of the Sunwapta River hydrometric station to the Athabasca glacier, the observed daily flows from this station and the simulated daily melt runoff of the Athabasca glacier were used for model validation, calibration, and uncertainty assessment. Due to the data availability of both climate data for model simulations and observed daily flows, the calibration period was 2011-2018 and the validation period was 2006-2010. Separate calibration and validation periods have been used in other glacier modeling studies, including TIM-based models (Pellicciotti et al. 2005) and basin-scale glacier mass balance volume-area scaling models (Stahl et al., 2008). Having a separate validation period allows us to assess the model's predictive capability after calibration.

2.3.4.3 Calibration, Validation, Uncertainty Assessment approach description

For calibration and uncertainty assessment we developed a similar approach as Abbaspour et al. (2004) and sampled the parameters using the LHS approach (McKay et al., 1979). A total of 1000 samples were taken from the maximum physically meaningful range that was identified for

each parameter based on an extensive literature review (see Table 1). The coefficient of determination (R^2), slope-based modified coefficient of determination (bR^2), and Nash–Sutcliffe efficiency (NS) were used as objective functions to compare simulated versus observed glacier melt runoff on a daily basis. The parameter set samples were fed into our coupled glacier melt, mass balance, and evolution model to generate 1000 simulation outputs for the calibration period based on the sampled parameters. After each iteration of 1000 simulations, the range of parameters was narrowed based on the simulation closest to the observed runoff, as determined by our chosen objective functions. The 1000 simulations based on optimized parameter ranges in the final iteration generated a 95% prediction uncertainty (95PPU) of the output variables (i.e., glacier melt runoff) that were calculated at the 2.5% and 97.5% levels of the cumulative distribution functions of glacier melt runoff. Two statistical criteria were used for assessment of model performance and uncertainty including p-factor and r-factor. The p-factor is the percentage of observed data bracketed by the 95PPU, and the r-factor represents the thickness of the 95PPU, which is calculated as the ratio of the average width of the 95PPU to the standard deviation of the measured variable (i.e., measured daily melt runoff). Ideally, a p-factor value of 1 and a r-factor value of zero is expected, however in large scale studies due to inherent uncertainties in input data, physical parameters, and model conceptualization a p-factor of above 0.5 and an r-factor of around 1-2 is considered satisfactory in hydrologic studies (Faramarzi et al., 2009, 2017; Sao et al., 2020). In this study, during the iterative calibration procedure, a total of 18000 model runs were performed in a R environmnet and simulations were parallelized in a 40-core computer.

To assess the response of glacier melt, SMB, and dynamics to physical parameters that are driven based on their maximum physically meaningful spectrum (as listed in Table 1), one-at-a-time (OAT) parameter perturbations were performed. The idea was to examine how a selection of

parameter values from empirical studies on a limited number of glaciers would be realistic as an input in melt runoff simulations of other glaciers at a regional scale. A reference simulation was also performed using the calibrated optimized parameter ranges for both CTIM-based and PTIM-based CGME models for the 2006-2018 period. Further, each parameter (listed in Table 1) was changed to an extreme value, either an extreme minimum or an extreme maximum within its physically meaningful range, while all other parameters were held unchanged. This process was repeated for each parameter until simulations were run for a minimum and a maximum for all parameters. These simulations were compared to the reference simulation.

2.4. Results and discussion

2.4.1 Calibration, validation, and uncertainty assessment based on Athabasca glacier measured runoff

Overall, the performance of our CTIM-based model for the entire simulation period, including both calibration and validation periods (2006-2018), was more successful than that of the PTIM-based model (Fig. 3a,b). However, the performance measures for the calibration period (2011-2018) were slightly different from those of the validation period (2006-2010) for both models. After a total of nine iterations, the CTIM-based CGME model results for the 2011-2018 calibration period indicated that the simulated glacier melt runoff for Athabasca glacier are satisfactory with a *p*-factor of 0.72 and an *r*-factor of 0.73. These were considered satisfactory, as a p-factor within 0.6-0.8 and an r-factor between 0 and 1 are considered satisfactory ranges (after Abbaspour et al., 2007; Sao et al., 2020). Based on the optimum parameter range resulting from the final iteration, the R^2, bR^2, and NS for the best performing model output was 0.78, 0.78, and 0.72 respectively. The calibration results showed that the best simulated daily melt runoff from

1000 model runs using the samples from optimized parameter ranges compared well with the observed melt runoff (Fig. S1 and S2).

For the PTIM-based CGME model, calibration results based on the final iteration indicated that simulated glacier melt runoff for Athabasca glacier are not as satisfactory as those of the CTIM-based model. The performance criteria for calibration of this model for the 2011-2018 period were 1.20 for the *r*-factor, 0.31 for the *p*-factor, 0.60 for R^2, 0.56 for bR^2, and 0.20 for NS (see Fig. S1).

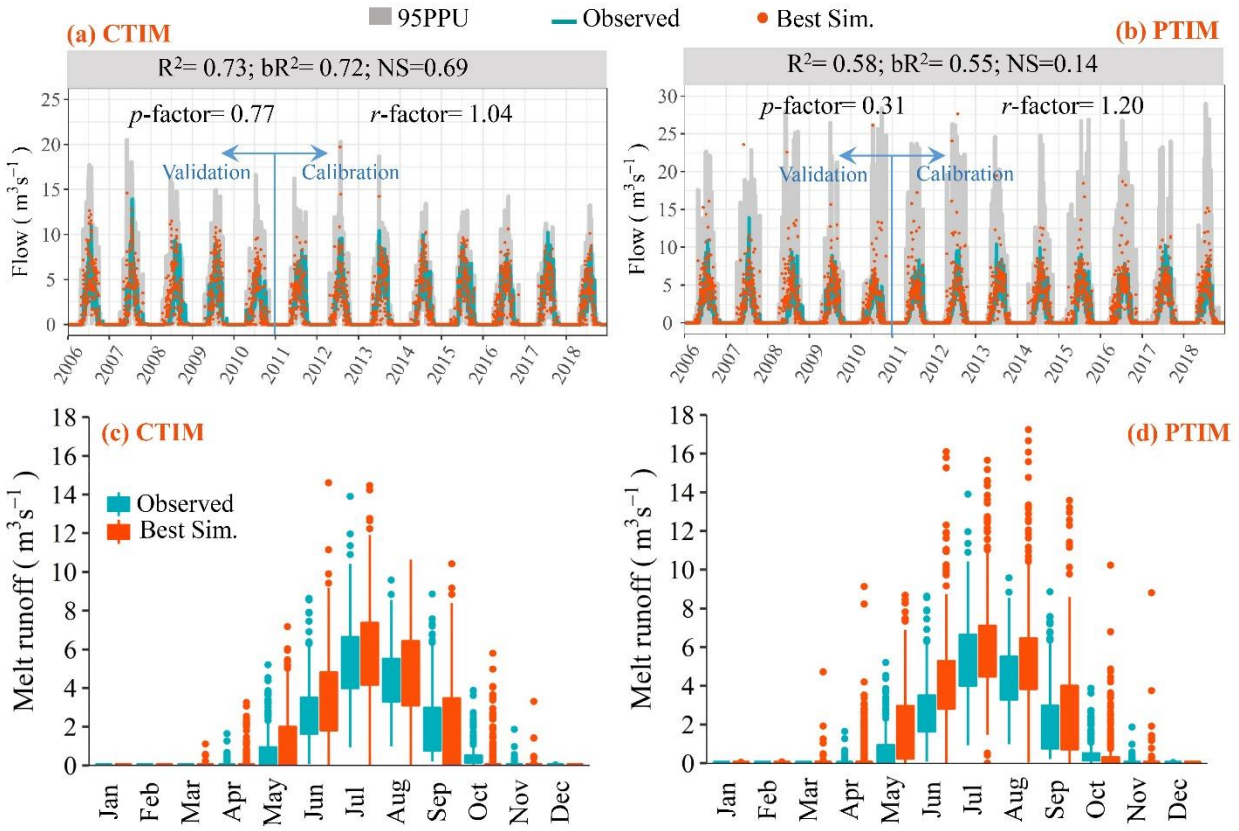

Figure 3. Comparison of the simulated daily melt runoff with observed data for the Athabasca Glacier based on (a) CTIM-based CGME, (b) PTIM-based CGME for the 2006-2018 calibration period. Simulated daily runoff based on the best parameter sets are indicated by orange dots, while observed flow data is indicated by the blue line. The 95 percent prediction uncertainty (95PPU) for 1000 simulations based on the optimal parameter ranges is indicated by the grey band. Bottom row panels illustrate the long-term (2006-2018) daily average data for different months based on the best simulated signals for: (c) CTIM-based CGMEM, (d) PTIM-based CGME.

To test the reliability of model predictions we performed a model validation for the 2006-2010 period. For the validation period, the climate data for model setup were obtained from the same meteorological station as those used for the calibration period (Jasper Warden station, Environment and Climate Change Canada). Jasper Warden station lies approximately 98 km north of Athabasca Glacier (where observed runoff for validation was measured) and at an elevation of 1020 m.a.s.l. Given that long-term times series data that correlate with observed streamflow data are not available for this station, our validation period was shorter than the calibration period. However, we covered at least five ablation-accumulation periods in our times series for the validation period to represent several years of seasonal variability. Similar to the calibration period, the validation performance fell within target ranges with a higher performance for the CTIM-based model (*p*-factor=0.64, *r*-factor=0.66, R^2=0.68, bR^2=0.68, and NS=0.51) than the PTIM-based model (*p*-factor=0.31, *r*-factor=1.02, R^2=0.54, bR^2=0.53, and NS=0.04) (Fig. S1, Table S1). Overall, while the CTIM-based CGME model performed well during the entire simulation period (Fig. 3a), the simulated melts occurred earlier in the season than observed flows. The model also slightly overestimated peak daily flows during the peak melt season in July and August.

Comparison of the CTIM-based and PTIM-based CGME model results indicate that the PTIM-based model overestimates peak daily flows during the peak melt season (July and August), which reduces the performance of the model for both the calibration and validation periods (see Fig. S2). The simulation results for the 2006-2018 period show that only 31 percent of observed data were represented by the predicted 95PPU in the PTIM-based model, and the R^2, bR^2, and NS were lower than those of the CTIM-based model (Fig. 3b). This is contrary to the assumption in the literature that PTIM is superior to other TIM approaches because of its capacity to involve

more process representation as compared to the other TIM-based approaches, e.g., consideration of incoming and reflected shortwave radiation (see Pellicciotti et al., 2005; Carenzo et al., 2009; Ragettli & Pellicciotti, 2012; Heynen et al., 2013). The overestimation of peaks and the low performance of the PTIM-based approach in our analyses is partially due to the lack of high resolution incoming solar radiation and snow and ice albedo observed data, and hence the use of estimated data in the model. The poor performance and a high uncertainty prediction of more sophisticated process-based models due to the lack of high quality input data has been reported in earlier studies (see Zaremehrjardy et al., (2020) and Engelhardt et al., (2013)). While simulated results at the 97.5th prediction percentile level (upper band of the 95PPU) indicated that the PTIM-based model significantly overestimated melt runoff during the warm season, the simulated data at the 2.5th prediction percentile level (lower band of the 95PPU) showed an underestimation of melt runoff during the ablation periods (Fig. 3b). This underestimation (Fig. 3b, Fig. S1 and S2) is consistent with another study performed in the CRM. Bash and Marshall (2014) found that the PTIM and an enhanced TIM they developed based on the PTIM also consistently underestimated melt compared to observations and exhibited high sensitivity. Some other studies indicated that the radiative-enhanced models are not always regarded as superior to temperature-based models, because ablation, especially at the glacier and larger scale, is most greatly impacted by temperature (see for example, Réveillet et al., 2017). While collinearity may be a factor in our PTIM model as well, we attribute the relatively poor PTIM performance to uncertainties related to PTIM model inputs, especially estimated values for radiative factors such as incoming shortwave radiation, α_{snow}, α_{ice}, SRF_{snow}, and SRF_{ice} (see section 2.2.4.1).

Analysis of the monthly data (Fig. 3c,d) showed that simulated melt runoff reflects variability of the observed monthly streamflow. Runoff was zero during the accumulation season

(Dec-Feb) and reached a maximum during the ablation season (Jun-Aug) for both the CTIM- and PTIM-based models. Between CTIM and PTIM, the PTIM-based model demonstrated greater inter-annual variability (Fig. 3b) and increased simulated melt runoff in the shoulder seasons, i.e., Mar-May and Sept-Nov (Fig. 3b,d). This is expected due to the incorporation of radiative melt factors in the PTIM-based model that allows simulation of some ice melt due to radiation energy absorption even on days when the daily temperature is below the melting threshold.

In general, both CTIM-based and PTIM-based model results predicted rather similar ranges of uncertainty (i.e., 95PPU represented by the *r*-factor), but the CTIM-base model reproduced more observed data points within its prediction uncertainty range (i.e., 71% of observed data were captured within predicted 95PPU) than PTIM-based model (i.e., 31% of observed data were bracketed within predicted 95PPU). In addition, the objective functions based on the comparison of observed with simulated melt runoff data were considerably higher in the CTIM-based model simulations. Overall, the uncertainty prediction and the model performance measures indicate that the CTIM model, which requires less volume of input data for model setup than the PTIM-based model, performs better. However, the PTIM-based model, which requires more input data and suffered from estimation of the inputs due to the lack of observations, generates poor performance with a similar range of uncertainty as that of CTIM-based model. Our findings are supported by other studies that reported similar conclusions (Vincent and Six, 2017; Zolles et al., 2019; Zaremehrjardy et al., 2020), especially at the glacier to basin-wide scale (Réveillet et al., 2017) that have high temporal resolution (Bash and Moorman, 2019).

2.4.2 Glacier melt runoff response to parameter perturbations

The results of OAT sensitivity analysis indicate the response of the simulated melt runoff to a change in each of the parameters used by our CTIM- and PTIM-based CGME models,

respectively (Figures 4 and 5). As shown in Figure 4, the CTIM-based simulated melt runoff increases in response to an increase in DDF_{snow}, DDF_{ice}, Ppara, RainC, SnowC, and GlacC or a decrease in T_{thres}, Rexp, LR, and LRGlacier (negligible response to changes in Prate or *rhe*). Simulated melt runoff using our PTIM-based model in Figure 5 increases in response to an increase in Ppara, RainC, SnowC, and GlacC or a decrease in LR, LRG, T_{thres}, and TF (negligible response to changes in Prate, rhe, SRF_{snow}, SRF_{ice}, or α_{ice}). In the following sections we provide analyses of the physical implications of parameter sensitivity by discussion of the parameters in more details.

2.4.2.1 Melt

By having and calibrating separate degree day factors for snow and ice (DDF_{snow} and DDF_{ice} respectively), the CTIM better differentiates surface properties as compared to the models that use single DDF representing both snow and ice conditions cumulatively (Braithwaite, 1995; Hock, 1999). Figure 4 (a) and (b) indicate that the model is highly sensitive to changes in values for both DDF_{snow} and DDF_{ice}, with increases in both DDF_{snow} and DDF_{ice} leading to increased total melt runoff. The DDFs are empirically derived and the melt calculation is simplistic, leading the CTIM approach to be sensitive to these parameters as they are reflecting several underlying processes (Hock, 1999; Tsai & Ruan, 2018). To further refine the DDF approach, an exposition factor (Rexp) is considered (Shea et al., 2015; Marshall et al., 2011); which modifies both DDF_{snow} and DDF_{ice} to vary with DEM-derived aspect and surface type. Our simulated data in Figure 4d indicates some sensitivity to changes in Rexp parameter, with a decrease in Rexp correlating to a slight increase in total melt runoff.

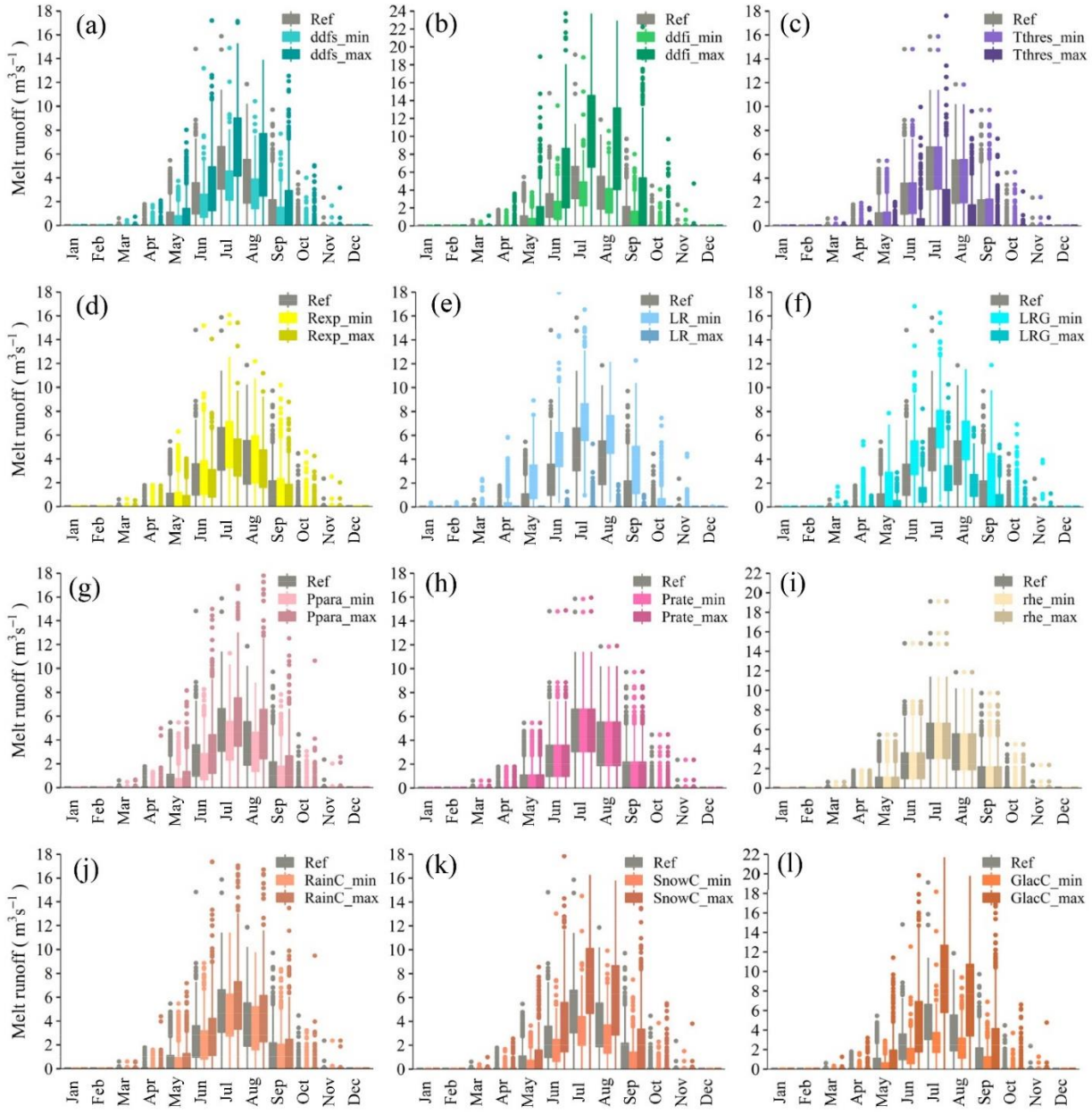

Figure 4. Monthly variability of CTIM-based coupled melt-mass balance-evolution model parameters, results of one-at-a-time parameter perturbations. Simulated daily glacier melt runoff is plotted by month for the period 2006-2018. A reference simulation using CTIM-based model optimized parameters is shown in grey, while melt runoff using an extreme minimum parameter value and an extreme maximum parameter value are shown to the right of reference. The parameter descriptions and ranges in figure panels (a-l) are listed in Table 1.

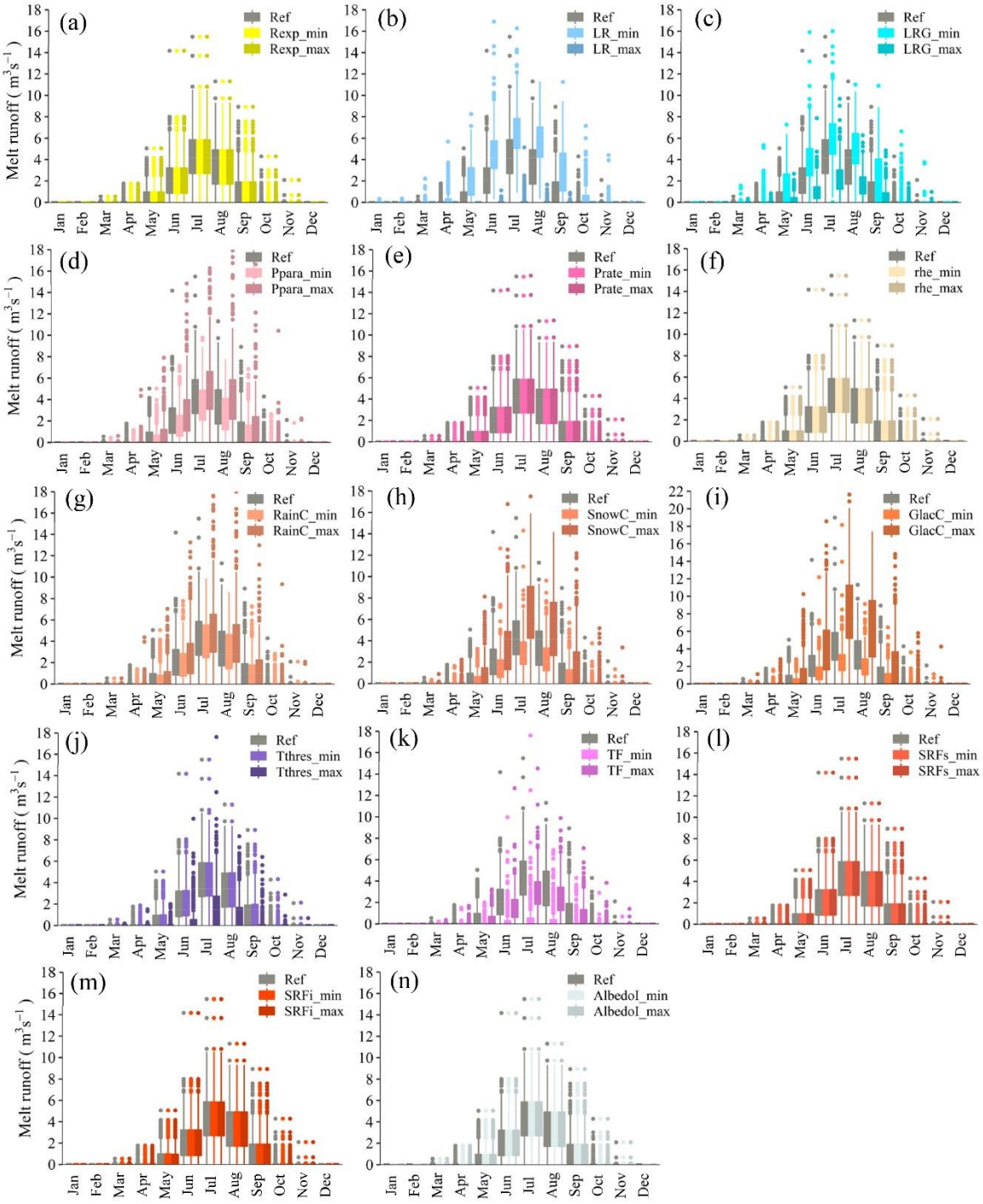

Figure 5. Monthly variability of PTIM-based coupled melt-mass balance-evolution model parameters, results of one-at-a-time parameter perturbations. Simulated daily glacier melt runoff is plotted by month for the period 2006-2018. A reference simulation using PTIM-based model optimized parameters is shown in grey, while melt runoff using an extreme minimum parameter value and an extreme maximum parameter value are shown to the right of reference. The parameter descriptions and ranges in figure panels (a-n) are listed in Table 1.

The PTIM uses the albedo, temperature melt factor (TF), incoming shortwave radiation, and shortwave radiation factor (SRF). By separating both albedo and SRF into those for snow and ice, we aimed to improve model performance by better simulating retention of radiation across the glacier surface. Figure 5 (l) and (m) indicate that changes in either SRF_{snow} or SRF_{ice} do not significantly affect the modelled melt runoff. Daily incoming shortwave radiation was a model input; observed incoming radiation was not available for the full study region, so it was estimated after Walter et al. (2005) and modified due to atmospheric conditions (e.g. thickness, aerosols) after Follum et al. (2015). As shown in Figure 5 (n), the albedo of ice does not significantly affect the modelled total melt runoff. This is contrary to the findings of Marshall and Miller (2020), whose observations at Haig glacier in Alberta found strong variability in glacier surface albedo and corresponding runoff during the melt season. Other studies show that albedo affects glacier melt at sub-daily time scales, whereas the most commonly used models (similar to the one developed here) simulate at the daily time scale (Pellicciotti et al., 2005; Heynen et al., 2013), which may explain why the effects of albedo are not profoundly observed in the simulations. This demonstrates the limitations of approximated albedo values for snow, even when the albedos of snow and ice are separated.

The final PTIM parameter, temperature melt factor (TF), was found to have some effect on PTIM overall model performance. This is shown in Figure 5 (k), which also indicates that low values of TF greatly decrease modelled total melt runoff.

The other melt model parameters, required by both CTIM and PTIM are a threshold temperature for snow melt (T_{thres}), the coefficients of glacier ice melt, snowmelt, and rainfall (GlacC, SnowC, and RainC, respectively). These are used with modelled melt from either CTIM or PTIM to calculate total runoff per elevation band, which is later used to find the surface mass

balance of the elevation band (see section 2.3.2.2.) As shown in Figure 4 c, j, k, and l and Figure 5 g, h, i, and j, both CTIM and PTIM versions of the model showed similar sensitivities to these parameters; an increase in total simulated melt runoff in response to an increase in GlacC, SnowC, or RainC or a decrease in T_{thres}. This is consistent with other studies, though Ragettli and Pellicciotti (2012) found their PTIM-based model was more sensitive to the SRF than these coefficients. Our study, unlike theirs, did not account for the percolation and storage of meltwater in nearby soils, which may be one cause of the difference.

2.4.2.2 Surface Mass Balance (SMB)

In this study, the processes that affect SMB are those that contribute to snowfall (accumulation) and total melt runoff (ablation). The parameters used by the coupled mass balance dynamic evolution model that govern snowfall and total melt runoff (aside from those used by the TIM in Module 1, as explained in the previous section) are the precipitation gradient (Prate), precipitation parameter (Ppara), Altitudinal lapse rate (LR), and lapse rate along the glacier surface (LRGlacier). These plus the model inputs of daily observed precipitation and temperature allow for the calculation of temperature and amount of precipitation at each elevation band.

By using LHS and 95PPU through our calibration procedure, we were able to predict an uncertainty range for both LR and LRGlacier. This is an improvement compared to studies that use a single fixed value for the lapse rate. Figure 6 (e) and (f) and Figure 7 (b) and (c) show that both CTIM and PTIM-based versions of the model are highly sensitive to variations in both LR and LRGlacier and that a decrease in either LR or LRGlacier leads to an increase in simulated melt runoff. This is consistent with what has been observed (such as by Arendt & Sharp, 2009) as a large lapse rate would lead to estimations of lower temperatures at higher elevations, causing higher simulated snowfall and lower simulated melt runoff.

Similarly, the choice of precipitation gradient (Prate), which extrapolates precipitation by elevation, affects TIM-based glacier melt models (Engelhardt et al., 2013; Heynen et al., 2013). This is in conjunction with a precipitation correction parameter (Ppara) which is empirically derived to correlate winter mass balance and climate station elevation to better simulate SMB and melt runoff (Stahl et al., 2008). Both CTIM and PTIM-based models show slight sensitivity to Ppara, with a response of increased melt runoff to an increase in Ppara, indicated in Figure 6 (g) and Figure 7 (d). Negligible sensitivity to Prate in both models is illustrated in Figure 6 (h) and Figure 7 (e). This may be because the precipitation distribution to each elevation band by Prate is less significant to total melt runoff than the distribution of precipitation type (rain or snow) governed by temperature-based processes.

While the simulated process of surface mass balance is simplistic in this model (snowfall – total melt runoff), it is the aim of this study to refine it by calculating daily SMB using estimated melt runoff (as described in 3.2.1.); distributing temperature and precipitation to each elevation band by using calibrated ranges of LR, LRGlacier, Prate, and Ppara; and distinguishing between solid and liquid precipitation (i.e. snow or rainfall.) From this daily, elevational SMB, the total annual SMB for the entire glacier can be determined and used to simulate glacier dynamic evolution.

2.4.2.3 Evolution

In this study, initial glacier hypsometry is defined as model inputs (see section 2.3.4.1.) The only model parameter relating to dynamic evolution was the rheology parameter, which was calibrated using LHS and 95PPU from a physically meaningful range from other studies of mountain glaciers. In this model the rheology parameter is used in the calculation of ice flux and the change in the range of ice thickness (see Equations 2 and 3). Figure 6 (i) and Figure 7 (f) show

negligible sensitivity in simulated melt runoff to changes in the rheology parameter in both CTIM and PTIM-based models. Calibrated ranges for the rheology parameter in both models (see Table 2) agree with values found by other studies in the CRM (Marshall et al., 2011).

2.4.3. Parameter transferability and the use of a range of parameters at the regional scale

To examine the issue of parameter transferability and prediction uncertainty of glacier melt, mass balance, and evolution modeling at a regional scale, we applied our calibrated-validated model to predict melt runoff in 258 glaciers in the Athabasca River Basin for the historical period 1984-2007. This period was selected due to limitations in data availability at the regional scale, as the glaciers are distributed across 15 sub-basins of the Athabasca River Basin and contiguous meteorological observations are not available across these sub-basins. Instead, we used a gridded climate product, which covered 1984-2007, that was downscaled to our study's spatial resolution (see Faramarzi et al., 2015). Due to its better performance and limited input observations, we used the CTIM version of the model. For each glacier we performed 100 simulations using the optimum parameter ranges that were obtained through the calibration iterations for the Athabasca glacier. The simulations were based on 100 sets of new sampled parameters from the optimum range using the LHS approach explained in Section 2.3.2.1.

The simulation results indicate that depending on the glacier size and location, the average annual cumulative melt runoff ranges from ~ 0.005 m^3 sec^{-1} to ~ 75 m^3 sec^{-1} using L95PPU, which refers to the 2.5th prediction percentiles (Fig. 6a); from ~ 0.046 m^3 sec^{-1} to ~ 205 m^3 sec^{-1} using U95PPU, which refers to 97.5th prediction percentiles (Fig. 6b), and from ~ 0.01 m^3 sec^{-1} to ~ 132 m^3 sec^{-1} M95PPU, which refers to the median of predictions (Fig. 6c) across the region. The

predicted uncertainty range, which is calculated as the difference between L95PPU (m^3 sec^{-1}) and U95PPU (m^3 sec^{-1}) for each glacier (Δ95PPU (m^3 sec^{-1})), varied from 0.04 m^3 sec^{-1} to ~ 134 m^3 sec^{-1} (Fig. 6d) across glaciers. Prediction of such

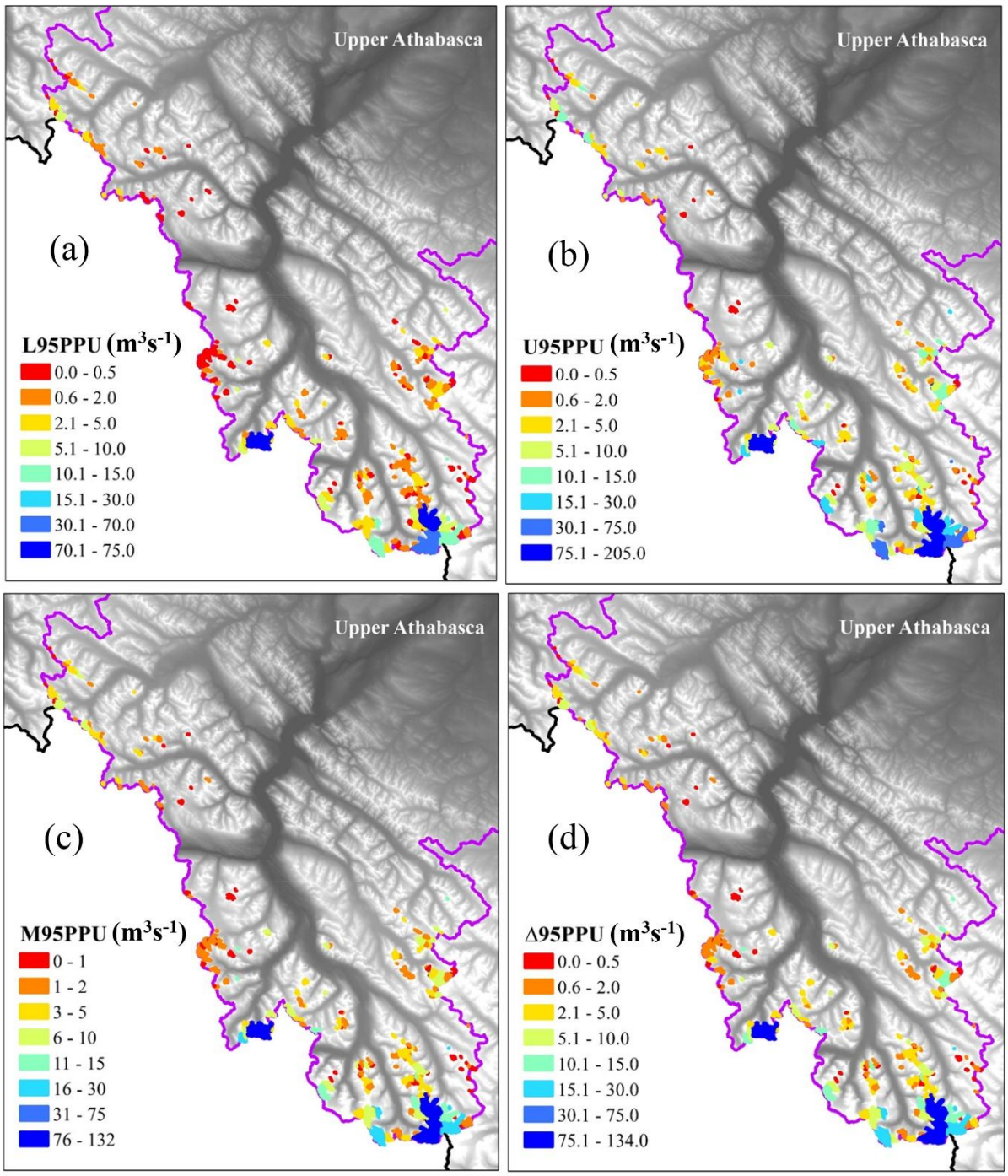

Figure 6. Maps of the 258 glaciers in the Athabasca River Basin, indicating the average annual cumulative melt runoff per glacier (m^3 sec^{-1}) for the Lower (a), Upper (b), and Median of 95% Prediction Uncertainty (95PPU) for the period 1984-2007, from 100 simulations of the CTIM CGBMDEM using optimized parameter ranges. Bottom right (d) is the difference between Lower and Upper bands (Δ95PPU). The cumulative melt runoff was calculated as the sum of daily melt runoff (m^3 sec^{-1}) for all days of the given year.

a range of runoff for each glacier rather than a single runoff value demonstrates the issue of parameter transferability, and indicates that the simulated runoff is strongly dependent on the value of input parameters. In these glaciers different sets of input parameter values in the model results in a different runoff accumulation, with the largest predictions which can stay up to 134 m^3 sec^{-1} apart from their predicted L95PPU (m^3 sec^{-1}). The results indicate that the large values of Δ95PPU are observed only in large glaciers which count for < 3% of the total number of glaciers in the region (Fig. 6d). However, the lesser Δ95PPU (m^3 sec^{-1}) in small size glaciers do not understate the parameter transferability issue because of the mathematical error propagation, where the Δ95PPU (m^3 sec^{-1}) values are magnified in large quantities (e.g., large cumulative runoff from larger glaciers) as compared to small values. To mask the effect of error propagation issues in the interpretation of our results, we normalized the predicted uncertainty ranges by dividing their Δ95PPU (m^3 sec^{-1}) to the median of the predicted runoff values (i.e., M95PPU (m^3 sec^{-1})) for each of the glaciers (Fig. 7a) and presented them as their share from the maximum value (Fig. 7b). The normalized uncertainty prediction (Rn) varied from 0.37 to 1 across glaciers (Fig. 6d), which showed ~ 63% of the glaciers in the region had an Rn value of greater than 0.5 and only in less than 37% of the glaciers the R value was less than 0.5. Note that the larger the Rn indicates the greater the share of their normalized uncertainty prediction and, therefore, demonstrates a greater sensitivity of the predicted melt runoff to their underlying input parameters. This indicates that in more than 63% of the glaciers in the region, the input parameters for melt-mass balance-evolution modeling (such as the one developed in this study) cannot be driven from empirical measurements from other adjacent glaciers such as the Athabasca. However, in less than 37% of the glaciers in the region the parameter values can be transferred from their adjacent glaciers with relatively smaller uncertainty in their runoff predictions (Rn < 0.5) as compared to the other glaciers (with

Rn > 0.5). While other TIM-based studies note that parameterization has limited transferability due to being based upon and calibrated to site-specific measurements (Litt et al., 2019; Marshall & Miller, 2020), Carenzo et al., (2009) note that parameterization can be transferred across spatial and temporal scales in general mountain regions with minimal loss to performance, and of the models analyzed by Réveillet et al. (2017) not one model type offered better transferability over the others. By using a range of parameter values, calibrated from the maximum physically meaningful range for each parameter from an adjacent glacier (e.g., Athabasca glacier in this study), we demonstrate different levels of uncertainty arising from the parameter transferability in each glacier.

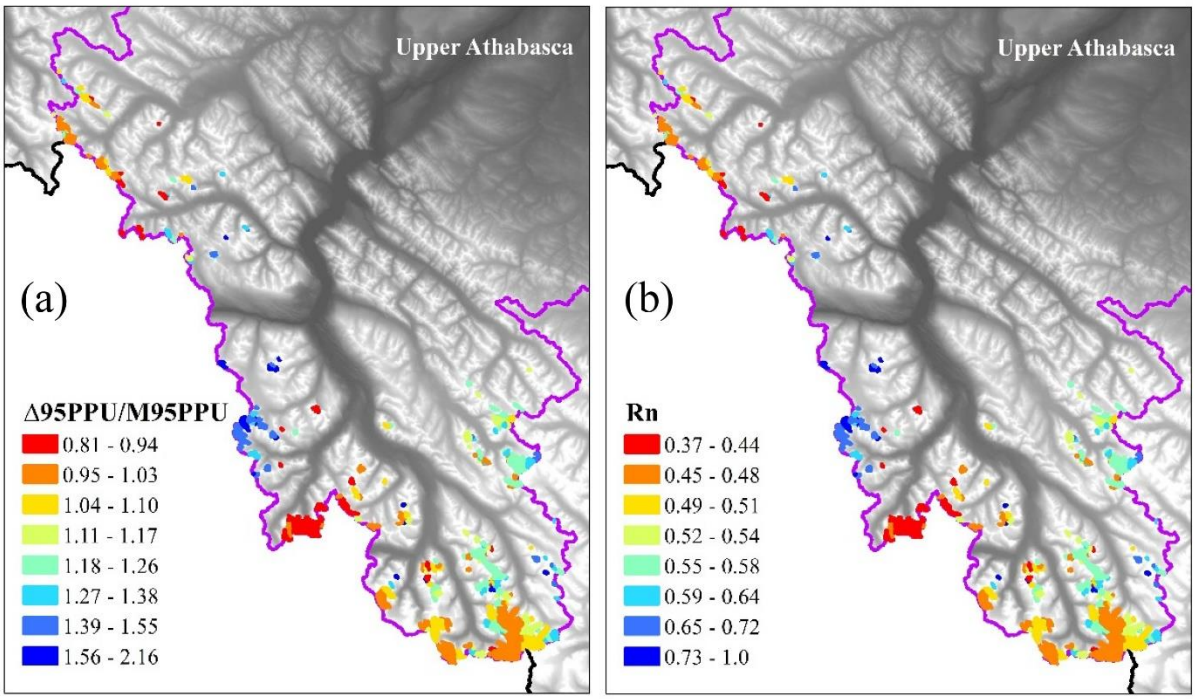

Figure 7. Maps of the 258 glaciers in the Athabasca River Basin, indicating normalized uncertainty range of melt runoff (a), calculated as as: Δ95PPU/M95PPU, and share of normalized range from their maximum value (b), calculated as: Rn = (Δ95PPU/M95PPU)/2.16.

To further investigate how glacier size plays a part in parameter transferability issue, we categorized all glaciers of the region into 3 size classes after Chinn (2001) and calculated the cumulative melt runoff differences (Δ95PPU (m^3 sec^{-1})) and % difference of cumulative melt runoff for each category. It was determined that 46.5% of total glacier count are small glaciers and they account only for ~ 5.8% of total initial glacier area in the region. Medium size glaciers make up 45% of the total glacier count, and accounted for 35.8% of total initial surface area. Large glaciers, at 8.5% of the total glacier count, accounted for 58.4% of the total initial surface area. The total predicted Δ95PPU for small, medium, and large size glaciers were 697.4 m^3 sec^{-1}, 326.1 m^3 sec^{-1}, and 529.5 m^3 sec^{-1}, respectively (Table 3). It is evident that, while large glaciers account for the largest cumulative Δ95PPU of melt runoff due to their size, small glaciers have a greater cumulative melt runoff difference arising from the input parameter variability. This indicates larger parameter dependence of the melt-mass balance-evolution modeling in smaller glaciers. While a majority of glacio-hydrological studies have focused on modeling of large glaciers across the world (Radic et al., 2014; Kraaijenbrink et al., 2017; Immerzeel et al., 2019), reliable prediction of the response of small glaciers to future climate changes are of utmost importance not only due to their cumulative impact on their downstream water resources for economic sectors, but also for their ecological impacts (Brown et al., 2006; Cauvy-Fraunié et al., 2016). Small glaciers feed numerous stream tributaries worldwide, and they play a key role in regulating stream temperature, stream biochemical makeup, and stream type/channel evolution. Even small changes in glacier streamflow contribution can cause rapid, dramatic changes in the surrounding ecosystem, including stream microscopic biota, algal growth, fish and other macro-organism populations, and surrounding vegetation cover and type (Brown et al., 2006; Cauvy-Fraunié et al., 2016; Cannone

et al., 2008; Milner et al., 2009). An accurate and reliable simulation of these glaciers and prediction of their changes in the future are key for adaptation and mitigation strategies.

Table 2.3. Summary data of glaciers in the Athabasca River Basin and the difference in Lower (L) and Upper (U) 95 percent prediction uncertainty (95PPU) estimates of cumulative melt runoff for the period 1984-2007 from 100 simulations using the CTIM calibrated parameter range.

Category	Size (km^2)	Count	% of total glacier count	Initial surface area (km^2)	% of total initial surface area	Cumulative melt runoff difference Δ95PPU (m^3 sec^{-1})
Small	0.01-0.32	120	46.50%	17.46	5.80%	697.4
Medium	0.32-2.56	116	45.00%	108.1	35.80%	326.1
Large	2.56-29.95	22	8.50%	176.32	58.40%	529.5
Total	_	258	100.00%	301.88	100.00%	_

2.5. Summary, conclusions, and future directions

We revisit widely used glacier models (CTIM, PTIM, SMB, and spline-based VAS models), incorporating them into a coupled glacier mass balance dynamic evolution model (CGME) to characterize uncertainty associated with physical input parameters and assess the suitability of using such models at the regional scale and when input data is limited. We examined the response of glacier melt, SMB, and dynamics to physical parameters that are driven based on their maximum physically meaningful spectrum rather than a fixed value for each parameter.

Calibration and validation determined that while both versions of the CGME with different melt models (CTIM or PTIM) gave similar ranges of uncertainty for melt runoff from 1000 simulations forced by the maximum meaningful parameter range for each model, representation of observed data by the simulated predictions were vastly different. Using 95 percent prediction uncertainty (95PPU), it was found that 31% of observed data were represented by prediction

95PPU in the PTIM-based model versus the 71% represented by the CTIM-based model. There was high uncertainty associated with both overestimation and underestimation of melt runoff in the PTIM-based model. While model performance may be improved by using a range of parameter values compared to a singular value, prediction uncertainty may still be high due to model selection and quality of input data.

One-at-a-time (OAT) sensitivity analysis of each parameter for both model types showed the sensitivity of simulated melt runoff to each parameter. Both were found to be highly sensitive to similar parameters associated with temperature and melt runoff, with even small changes in parameter values leading to large changes in runoff. This highlights the importance and associated uncertainty of parameter selection and parameter transferability both spatially and temporally.

Assessment of 95PPU of melt runoff at a larger spatiotemporal scale reinforced this idea. Differences between U95PPU and L95PPU average annual cumulative melt runoff for each glacier (Δ95PPU (mm)), varied from 0.04 mm to ~ 134 mm across the 258 glaciers simulated. Normalized uncertainty prediction (Rn), which accounts for differences in glacier area, varied from 0.37 to 1 and ~63% of glaciers had Rn between 0.5-1. This demonstrates higher sensitivity of the predicted melt runoff to their underlying input parameters and that these glaciers ought not to be driven with parameters from empirical measurements from other adjacent glaciers. We also assessed cumulative melt runoff differences (Δ95PPU (mm)) and % difference of cumulative melt runoff based on glacier size. This determined that small glaciers have a greater cumulative melt runoff difference arising from the input parameter variability and larger parameter dependence at a regional scale. From this, we conclude that small glaciers have a wide range of potential cumulative melt runoff values that are regionally significant and ought not to be overlooked in examinations and discussions of regional projections.

Overall, we explored different levels of uncertainty in using ranges of parameter values in CGME modeling approaches. We determined that ranges of model predictions compared to observed data can be improved (and we developed optimized ranges for each parameter and modeling approach), but improvement is dependent on available input data and associated model selection. The models are more sensitive to changes in the range of some parameters and not responsive to others, which can help identify sources of uncertainty. We also assessed uncertainty at the regional scale, determining that even when using an optimized parameter range for simulated melt runoff, parameter range transferability is not appropriate for the majority of glaciers in the region and that small glaciers are especially sensitive to input parameter variability.

Applications of the optimized parameter ranges used with this model include being used to examine glacier melt runoff, mass balance, and evolution (such as change in ice area or glacier thickness) in regions where observations are sparse. They could also be used to generate predictions of simulated melt runoff to be coupled with other hydrological models to explore the impacts of glacier melt runoff to a watershed, such as volume and timing of seasonal melt runoff or the ecological and environmental impacts to stream temperature. Future work will focus on incorporating the range of predictions into projections of glacial changes through the end of this century under various climate change scenarios.

2.6. Acknowledgements

Funding for this study was primarily provided by the Natural Sciences and Engineering Research Council of Canada Discovery Grant (Grant #RES0043463) and Campus Alberta Innovation Program Chair (Grant #RES0034497).

2.7. References:

Abbaspour, K. C., Johnson, C. A., & Genuchten, M. T. van. (2004). Estimating Uncertain Flow and Transport Parameters Using a Sequential Uncertainty Fitting Procedure. *Vadose Zone Journal*, *3*(4), 1340–1352. https://doi.org/10.2136/VZJ2004.1340

Abbaspour, K. C., Yang, J., Maximov, I., Siber, R., Bogner, K., Mieleitner, J., Zobrist, J., & Srinivasan, R. (2007). Modeling hydrology and water quality in the pre-alpine/alpine Thur watershed using SWAT. *Journal of Hydrology*, *333*(2–4), 413–430. https://doi.org/10.1016/J.JHYDROL.2006.09.014

Adhikari, S., & Marshall, S. J. (2013). The Cryosphere Influence of high-order mechanics on simulation of glacier response to climate change: insights from Haig Glacier, Canadian Rocky Mountains. *The Cryosphere*, *7*, 1527–1541. https://doi.org/10.5194/tc-7-1527-2013

Arendt, A., & Sharp, M. (1999). Energy balance measurements on a Canadian high Arctic glacier and their implications for mass-balance modeling. (*Symposium at Birmingham, 1 July 1999 – Interactions between the Cryosphere, Climate and Greenhouse Gases, 165–172, 1999). International Association of Hydrological Sciences Publications, Issue 256.*

Bash, E. A., & Marshall, S. J. (2014). Estimation of glacial melt contributions to the Bow River, Alberta, Canada, using a radiation-temperature melt model. *Annals of Glaciology*, *55*(66), 138–152. https://doi.org/10.3189/2014AoG66A226

Bawden, A. J., Linton, H. C., Burn, D. H., & Prowse, T. D. (2014). A spatiotemporal analysis of hydrological trends and variability in the Athabasca River region, Canada. *Journal of Hydrology*, *509*, 333–342. https://doi.org/10.1016/j.jhydrol.2013.11.051

Bolch, T., Menounos, B., & Wheate, R. (2010). Landsat-based inventory of glaciers in western Canada, 1985-2005. *Remote Sensing of Environment, 114(1)*, 127–137. https://doi.org/10.1016/j.rse.2009.08.015

Braithwaite, R. J. (1995). Positive degree-day factors for ablation on the Greenland ice sheet studied by energy-balance modeling. *Journal of Glaciology, 41(137),* 153–160. https://doi.org/10.3189/s0022143000017846

Braithwaite, R. J. and Olesen, O. B. (1985.) Ice ablation in West Greenland in relation to air temperature and global radiation. *Zeitschrift für Gletscherkunde und Glazialgeologie, 20,* 155–168. Retrieved February 23, 2021, from https://www.research.manchester.ac.uk/portal/files/24283613/POST-PEER-REVIEW-PUBLISHERS.PDF

Braun, L.N., Grabs, W., & Rana, B. (1993) Application of a Conceptual Precipitation Runoff Model in the Langtang Kfaola Basin, Nepal Himalaya. *Snow and Glacier Hydrology (Proceedings of the Kathmandu Symposium, November 1992). International Association of*

Hydrological Sciences Publications no. 218. Retrieved February 23, 2021, from https://www.researchgate.net/publication/242567643

Brock, B. W., & Arnold, N. S. (2000). A spreadsheet-based (microsoft excel) point surface energy balance model for glacier and snow melt studies. *Earth Surface Processes and Landforms, 25(6)*, 649–658. https://doi.org/10.1002/1096-9837(200006)25:6<649::AID-ESP97>3.0.CO;2-U

Brown, L. E., Hannah, D. M., & Milner, A. M. (2007). Vulnerability of alpine stream biodiversity to shrinking glaciers and snowpacks. *Global Change Biology*, *13*(5), 958–966. https://doi.org/10.1111/J.1365-2486.2007.01341.X

Cannone, N., Diolaiuti, G., Guglielmin, M., & Smiraglia, C. (2008). ACCELERATING CLIMATE CHANGE IMPACTS ON ALPINE GLACIER FOREFIELD ECOSYSTEMS IN THE EUROPEAN ALPS. *Ecological Applications*, *18*(3), 637–648. https://doi.org/10.1890/07-1188.1

Cauvy-Fraunié, S., Andino, P., Espinosa, R., Calvez, R., Jacobsen, D., & Dangles, O. (2016). Ecological responses to experimental glacier-runoff reduction in alpine rivers. *Nature Communications 2016 7:1*, *7*(1), 1–7. https://doi.org/10.1038/ncomms12025

Clarke, G. K. C., Anslow, F. S., Jarosch, A. H., Radić, V., Menounos, B., Bolch, T., & Berthier, E. (2013). Ice volume and subglacial topography for western Canadian glaciers from mass-balance fields, thinning rates, and a bed stress model. *Journal of Climate*, *26*(12), 4282–4303. https://doi.org/10.1175/JCLI-D-12-00513.1

Clarke, G. K. C., Jarosch, A. H., Anslow, F. S., Radić, V., & Menounos, B. (2015). Projected deglaciation of western Canada in the twenty-first century. *Nature Geoscience, 8(5),* 372–377. https://doi.org/10.1038/ngeo2407

Comeau, L., Pietroniro, A., Demuth, M. *et al.* (2009) Glacier contribution to the North and South Saskatchewan Rivers. *Hydrological Processes.* 23, 2640–2653 DOI: 10.1002/hyp.7409

Engelhardt, M., Schuler, T. V., & Andreassen, L. M. (2013). Glacier mass-balance of Norway 1961-2010 calculated by a temperature-index model. *Annals of Glaciology*, *54*(63), 32–40. https://doi.org/10.3189/2013AoG63A245

Eyring, V., Bony, S., Meehl, G. A., Senior, C. A., Stevens, B., Stouffer, R. J., & Taylor, K. E. (2016). Overview of the Coupled Model Intercomparison Project Phase 6 (CMIP6) experimental design and organization. *Geoscientific Model Development*, *9*(5), 1937–1958. https://doi.org/10.5194/gmd-9-1937-2016

Farinotti, D., Huss, M., Bauder, A., Funk, M., & Truffer, M. (2009). A method to estimate the ice volume and ice-thickness distribution of alpine glaciers. *Journal of Glaciology, 55(191),* 422–430. https://doi.org/10.3189/002214309788816759

Faramarzi, M., Abbaspour, K. C., Adamowicz, V., Lu, W., Fennell, J., Zehnder, A. J. B., & Goss, G. G. (2017). Uncertainty based assessment of dynamic freshwater scarcity in semi-arid watersheds of Alberta, Canada. *Journal of Hydrology: Regional Studies*, *9*, 48–68. https://doi.org/10.1016/j.ejrh.2016.11.003

Finsterwalder, S., Schunk, H., 1887. Der Suldenferner. *Zeitschrift des Deutschen und Oesterreichischen Alpenvereins 18,* 72–89

Follum, M. L., Downer, C. W., Niemann, J. D., Roylance, S. M., & Vuyovich, C. M. (2015). A radiation-derived temperature-index snow routine for the GSSHA hydrologic model. Journal of Hydrology, 529(P3), 723–736. https://doi.org/10.1016/j.jhydrol.2015.08.044

Frey, H., Machguth, H., Huss, M., Huggel, C., Bajracharya, S., Bolch, T., Kulkarni, A., Linsbauer, A., Salzmann, N., & Stoffel, M. (2014). Estimating the volume of glaciers in the Himalayan-Karakoram region using different methods. *Cryosphere, 8(6),* 2313–2333. https://doi.org/10.5194/tc-8-2313-2014

Gardner, A. S., & Sharp, M. (2009). Sensitivity of net mass-balance estimates to near-surface temperature lapse rates when employing the degree-day method to estimate glacier melt. *Annals of Glaciology*, *50*(50), 80–86. https://doi.org/10.3189/172756409787769663

Gardner, A. S., Sharp, M. J., Koerner, R. M., Labine, C., Boon, S., Marshall, S. J., Burgess, D. O., & Lewis, D. (2009). Near-surface temperature lapse rates over arctic glaciers and their implications for temperature downscaling. *Journal of Climate, 22(16),* 4281–4298. https://doi.org/10.1175/2009JCLI2845.1

Gleick, P. H., & Palaniappan, M. (2010). Peak water limits to freshwater withdrawal and use. *Proceedings of the National Academy of Sciences of the United States of America*, *107*(25), 11155–11162. https://doi.org/10.1073/pnas.1004812107

Haslinger, K., Koffler, D., Schöner, W., & Laaha, G. (2014). Exploring the link between meteorological drought and streamflow: Effects of climate-catchment interaction. *Water Resources Research*, *50*(3), 2468–2487. https://doi.org/10.1002/2013WR015051

Heynen, M., Pellicciotti, F., & Carenzo, M. (2013). Parameter sensitivity of a distributed enhanced temperature-index melt model. *Annals of Glaciology*, *54*(63), 311–321. https://doi.org/10.3189/2013AOG63A537

Hock, R. (1999). A distributed temperature-index ice- and snowmelt model including potential direct solar radiation. *Journal of Glaciology, 45(149),* 101–111. https://doi.org/10.3189/s0022143000003087

Hock, R. (2003). Temperature index melt modeling in mountain areas. *Journal of Hydrology*, *282*(1–4), 104–115. https://doi.org/10.1016/S0022-1694(03)00257-9

Huss, M., & Farinotti, D. (2012). Distributed ice thickness and volume of all glaciers around the globe. *Journal of Geophysical Research: Earth Surface*, *117*(F4), 4010. https://doi.org/10.1029/2012JF002523

Huss, M., & Hock, R. (2015). A new model for global glacier change and sea-level rise. *Frontiers in Earth Science, 3*, 54. https://doi.org/10.3389/feart.2015.00054

Immerzeel, W. W., van Beek, L. P. H., Konz, M., Shrestha, A. B., & Bierkens, M. F. P. (2012). Hydrological response to climate change in a glacierized catchment in the Himalayas. *Climatic Change*, *110*(3–4), 721–736. https://doi.org/10.1007/s10584-011-0143-4

Immerzeel, W.W., Lutz, A.F., Andrade, M. et al. (2020) Importance and vulnerability of the world's water towers. *Nature 577*, 364–369 https://doi.org/10.1038/s41586-019-1822-y

Intergovernmental Panel on Climate Change (2019) IPCC Special Report on the Ocean and Cryosphere in a Changing Climate https://www.ipcc.ch/report/srocc/

Intsiful, A., & Ambinakudige, S. (2020). Glacier Cover Change Assessment of the Columbia Icefield in the Canadian Rocky Mountains, Canada (1985–2018). *Geosciences*, *11*(1), 19. https://doi.org/10.3390/geosciences11010019

Jarvis, A., Reuter, H. I., Nelson, A., & Guevara, E. (2008). Hole-filled shuttle radar topography mission (SRTM) for the globe Version 4. *Consultative Group on International Agricultural Research-Consortium for Spatial Information (CGIAR-CSI), Washington, DC Available from https://srtm.csi.cgiar.org (accessed Oct 2022)*.

Jóhannesson, T. (1997). The response of two Icelandic glaciers to climatic warming computed with a degree-day glacier mass-balance model coupled to a dynamic glacier model. *Journal of Glaciology, 43(144)*, 321–327. https://doi.org/10.3189/s0022143000003270

Jóhannesson, T., Sigurdsson, O., Laumann, T., & Kennett, M. (1995). Degree-day glacier mass-balance modeling with applications to glaciers in Iceland, Norway and Greenland. *Journal of Glaciology, 41(138)*, 345–358. https://doi.org/10.3189/s0022143000016221

Khadka, M., Kayastha, R. B., & Kayastha, R. (2020). Future projection of cryospheric and hydrologic regimes in Koshi River basin, Central Himalaya, using coupled glacier dynamics and glacio-hydrological models. *Journal of Glaciology*, *66*(259), 831–845. https://doi.org/10.1017/jog.2020.51

Klein Goldewijk, K., Beusen, A., Van Drecht, G., & De Vos, M. (2011). The HYDE 3.1 spatially explicit database of human-induced global land-use change over the past 12,000 years. *Global Ecology and Biogeography*, *20*(1), 73–86. https://doi.org/10.1111/j.1466-8238.2010.00587.x

Kraaijenbrink, P. D. A., Bierkens, M. F. P., Lutz, A. F., & Immerzeel, W. W. (2017). Impact of a global temperature rise of 1.5 degrees Celsius on Asia's glaciers. *Nature, 549(7671),* 257–260. https://doi.org/10.1038/nature23878

Krause, P., Boyle, D. P., & Bäse, F. (2005). Comparison of different efficiency criteria for hydrological model assessment. *Advances in Geosciences*, *5*, 89–97. https://doi.org/10.5194/adgeo-5-89-2005

Li, Z., Yang, Y., Kan, G., & Hong, Y. (2018). Study on the applicability of the Hargreaves potential evapotranspiration estimation method in CREST distributed hydrological model (version 3.0) applications. *Water (Switzerland)*, *10*(12), 1–15. https://doi.org/10.3390/w10121882

Lute, A. C., & Abatzoglou, J. T. (2021). Best practices for estimating near-surface air temperature lapse rates. *International Journal of Climatology*, *41*(S1), E110–E125. https://doi.org/10.1002/JOC.6668

Marshall, S. J., & Miller, K. (2020). *Seasonal and Interannual Variability of Melt-Season Albedo at Haig Glacier, Canadian Rocky Mountains*. https://doi.org/10.5194/tc-2020-87

Marshall, S., & White, E. (2010). *Alberta Glacier Inventory and Ice Volume Estimation*. Report for the Alberta Water Research Institute, 55 pp. https://albertawater.com/dmdocuments/01_2010_12_Alberta_Glacier_Inventory_and_Ice_Volume_Estimation_Marshall_et_al%20(15).pdf

Marshall, S. J., White, E. C., Demuth, M. N., Bolch, T., Wheate, R., Menounos, B., Beedle, M. J., & Shea, J. M. (2011). Glacier Water Resources on the Eastern Slopes of the Canadian Rocky Mountains. *Canadian Water Resources Journal, 36(2),* 109–134. https://doi.org/10.4296/cwrj3602823

Martinec, J., Rango, A., & Roberts, R. (2008). Snowmelt runoff model (SRM) user's manual. *Agricultural Experiment Station Special Report 100*, 180. https://doi.org/10.3882/j.issn.1674-2370.2010.03.003

Masud, B., Cui, Q., Ammar, M. E., Bonsal, B. R., Islam, Z., & Faramarzi, M. (2021). Means and Extremes: Evaluation of a CMIP6 Multi-Model Ensemble in Reproducing Historical Climate Characteristics across Alberta, Canada. *Water 2021, Vol. 13, Page 737*, *13*(5), 737. https://doi.org/10.3390/W13050737

McKay, M. D., Beckman, R. J., & . Conover, W. J (1979) Comparison of Three Methods for Selecting Values of Input Variables in the Analysis of Output from a Computer Code, *Technometrics*, 21:2, 239-245https://doi.org/10.1080/00401706.1979.10489755

Milner, A. M., Brown, L. E., & Hannah, D. M. (2009). Hydroecological response of river systems to shrinking glaciers. *Process*, *23*, 62–77. https://doi.org/10.1002/hyp.7197

Ohmura, A. (2001). Physical basis for the temperature-based melt-index method. *Journal of Applied Meteorology, 40(4)*, 753–761. https://doi.org/10.1175/1520-0450(2001)040<0753:PBFTTB>2.0.CO;2

Omani, N., Srinivasan, R., Smith, P.K. & Karthikeyan, R. (2017) Glacier mass-balance simulation using SWAT distributed snow algorithm, Hydrological Sciences Journal, 62:4, 546-560, https://doi.org/10.1080/02626667.2016.1162907

Payne, J.T., Wood, A.W., Hamlet, A.F. et al. (2004) Mitigating the Effects of Climate Change on the Water Resources of the Columbia River Basin. *Climatic Change 62,* 233–256. https://doi.org/10.1023/B:CLIM.0000013694.18154.d6

Pellicciotti, F., Brock, B., Strasser, U., Burlando, P., Funk, M., & Corripio, J. (2005). An enhanced temperature-index glacier melt model including the shortwave radiation balance: development and testing for Haut Glacier d'Arolla, Switzerland. *Journal of Glaciology, 51(175)*, 573–587. https://doi.org/10.3189/172756505781829124

Peters, D. L., Atkinson, D., Monk, W. A., Tenenbaum, D. E., & Baird, D. J. (2013). A multi- scale hydroclimatic analysis of runoff generation in the Athabasca River, western Canada. *Hydrological Processes, 27(13)*, 1915–1934. https://doi.org/10.1002/hyp.9699

Pfeffer, W. T., Arendt, A. A., Bliss, A., Bolch, T., Graham, J., Gardner, A. S., Hagen, J.-O., Hock, R., Kaser, G., Kienholz, C., Miles, E. S., Moholdt, G., Mo¨lg, N., Mo¨lg, M., Paul, F., Radic´, V., Radic´, R., Rastner, P., Raup, B. H., … Consortium, R. (2017). *The Randolph Glacier Inventory: a globally complete inventory of glaciers*. https://doi.org/10.3189/2014JoG13J176

Quick, M. C., & Pipes, A. (1977). U.b.c. watershed model. *Hydrological Sciences Bulletin*, *22*(1), 153–161. https://doi.org/10.1080/02626667709491701

Radić, V., Hock, R., & Oerlemans, J. (2007). Volume-area scaling vs flowline modeling in glacier volume projections. *Annals of Glaciology*, *46*, 234–240. https://doi.org/10.3189/172756407782871288

Ragettli, S., & Pellicciotti, F. (2012). Calibration of a physically based, spatially distributed hydrological model in a glacierized basin: On the use of knowledge from glaciometeorological processes to constrain model parameters. *Water Resources Research*, *48*(3). https://doi.org/10.1029/2011WR010559

Rokaya, P., Peters, D. L., Elshamy, M., Budhathoki, S., & Lindenschmidt, K. (2020). Impacts of future climate on the hydrology of a northern headwaters basin and its implications for a downstream deltaic ecosystem. *Hydrological Processes*, *34*(7), 1630–1646. https://doi.org/10.1002/hyp.13687

Sao, D., Kato, T., Tu, L. H., Thouk, P., Fitriyah, A., & Oeurng, C. (2020). Evaluation of different objective functions used in the sufi-2 calibration process of swat-cup on water balance analysis: A case study of the pursat river basin, cambodia. *Water (Switzerland)*, *12*(10), 1–22. https://doi.org/10.3390/w12102901

Schaefli, B., & Huss, M. (2011). Integrating point glacier mass-balance observations into hydrologic model identification. *Hydrology and Earth System Sciences*, *15*(4), 1227–1241. https://doi.org/10.5194/HESS-15-1227-2011

Shea, J. M., Immerzeel, W. W., Wagnon, P., Vincent, C., & Bajracharya, S. (2015). Modeling glacier change in the Everest region, Nepal Himalaya. *Cryosphere, 9(3),* 1105–1128. https://doi.org/10.5194/tc-9-1105-2015

Shea, J. M., Moore, R. D., & Stahl, K. (2009). Derivation of melt factors from glacier mass-balance records in western Canada. *Journal of Glaciology*, *55*(189), 123–130. https://doi.org/10.3189/002214309788608886

Silwal, G., Ammar, M.E., Thapa, A., Bonsal, B., Faramarzi, M. (2023), Response of glacier melt modelling parameters to time, space, and model complexity: examples from eastern slopes of Canadian Rocky Mountains. *Science of the Total Environmnet*, In review.

Stahl, K., Moore, R. D., Shea, J. M., Hutchinson, D., & Cannon, A. J. (2008). Coupled modeling of glacier and streamflow response to future climate scenarios. *Water Resources Research, 44(2).* https://doi.org/10.1029/2007WR005956

Todd, W., M., Brooks, E. S., McCool, D. K., King, L. G., Molnau, M., & Boll, J. (2005). Process-based snowmelt modeling: does it require more input data than temperature-index modeling? *Journal of Hydrology*, *300*(1–4), 65–75. https://doi.org/10.1016/J.JHYDROL.2004.05.002

Tsai, V. C., & Ruan, X. (2018). A simple physics-based improvement to the positive degree day model. Journal of Glaciology, 64(246), 661–668. https://doi.org/10.1017/jog.2018.55

Viviroli, D., Dürr, H. H., Messerli, B., Meybeck, M. & Weingartner, R. (2007). Mountains of the world, water towers for humanity: typology, mapping, and global significance. *Water Resources Research 43*, 1–13

Walter, M. T., Brooks, E. S., Mccool, D. K., King, L. G., Molnau, M., & Boll, J. (n.d.). Process-based snowmelt modeling: does it require more input data than temperature-index modeling? https://doi.org/10.1016/j.jhydrol.2004.05.002

Wortmann, M., Bolch, T., Su, B., & Krysanova, V. (2019). An efficient representation of glacier dynamics in a semi-distributed hydrological model to bridge glacier and river catchment scales. *Journal of Hydrology*, *573*, 136–152. https://doi.org/10.1016/J.JHYDROL.2019.03.006

CHAPTER III – MANUSCRIPT 2

Assessment of the response of mountain glaciers to climate change based on their size and elevation using CMIP6 climate model data and scenarios

Amanda J. Kotila[1], Edward Bam[1], Andrew B.G. Bush[2], Monireh Faramarzi[1]

[1] Watershed Science & Modelling Laboratory, Department of Earth and Atmospheric Sciences, Faculty of Science, University of Alberta, Edmonton, AB T6G 2R3, Canada

[2] Department of Earth and Atmospheric Sciences, Faculty of Science, University of Alberta, Edmonton

3.1 Abstract

While they are important sources of freshwater, mountain glaciers are responsive and vulnerable to changes in climate. Modeling can provide insight to potential future changes, but regional-scale predictions can be difficult where limited input data and high spatiotemporal variability can lead to high uncertainty in model results. We aim to explore potential future glacier behaviour by taking into account the uncertainty arising from series of predictive models including glacier melt, mass balance, evolution simulators (CGME) and global climate models (GCMs), as well as future shared socioeconomic scenarios (SSPs).

We evaluate glacier melt runoff and area-volume change simulations by applying a modeling framework that couples empirical melt, surface mass balance, and spline-based volume-area scaling models. Our calibrated-validated CGME is forced using projected climate data from four GCMs of the Coupled Model Intercomparison Project 6 (CMIP6) series, and two SSP scenarios (SSP126 and SSP585) for the 258 glaciers in the Athabasca Watershed in Alberta, Canada for the period 1980-2100. The CGME model uncertainty is quantified by performing 100 sets of model input parameters from their maximum physically meaningful range and are used with a series of downscaled future climate data to force 100 simulations for each glacier. This allows us to explicitly quantify the uncertainty related to GCME model projections (via the 95 Percent Prediction Uncertainty, 95PPU) stemming from input parameterization, as well as those related to GCM model spread and different SSPs.

Glacier changes are assessed based on two categorization schemes, including glacier size class and their elevation class. The former is identified based on glacier initial area, and the later is defined based on glacier initial elevation. Our results based on size show that small-to-large glaciers are predicted to decrease in volume 75% (small)-80% (large), decrease in area 72%

(small)-78% (large), and discharge 70% (small)-80% (large) of their potential melt runoff in the first forty years of the simulation period (1980-2019, the historical period). Monthly predicted flow regimes not only indicate greatly reduced melt runoff as the century progresses, but also the loss of late spring and early fall melt runoff. Assessing potential changes by glacier initial elevation indicated similar trends, though low elevation glaciers are predicted to be especially responsive, discharging ~95% of their melt runoff during the historical period. Monthly melt runoff reflects similar trends to those found in the size analysis, though low elevation glaciers have the most extreme response. These assessments show the potential range of recent and imminent glacier retreat and related impacts on the glacio-hydrological regime.

Keywords: glacier model uncertainty, CMIP 6, SSP126, SSP585, glacier volume and area, glacier melt runoff

3.2 Introduction

Mountain glaciers have undergone many changes in the last century, including dramatic area loss (Tennant et al., 2012; Paul & Mölg, 2014) and increased contribution to streamflow (Comeau et al., 2009; Liu et al., 2022). Continued drastic changes in the current century is expected in alpine environments across the world (Clarke et al. 2015; Gan et al., 2015; Hock et al., 2019), affecting runoff regimes (Huss et al., 2010), surface water availability (Duethmann et al., 2016), and glacio-hydrological processes in mountainous catchments (Gan et al., 2015). The potential effects of changing hydrology, including water quality and quantity, has significant implications for downstream human and ecologic systems (Tolotti et al., 2020; Bash & Marshall, 2014; Jost et al., 2012). Much work has been done to project potential changes in glacier melt runoff, mass balance, and volume and area at the global, regional, and local levels (Radić et al., 2014; Clarke et al., 2015; Ambinakudige & Intsiful, 2022). However, characterizing future changes using model projections is difficult due to the inherent uncertainties stemming from spread in (i) global climate model projections, i.e., portrayals of elements of the atmosphere, ocean, land surface, and ice system that models emphasize on their process simulation, and their downscaling when applied for regional to local studies (Intergovernmental Panel on Climate Change 6th Assessment Report, IPCC AR6, 2019) ; (ii) emissions scenarios, e.g., Shared Socioeconomic Pathways, SSPs, which reflect the uncertainty of the future radiative forcing affecting the GCM projections (IPCC AR6); (iii) glacier model uncertainty, including process representation and downscaling procedures, model parameterization uncertainty, and uncertainty related to input data quality, including initial glacier geometry (Huss et al., 2014; Marzeion et al., 2020). Combined, these can lead to a range of possibilities, e.g. in glacier area loss (-100% to -63%) and the change in annual runoff (-57% to +25% relative to today) in projections through 2100 of glacierized catchments (Huss et al., 2014).

While many studies have been dedicated to characterizing the source and range of uncertainty to one of these factors (e.g., downscaling, Radić & Hock, 2006; initial ice geometry, Farinotti et al., 2009; and ice melt, Pellicciotti et al., 2005), others have attempted to quantify uncertainty ranges (Huss et al., 2014) or partition sources of uncertainty in projection ensembles (Hock et al., 2019; Marzeion et al., 2020). Framing future emissions scenarios as SSPs can assist in characterizing the uncertainty and assist in adaptation and mitigation assessments (O'Neill et al., 2017), given that the greatest source of uncertainty in 21st century projections of glacier mass, area, and runoff changes are reported to be emissions scenarios and climate models, especially later in the century (Huss et al., 2014; Marzeion et al., 2020). However, the share of uncertainty sources in impact assessments can vary spatially and temporally in regional studies. In an earlier study, Zaremehrjardy et al. (2021) showed that in hydrological and snow depth modeling of a snow dominated watershed, the uncertainty related to input data can dominate other sources of uncertainty such as the emission scenarios and GCMs depending on the ecoregion. Overall, assessment of the uncertainty range of future glacier melts can help society today to plan for a breadth of potential impacts in regions affected by glacier retreat (Milner et al., 2017). In this study, we aim to characterize the spectrum of possible glacier responses to future climate by forcing a CGME model not only with a GCM-SSP ensemble but also with a range of optimum values for each input parameter (i.e., model parameter uncertainty). Thus we can assess the range of uncertainty associated with model output uncertainty in addition to that from future climate.

This study focuses on regional glacio-hydrological changes and uses the Canadian Rocky Mountain (CRM) glaciers of Alberta, Canada as a study area. Numerous glacier melt and change studies have noted the potential vulnerability of CRM glaciers and water resources to rapid glacier retreat and deglaciation (e.g., Anderson & Radić, 2020; Bonsal et al., 2020; Clarke et al., 2015;

DeBeer et al. 2016; Ambinakudige & Intsiful, 2022). Regional glacier studies of observed change in ice cover extent (Marshall et al., 2011), glacier area (Moore et al., 2009), and modelled estimates of glacier melt and streamflow contribution (Bash & Marshall, 2014; Comeau et al., 2009) have shown that glacial discharge at present contributes between 39 – 64% of streamflow in the summer season and glacier loss during the past decades has been affecting downstream users and ecosystems (Payne et al., 2004). Furthermore, the projected deglaciation of western Canada (by Clarke et al., 2015) shows that by 2100, the volume of glacier ice in western Canada will shrink by 70 $\pm$ 10% relative to 2005 levels. Similarly, the projected maximum rate of ice volume loss, corresponding to peak input of deglacial meltwater to streams and rivers, will occur around 2020 and 2040 (Clarke et al., 2015). In some glacierized basins, streamflow is estimated to decrease by 40% by 2050 and changes in monthly discharge regimes are expected, especially after 2070 (Chernos et al., 2020). The potential implications of these changes in glacial area and volume are envisaged to result in the decline of water supply for aquatic ecosystem function, agriculture, forestry, alpine tourism, and quality in the region (Clarke et al., 2015). While this is important information about mountain glacier behaviour throughout the 21st century, the uncertainty in projected regional glacier behaviour can be different due to heterogeneity in intial glacier characteristics. A major factor for determining mountain glacier behaviour is initial glacier area. It has been shown in historical observations (Paul & Mölg, 2014; Ambinakudige & Intsiful, 2022), in modeling studies (e..g Radić et al., 2007), and glacio-hydrological projections (Gan et al., 2015; Liu et al., 2022) that the runoff and area changes in relatively small glaciers are drastically different to relatively larger glaciers in the same region. They have been found to be more sensitive to the various emissions scenarios (Gan et al., 2015) leading to increased uncertainty (Duethmann et al., 2016). Another characteristic that determines how a glacier has and may continue to change is

elevation. The empirical, data driven, and modeling studies (e.g. Tennant et al., 2012; Huss et al., 2014; Gan et al., 2015; Perroud et al., 2019) have shown that a glacier's elevation greatly influences the changes in its melt runoff, area/volume change, and mass balance. A glacier at high elevation responds differently to the regional changes in climate than a similar glacier at lower elevation. These studies either provided average estimates of projected glacier melt contribution to streamflow and projected glacier area change at the catchment scale (Liu et al., 2022; Gan et al., 2015) or characterized projected glacier volume-area change based on individual sample glaciers of various sizes (Radić et al., 2007) or projected mass balance of sample glacier based on elevation (Perroud et al., 2019). Of these studies, Duethmann et al. (2016) presented the most uncertainty analysis and 5-95 percentile ensemble spread estimates at the catchment scale, but did not explore glacial regimes based on size or elevation. We aim to explore regional projections of glacier melt runoff, volume and area change. To account for glacier behaviour due to differences in size and in initial elevation at a large regional scale, we organize our study glaciers into size classes and elevation classes and evaluating potential changes using these classifications. We seek to characterize a range of potential glacio-hydrological futures in the region by characterizing uncertainty based on climate model ensemble spread, model parametrization, and size and elevation class.

In addition, projections by earlier studies were centred on application of CMIP5 models and Representative Concentration Pathways (IPCC, 2007). This study will explore regional changes in glacier runoff, area, and volume in response to the future climate models and radiative forcing presented in CMIP6 (IPCC, 2019). The CMIP6 provides the means to simulate climate change scenarios from the state-of-the-art GCMs which are now included in the 6th assessment report (AR6) of the IPCC (Eyring et al., 2016; Masud et al., 2021). A major difference between

CMIP5 and CMIP6 is the set of future scenarios used to project climate evolution. The CMIP6 offers scenarios based on socioeconomic trajectories (i.e., Shared Socioeconomic Pathways or SSPs), which work in harmony with the Representative Concentration Pathways (RCP) from CMIP5. The development of CMIP6 helps overcome and improve the limitations identified in CMIP5, namely identifying and interpreting systematic errors in simulations, improving the estimation of radiative forcing, identifying the response of climate to aerosol forcing, and improving the representation of impacts of land use changes on climate (Eyring et al., 2016; Masud et al., 2021; Voldoire et al., 2019). Recent climate change studies in Canada which employed CMIP6 data (Masud et al., 2021; Papalexiou et al., 2019; Voldoire et al., 2019) were focused on evaluating the performance of CMIP6 in models to reproduce the historical simulations, mean and extreme climate characteristics and drought duration and severity at local scales. We utilize four GCMs of CMPI6 series and two most extreme SSPs (i.e., SSP126, which assumes the least warming effects, and SSP585, which representes the most warming effects due to socioeconomic developments) to project the ranges of potential glacier behaviour based on the latest climate scenarios and models, which will be useful for adaptive planning and mitigation (Bonsal et al., 2020; Hindshaw et al., 2011; Wheater & Gober, 2013).

The hydro-glaciological model used in this study is a calibrated, validated CGME model which quantifies the prediction uncertainty range (Kotila et al., in review). It is composed of three modules, which calculate daily melt runoff from the glacier, daily surface mass balance (SMB) of the glacier, and the annual changes in glacier surface area, depth, and volume in response to the change in mass. The coupling between these sections of the model allows for refined modeling of the long-term feedback between SMB and changes in glacier geometry such as length, area, and ice thickness (Kraainjenbrink et al., 2017) and for projections of glacier response to climate

change. This approach enables analysis of not only mass loss due to volume-area dynamics but also changes in the discharge regime downstream (Huss & Hock, 2015) and is appropriate at the basin or regional scale (Immerzeel et al., 2012) and multi-decade to multi-century timescales (Radić et al., 2007). In addition to the coupled glacier mass balance dynamic evolution components, the model also uses an elevation-band approach. Other studies, such as that by Huss and Hock (2015) have used elevation bands when doing temperature-based melt modeling. The elevation-band approach delineates each glacier into bands of equal mean elevation based on glacier size and area. The daily melt runoff, SMB, and volume-area changes are simulated for each band individually, allowing for a more refined model of the entire glacier's mass flux and geometry changes through time. Using this model, we can project not only the quantity and timing of glacier melt runoff but also corresponding changes in glacier volume, area, and ice thickness. In addition, the model can be forced using a range of values for each model parameter (which includes meteorological, glacial, and temperature-index parameters). In this study, we forced the projections with 100 parameter sets, sampled from the maximum physically meaningful range for each parameter (Kotila et al., in review) using Latin Hypercube Sampling (LHS, Mckay et al., 1979). This approach allows quantification of model output uncertainty using 95 Percent Prediction Uncertainty (95PPU). 95PPU predicts an uncertainty band calculated at the 2.5% and 97.5% levels of the cumulative distribution of model output in response to parameter uncertainty (Abbaspour et al., 2007), instead of a single modelled value reponse to a single parameter. Kotila et al. (in review) optimized the parameter ranges for this model in this region using historical observed glacier melt runoff, ensuring bracketing most of the data within the 95PPU while seeking the smallest possible uncertainty band. By applying this parameterization in this study, we seek to

keep the uncertainty band due to model parameterization narrow while still exploring the possible range of predictions in glacier behaviour and avoiding a single value for each input parameter.

The overarching goal of this study is to characterize mountain glacier dynamics based on their size and elevation and by quantifying the range of uncertainty arising from various sources. We use a coupled glacier melt, mass balance, evolution modeling framework to evaluate the changes in the past (1980-2019) and future (2020-2100) years using projections from CGME model, four GCMs of the CMIP6, under two SSP scenarios. The specific objectives in this study are as follows:

(i) Characterize uncertainty due to both projected future climate uncertainty and predicted model uncertainty for the projected glacier dynamics (changes in melt runoff, volume, and area.)

(ii) Compare the behaviour and associated uncertainty of three populations of glaciers ("small", "medium", and "large") classified based on initial surface area.

(iii) Compare the behaviour and associated uncertainty of three populations of glaciers ("low", "medium", and "high") classified based on initial median elevation.

Our model is applied to the western boundary of the Canadian Rocky Mountains (CRM) at the upstream of the Athabasca River basin (ARB) that drains melt water from 258 glaciers. The region is characterized by heterogeneous hydro-climate and geospatial conditions, as well as a diverse range of glacier sizes (ranging from approximately 0.01 to 29.96 km^2) and glacier elevations, ranging from a median elevation of approximately 2050 to 3300 m.a.s.l. This glacio-hydrological heterogeneity, as well as the ARB being an important catchment to downstream ecosystems and users (Payne et al., 2004; Rokaya et al., 2020) altogether makes the upper ARB a suitable study region for examining our study objectives.

3.3 Material and methods

3.3.1 Study Area

The province of Alberta in western Canada covers about 661,000 km² and extends from 49° N –60° N and 110° W–120° W along its widest extent. Elevation ranges from 152m at Slave River in the northeast to 3747 m at Mount Columbia in the Canadian Rocky Mountains along the southwest border of the province. Seventeen river basins intersect Alberta, five of which are glacierized (the Athabasca, Bow, North Saskatchewan, Peace, and Red Deer watersheds). Six hundred sixty-eight glaciers lie at elevations from 2,200-3,500m (approximately within the region from 117-120°W and 52-54°N; Pfeffer et al., 2017). Most of Alberta lies leeward of the Rocky Mountains, and thus has a semi-arid continental climate with 350 – 500 mm of average annual precipitation (Mwale et al., 2009) and a mean annual temperature ranging from 3.6 to 4.4 °C (with a winter temperature typically varying between −25.1 and −9.6 °C, and a summer temperature between 8.7 and 18.5 °C; Jiang et al., 2015). At higher elevations (above 1500m), annual average precipitation can be 600 mm or more (Mwale et al., 2009) due to orographic precipitation and average daily temperatures of about -11°C in January, 11°C in July and 0°C at these elevations (30-year averages, Environment and Climate Change Canada, 2022).

There are 258 glaciers in our study area, the Athabasca river basin,. They lie on the eastern slope of the CRM. The Athabasca Glacier (part of the Columbia Icefield) feeds one of the main tributaries in the Athabasca River basin (which were used for calibration and validation of the glacier model; Kotila et al., in review); there are other tributaries fed by smaller mountain glaciers present in the upper Athabasca region which are also affected by the decrease in their extent. Negative changes in glacier extent have been reported for other glaciers in the region, including

other portions of the Columbia Icefield (Clarke et al., 2013; Intsiful & Ambinakudige, 2020) that run off to the North Saskatchewan River basin (Alberta) and the Columbia River basin (British Columbia). To meet our study objectives, the glaciers were organized in two ways. Firstly, into three size classes after Chinn et al., 2001 (see section 3.4.1.) based on initial area. Then into three groups based on initial median elevation (see section 3.4.2.). Figure 1 shows the study area and the two classification schemes.

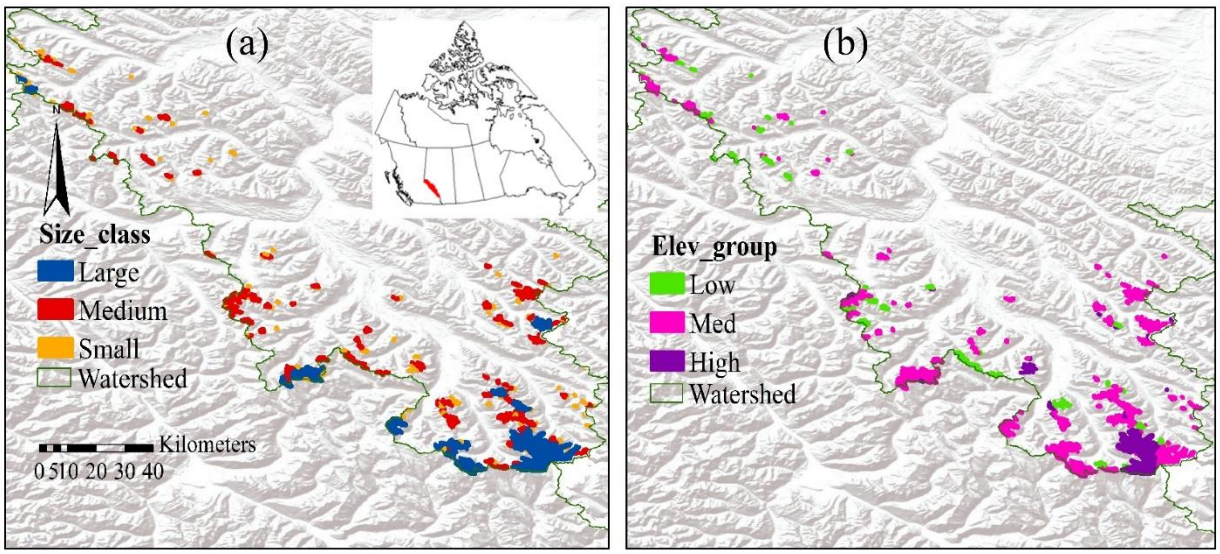

Figure 1. Study area, showing the upper (glacierized) end of the Athabasca river basin in western Alberta, Canada. Watershed boundaries and the 258 glaciers are highlighted (glacier boundaries are exaggerated to enhance visibility). Figure (a) shows the glaciers organized by size class, with small glaciers in yellow, medium glaciers in red, and large glaciers in blue. Figure (b) shows the glaciers organized by elevation group, with low elevation glaciers in green, medium glaciers in pink, and high glaciers in purple.

3.3.2. Glacier Model

The model used in this study is a coupled glacier mass balance dynamic evolution model (CGME). It is composed of three modules, which calculate daily melt runoff from the glacier (using a degree day factor temperature index model, TIM), daily and annual surface mass balance (SMB) of the glacier, and annual changes in glacier surface area, depth, and volume in response

to the change in mass. The model is driven with daily mean temperature (adjusted for elevation using an altitudinal lapse rate and a surface-of-glacier lapse rate) and precipitation (separated into rainfall and snowfall using a threshold temperature and adjusted for elevation using a precipitation gradient). Geometry changes are calculated annually using a smoothing spline predictor. For each module, the model also uses an elevation-band approach. The elevation-band approach delineates each glacier into bands of equal mean elevation based on glacier area. The daily melt runoff, SMB, and volume-area changes are simulated for each band individually, allowing for a more refined model of the entire glacier's mass flux and geometry changes through time. This is because it accounts for changes in temperature due to elevation (Hock, 2003; Ohmura, 2001) and changes in precipitation due to orographic lifting (Shea et al., 2015). A detailed description of the CGME can be found in Kotila et al. (in review) and Silwal et al. (2022).

The model uses 14 input parameters, including the meteorological modeling parameters that can vary spatiotemporally (e.g., temperature lapse rate and precipitation gradient), glacier characteristics (e.g., albedo of glacier ice, rheology parameter), and TIM parameters (e.g., degree day factor for ice, coefficient of ice melt). These input parameters fall within a physically meaningful range, described by previous empirical studies for glaciers with similar climate regimes (e.g., Gardner & Sharp, 2009; Shea et al., 2009; and Stahl et al., 2008); the optimization of the range for each parameter is described in Kotila et al. (in review). To examine the model prediction uncertainty for regional-scale studies (i.e., range of possible changes in the glacier dynamics across study region), a total of 100 samples from each parameter were created via the Latin Hypercube Sampling (LHS) technique (Krause et al., 2005). These 100 parameter sets were used to force the CGME model for each GCM and SSP to create projections for each glacier for the period 1980-2100.

3.3.3 Climate Model Selection

The climate data used in this study to force the model come from the simulations of the General Circulation Models (GCMs) included in the 6th assessment report (AR6) of the IPCC through the CMIP6 (Eyring et al., 2016). Four GCMs from CMIP 6 were used in this study: EC-Earth3 (Döscher et al., 2022), EC-Earth3-veg (Döscher et al., 2022), CNRM-CM6-1 (Voldoire et al., 2019), and MRI-ESM2.0 (Yukimoto et al., 2019). The climate input data for the model was previously downscaled for the province of Alberta using thin-plate spline interpolation and the 'ClimDown' R package (Cannon et al., 2016) after Masud et al. (2021). This is a statistical downscaling approach that utilizes multiple techniques (included in the 'ClimDown' R package, including climate imprint and quantile data mapping) and a high-resolution reference observed climate dataset. It calculates daily climate anomalies for the GCM dataset during the observed data set period, interpolates these to the observed dataset grid, calculates a monthly climatology, adds this to the climate imprint, and uses this imprint and the observations to perform a quantile mapping bias correction. This approach results in more accurate representation of event-scale spatial gradients, prevents the downscaled results from drifting away from the GCM's long-term trend, and can generate estimates of extreme events (Masud et al., 2021).

In this study, we force the CGME with the downscaled outputs for each of our 4 GCMs under two extreme scenarios: SSP 126 (low carbon intensity) and SSP 585 (high carbon intensity) for the period 1980-2100.

3.3.4. Data Description

Aside from the model input parameters, the model simulations also require geospatial and time series data. These data include observations of initial glacier geometry (i.e., DEM), initial surface area of the glaciers, initial ice thickness, aspect, hill slope, and a time series of climate for

the simulation period (i.e., daily maximum, minimum, mean, and difference between maximum and minimum temperature; daily precipitation; and daily incoming solar radiation at the glacier surface). The initial glacier surface area and aspect are used to initiate Module 2, which calculates the daily SMB. Initial ice thickness, slope, and extent (outline) for the glaciers are required as inputs for Module 3 to calculate initial volume (for the first year of the simulation); later years use the ice volume calculated at the end of the previous simulated year. Initial glacier outlines were obtained from the Randolph Glacier Inventory version 6 (RGI Consortium, Pfeffer et al., 2017). Glacier hypsometry was derived from a digital elevation model (DEM), with a grid resolution of 10 m ×10 m, sourced from maps Canada (http://maps.canada.ca/) based on Shuttle Radar Topography Mission (SRTM) DEM version 4 (Jarvis et al., 2008). Ice thickness used for model initiation in year 1 are from the estimates by Farinotti et al. (2019) who used glacier topography from SRTMv4, glacier outlines from RGIv6, and a combination of five ice thickness estimation models to provide an ensemble-based estimate for the ice thickness distribution (by inverting for local ice thickness using the principles of ice flow dynamics and the glacier's surface topography). Ice thickness data was resampled to 10m to match the DEM resolution. (Table of data sources in Appendix Table 2).

3.4 Results and discussion

3.4.1 Analysis by glacier size

Glaciers were categorized into three size classes ("small", "medium", and "large"), using their initial area extents from the RGI v6 (Pfeffer et al., 2017) and using the classification scheme developed by Chinn et al. (2001) for mountain glaciers, used by other mountain glacier inventories (e.g. Baumann et al., 2020). Using this categorization, small glaciers are those with an initial area

of 0.01- <0.32 km^2, medium glaciers are 0.32-2.56 km^2, and large glaciers are >2.56 km^2. In our study area 120 (46.51%) glaciers fell into the small category, 116 (44.96%) medium, and 22 (8.53%) large. Small glaciers had an initial area of 17.46 km^2 (which made up 5.78% of initial

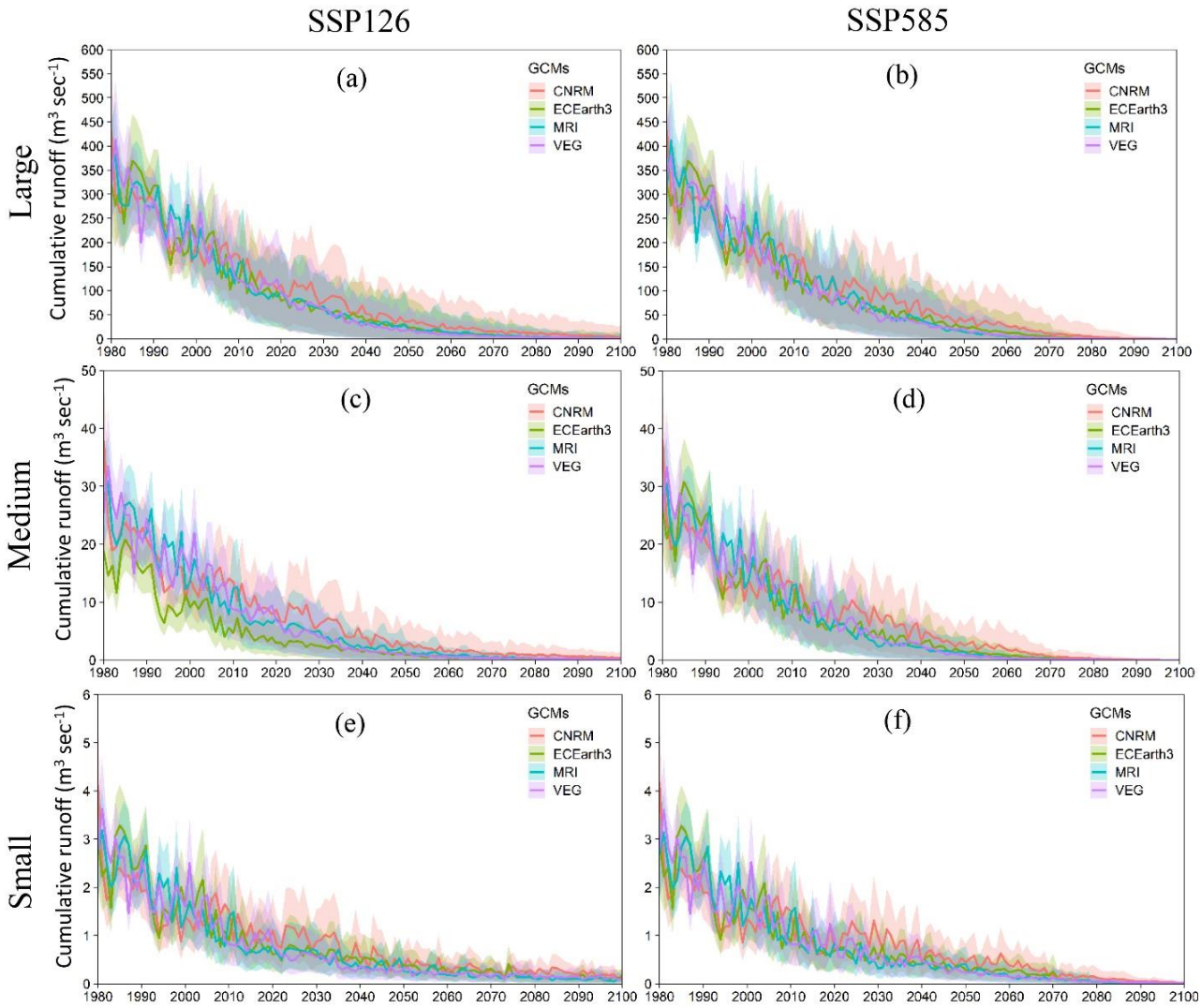

Figure 2. Multimodel ensemble projections of cumulative annual melt runoff for 1980-2100 for glaciers grouped by size. The coloured bands indicate the 95 percent prediction uncertainty (95PPU) resulting from CGME simulation under each of the GCM forcing. The single signals within each band represent median of CGME predictions (M95PPU). Figures (a), (c), and (e) show melt runoff under the SSP126 climate scenario, while figures (b), (d), and (f) show melt runoff under the SSP585 climate scenario.

glacier area coverage), medium glaciers covered 108.10 km^2 (35.81%), and large glaciers 176.32 km^2 (58.41%).

Daily melt runoff was accumulated to yearly melt runoff for each group of glaciers for each GCM and ninety-five percent prediction uncertainty (95PPU) performed on the 100 simulations for the period 1980-2100. Results reported in Table 1 are based on the median of the uncertainty range (M95PPU); annual cumulative average (ACA) is the yearly cumulative melt runoff averaged for the four GCMs. Table 1 presents ACA, summed for the whole period and for each sub-period ("historical", "near-future", and "far-future"). %ACA for the whole period (row 3) is calculated per sub-period; it is the percent of the ACA discharged each sub-period relative to the total ACA discharged over the whole period (per size class per SSP). %ACA relative to normal (row 7) is calculated per sub-period; it is the percent of ACA discharged in the near-future or far-future relative to the total ACA discharged during the historical period. The historical period is simulated M95PPU for the period 1980-2019; near-future is 2020-2059; and far-future is 2060-2100. The small size class had the smallest initial glacier area (5.78% of total initial glacier area); the medium class had in between (35.8%); and the large class had the largest (58.41%).

The multimodel ensemble projections of cumulative melt runoff indicate that glaciers in all size classes are expected to produce the greatest amount of melt runoff during the historical period (1980-2019), under both climate scenarios. Table 1 details the behaviour of each size class during each section of the simulation period, using the median of the uncertainty prediction (M95PPU) averaged across the four GCMs. Figure 3 indicates the monthly distribution and variability of cumulative melt runoff for each size class across the simulation periods under both SSPs. The largest amount of melt runoff is again expected during the historical period and runoff being greatly reduced in the far-future (2060-2100) period in both climate scenarios. It also shows

Table 1. Results of cumulative melt runoff predictions from four GCMs under two SSPs for glaciers grouped by size. Results reported below are for the median of the uncertainty range (M95PPU); annual cumulative average (ACA) is the yearly cumulative melt runoff averaged for the four GCMs and for the number of years in the sub-period.

		SSP126			SSP585			
	Units	Small	Medium	Large	Small	Medium	Large	Time period
Annual cumulative average (ACA), summed for whole period	m^3 sec^{-1}	94	716.6	10703.6	89.9	778.9	10313.6	Whole period (1980-2100)
ACA, summed for sub-period	m^3 sec^{-1}	66.2	577.5	8286.9	65.8	635	8271.1	Historical
		20.3	120.5	2064.8	20.4	134.9	1892.2	Near-future
		7.3	18.5	348.6	3.7	8.9	150.3	Far-future
%ACA summed for whole period	%	70.5	80.6	77.4	73.2	81.5	80.2	Historical
		21.7	16.8	19.3	22.7	17.3	18.3	Near-future
		7.8	2.6	3.3	4.1	1.2	1.5	Far-future
Summed ACA normalized by size class initial area	m^3 sec^{-1} per km^2	3.8	5.3	47	3.8	5.9	46.9	Historical
		1.2	1.1	11.7	1.2	1.2	10.7	Near-future
		0.4	0.2	2	0.2	0.1	0.9	Far-future
ACA	m^3 sec^{-1} yr^{-1}	1.69	14.8	212.5	1.7	16.3	212.1	Historical
		0.52	3.1	52.9	0.5	3.5	48.5	Near-future
		0.19	0.5	8.9	0.1	0.2	3.9	Far-future
ACA normalized by area	m^3 sec^{-1} yr^{-1} per km^2	0.097	0.137	1.205	0.097	0.151	1.203	Historical
		0.029	0.029	0.3	0.03	0.032	0.275	Near-future
		0.011	0.004	0.051	0.005	0.002	0.022	Far-future
%ACA relative to historical	%	100	100	100	100	100	100	Historical
		30.74	20.86	24.92	31.01	21.24	22.88	Near-future
		11.12	3.2	4.21	5.58	1.41	1.82	Far-future

the predicted evolution of monthly flows, with shoulder-season melt runoff (Apr-May, Sep-Oct) being substantially reduced or non-existent in the far-future period, especially under SSP585. It is to be noted that in this study a glaciological year is (accumulation and ablation periods) is not temporally defined, but daily simulations for each day in the period are performed. Thus, daily net accumulation or ablation (if any) is calculated, allowing for analysis of possible temporal trends. Details referred to in the following paragraphs can also be found in Table 1 (recall that these results

are the M95PPU averaged across the four GCMs and indicate the median of the predicted range of cumulative melt runoff). Overall, small glaciers are predicted to discharge the least

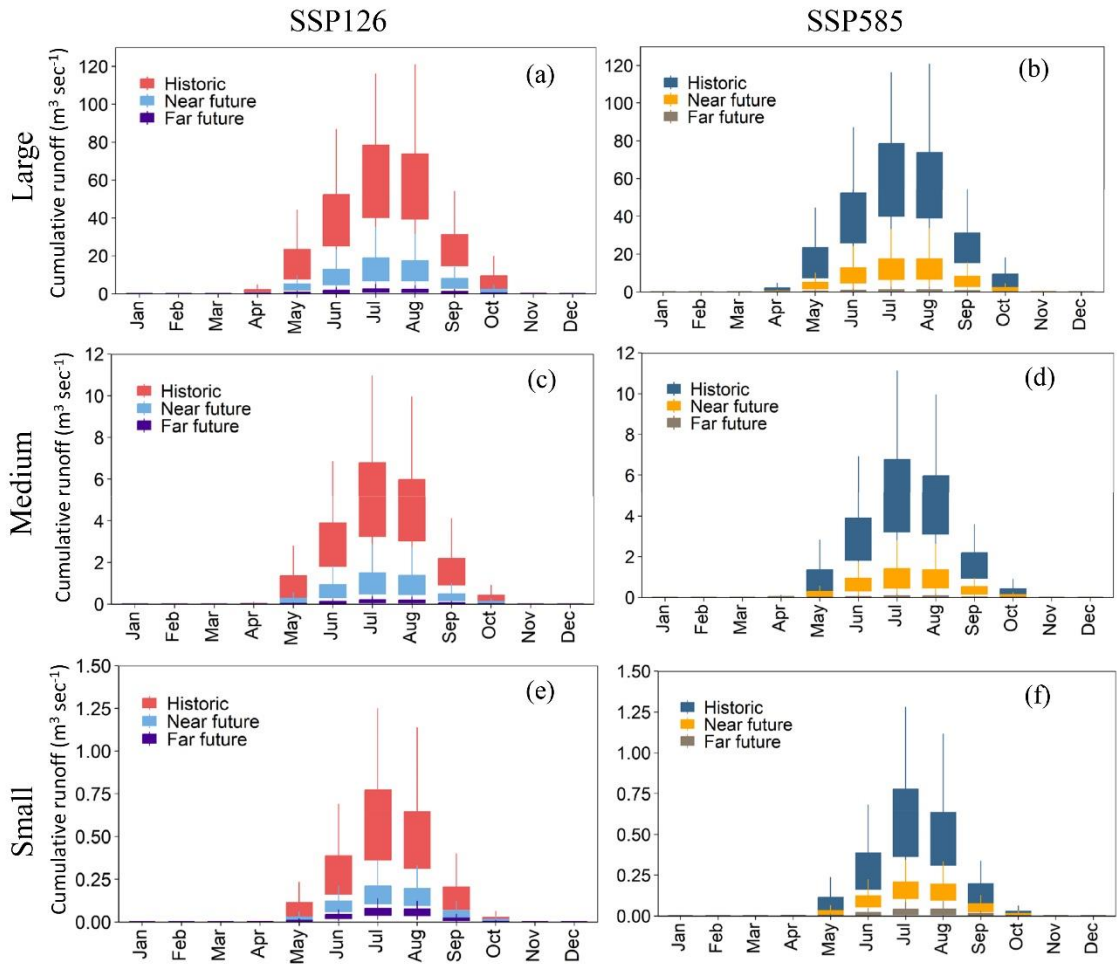

Figure 3. Historical (1980-2020) and multimodel ensemble projections of cumulative monthly runoff for near future (2020-2060) and far future (2060-2100) periods. The width of the box plot for historical periods is based on simulated runoff values for each month during 1980-2019. The width of the box plot for future periods is based on the monthly values for all years simulated from all GCMs in each period. In these figures only M95PPU were used, therefore the widths are not representing the CGME model parameter uncertainty.

melt runoff (94.0 m3 sec-^{1} and 89.9 m3 sec-^{1} under SSP126 and SSP585, respectively) over the full period (1980-2100), which is to be expected as they have the smallest initial area and volume. Of this total, small glaciers are predicted to discharge 71.9% during the historical period, 21.7%

during the near-future (under scenario SSP126; 22.7% under SSP 585), and 7.8% during the far-future (under SSP126; 4.1% under SSP 585). This indicates that a large portion of the glaciers' potential for melt runoff is discharged during the historical (1980-2019) period; relative to the discharge of the historical period, in the near-future they are predicted to discharge 30.86% of the melt runoff discharged during the historical period and in the far-future the prediction is 8.35% relative to historical. This is also indicated by the ACA normalized by initial glacier area for each period (shown in Table 1): 0.097 m^3 sec^{-1} yr^{-1} per km^2 during the historical; 0.029 m^3 sec^{-1} yr^{-1} per km^2 during the near-future 126 (and 0.030 for SSP585); and 0.011 m^3 sec^{-1} yr^{-1} per km^2 SSP 126 (0.005 SSP585) during the far-future. We expected quick meltdown of the small-sized glaciers, due to both their initial geometry, location, and the degree-day factor melt model approach (Huss et al., 2014). However, results may indicate that small glaciers will have the most gradual meltdown/discharge of melt runoff, with the lowest percentages of melt runoff throughout the period compared to the other glacier classes. Looking at the ACA normalized by area (Table 1), we see it is lower relative to the other, larger glaciers. This may be a function of the heterogeneity of small glaciers in the region, whose aspect, elevation, or proximity to larger glaciers may affect their microclimate and melt regimes. Another contributing factor may be GCM choice coupled with using M95PPU for analysis of the results. CNRM consistently predicts higher melt runoff (especially in the historical period) and greater 95PPU range (under both SSPs) than the other three GCMs, which produce relatively similar results. This notably affected the average M95PPU of all four GCMS (under both SSPs) and may have affected the predicted melt runoff, especially in the near-future and early far-future sub-periods, indicating a more sustained melt runoff regime than would have been indicated otherwise.

The general results are similar for the medium class glaciers (Table 1). They are predicted to discharge 716.6 m^3 sec^{-1} and 778.9 m^3 sec^{-1} of melt runoff under SSP126 and SSP585, respectively, over the full period (1980-2100). Of this total, medium class glaciers are predicted to discharge 81.1% during the historical period, 16.8% during the near-future, and 2.6% during the far-future (under scenario SSP126); it is predicted to be 17.3% and 1.2% respectively under SSP 585. Again, this indicates that the majority of the glaciers' potential for melt runoff will be discharged during the historical (1980-2019) period; in the near-future they are predicted to discharge 20.86% (SSP126; 21.24% for SSP585) of the melt runoff discharged during the historical period, and in the far-future the prediction is 3.20% for SSP126 (1.41% for SSP585) relative to historical. The ACA normalized by initial glacier area for each period reinforces this trend: during the historical (0.144 m^3 sec^{-1} yr^{-1} per km^2), 0.029 m^3 sec^{-1} yr^{-1} per km^2 under SSP 126 (0.032 under SSP585) during the near-future; and 0.004 m^3 sec^{-1} yr^{-1} per km^2 SSP 126 (0.002 SSP585) during the far-future.

Large glaciers exhibit similar behaviour (Figure 1, Table 1). The simulated M95PPU values indicate discharge of 10,703.6 m^3 sec^{-1} and 10,313.6 m^3 sec^{-1} of melt runoff under SSP126 and SSP585, respectively, over the full period (1980-2100). Of this total, large glaciers are predicted to discharge 78.8% during the historical period, 19.3% (SSP126; 18.3% for SSP585) during the near-future, and 3.3% (SSP126; 1.5% for SSP585) during the far-future. While again reflecting the majority of the glaciers' potential for melt runoff will be discharged during the historical (1980-2019) period, it also exhibits the expected resiliency of large glaciers due to their size; their loss rates are slightly lower and they are predicted to persist for slightly longer than smaller glaciers in the same basin. This is reinforced by the relative-to-historical period melt runoff; in the near-future they are predicted to discharge 23.90% relative to the melt runoff

discharged during the historical period, and in the far-future the projection is 4.21% for SSP126 (1.82% for SSP585) relative to the historical period. This higher-for-longer time melt runoff is highlighted by the ACA normalized values based on initial glacier area for each period: 1.204 m^3 sec^{-1} yr^{-1} per km^2 during the historical period, 0.300 m^3 sec^{-1} yr^{-1} per km^2 under SSP 126 (0.275 under SSP585) during the near-future period, and 0.051 m^3 sec^{-1} yr^{-1} per km^2 SSP under 126 (0.022 under SSP585) during the far-future period. This reflects the expected behaviour of large glaciers, whose large volume and mass allow for a more gradual and sustained change in predicted melt runoff (seen in observations of the region, Intsiful & Ambinakudige, 2020; and reflected in modeled mountain glaciers, e.g. Rounce et al., 2020). However, their melt regimes throughout the period but especially in the historical are similar to the other glacier size classes, with the highest amount of melt in the historical period. This was expected based on observed glacier retreat and melt runoff in the region (Bolch et al., 2010; Bawden et al., 2014) and modeled projections or melt runoff trends (Clarke et al., 2015; Chernos et al., 2020).

Comparing results between SSP126 and SSP585, both the percent of ACA for each sub-period relative to the ACA for the whole period and the normalized-by-area ACA for each sub-period are generally similar (for all size classes) in the historical period and the near-future period under both scenarios. For instance, it is 70.5% under SSP126 (73.2% under SSP585) for small glaciers, 80.6% under SSP126 (81.5% under SSP585) for medium glaciers, and 77.4% under SSP126 (80.2% under SSP585) for large glaciers during the historical period. During the near-future, it is 21.7% under SSP126 (22.7% under SSP585) for small glaciers, 16.7% under SSP126 (17.3% under SSP 585) for medium glaciers, and 19.3% under SSP126 (18.3% under SSP585) for large glaciers. However, in the far-future period there is a relatively greater difference between SSPs. For instance, it is 7.8% under SSP126 (4.1% under SS585) for small glaciers, 2.6% under

SSP126 (1.2% under SSP585) for medium glaciers, and 5.0% under SSP126 (2.6% under SSP585) for large glaciers. This is also evident looking at the normalized ACA; while similar in the historical and near-future sub-periods, in the far-future it is relatively different between the SSPs for all glacier sizes. It is 0.011 under SSP126 (0.005 under SSP585) for small glaciers, 0.004 under SSP126 (0.002 under SSP585) for medium glaciers, and 0.051 under SSP126 (0.022 under SSP585) for large glaciers (all values in m^3 sec^{-1} yr^{-1} per km^2). Both metrics indicate that, while the values of melt runoff in the far future are miniscule compared to those predicted in the historical and near-future periods, the difference between climate scenarios is striking. While both SSPs predict similar behaviour and amounts during 1980-2059, in the far-future (2060-2099) SSP585 consistently predicts melt runoff half that predicted by SSP126. This may indicate a sooner meltdown of glaciers with less far-future discharge under a SSP585-like climate scenario. Another factor may be downscaling techniques of the GCM ensemble and potential shifts in precipitation regime noted in this downscaled data. Khalili et al. (2021) found that in southwest Alberta projected precipitation anomalies under SSP585 project a decrease in precipitation in the mountainous regions compared to historical periods.

This is reinforced by looking at the predicted volume and area change. Recall that the model uses the annual mass balance to adjust glacier geometry, which is then the input to the subsequent simulated year. Figure 4 and Figure 5 show the area and volume change over time for each size class, under the SSP126 and SSP585 climate scenarios, respectively.

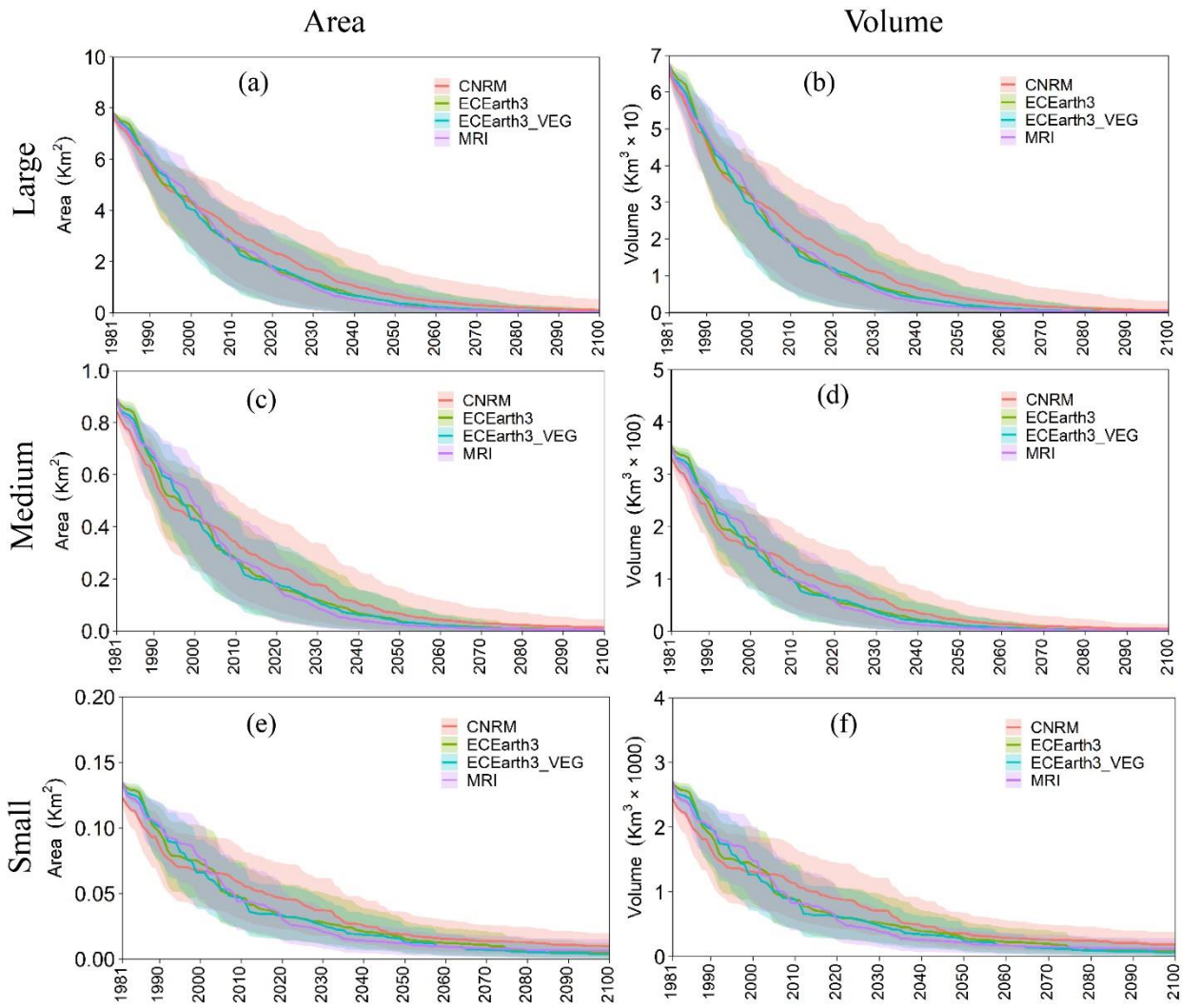

Figure 4. Multimodel ensemble projections of annual change in area and volume for 1980-2100 for glaciers grouped by size under SSP126. The coloured bands indicate the 95 percent prediction uncertainty (95PPU) resulting from CGME simulation under each of the GCM forcing. The single signals within each band represent median of CGME predictions (M95PPU). Panels (a), (c), and (e) show change in area, while panels (b), (d), and (f) show change in volume.

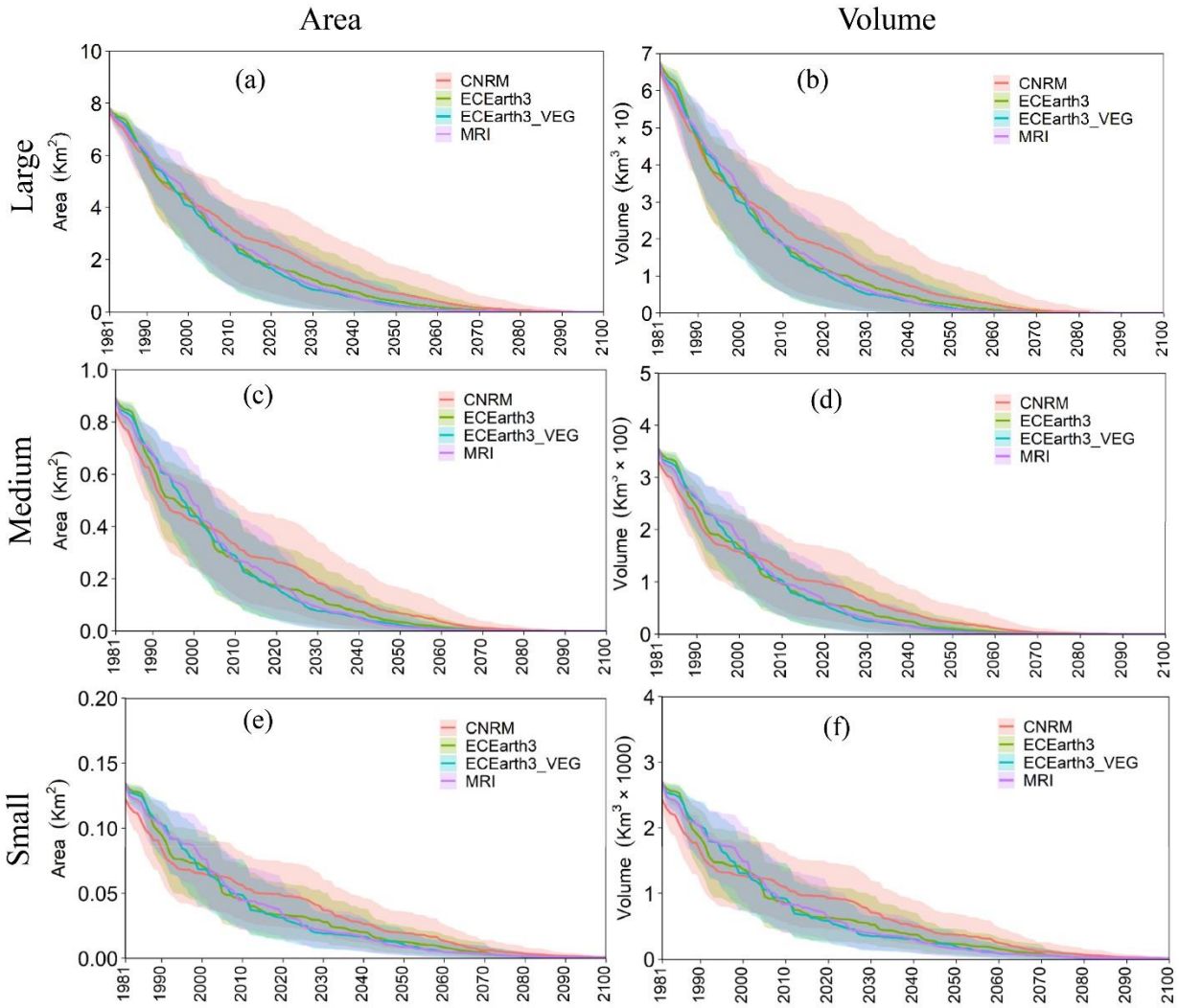

Figure 5. Multimodel ensemble projections of annual change in area and volume for 1980-2100 for glaciers grouped by size under SSP585. The coloured bands indicate the 95 percent prediction uncertainty (95PPU) resulting from CGME simulation under each of the GCM forcing. The single signals within each band represent median of CGME predictions (M95PPU). Panels (a), (c), and (e) show change in area, while panels (b), (d), and (f) show change in volume.

As was indicated by the melt runoff, all glacier size classes are predicted to decrease in both area and size rapidly during the historical (1980-2019) period under both SSP126 and SSP585. For small glaciers, 74.4% of the decrease of surface area occurs during the historical period, 18.4% during the near-future, and 4.1% during the far-future under SSP126 (21.1% and 5.4% respectively under SSP585.) Similar behaviours are indicated for the medium and large size classes of glaciers for their area and volume as reported in Table 2 below.

Table 2. Results of area and volume change predictions from four GCMs under two SSPs for glaciers grouped by size. Results reported below are based on M95PPU. Change in area (volume) is the difference in area (volume) over the period averaged for the four GCMs. Rate of change is the difference in area (volume) per number of years in the sub-period. Percent change of area (volume) indicate the percentage of change of that sub-period compared to change over the whole period. The historical period is simulated M95PPU for the 1980-2019, near-future is 2020-2059, and far-future is 2060-2100.

		SSP126			SSP126			
	Unit	Small	Medium	Large	Small	Medium	Large	Time period
Change of surcae area	km^2	-0.125	-0.869	-7.699	-0.131	-0.875	-7.742	Whole period
		-0.096	-0.685	-5.83	-0.094	-0.679	-5.797	Historical
		-0.023	-0.157	-1.559	-0.028	-0.171	-1.678	Near-future
		-0.005	-0.017	-0.205	-0.007	-0.015	-0.171	Far-future
Rate of change of surface area	$km^2\ yr^{-1}$	-0.001	-0.0073	-0.0642	-0.0011	-0.0073	-0.0645	Whole period
		-0.0024	-0.0171	-0.1458	-0.0024	-0.0169	-0.1449	Historical
		-0.0006	-0.0039	-0.0389	-0.0007	-0.0043	-0.0419	Near-future
		-0.0001	-0.0004	-0.0051	-0.0002	-0.0004	-0.0043	Far-future
Percent change in area relative to whole period	%	76.5	78.8	75.7	72.3	77.6	74.9	Historical
		18.4	18	20.2	21.1	19.6	21.7	Near-future
		4.1	1.9	2.7	5.4	1.7	2.2	Far-future
Percent change in area relative to historical period	%	100	100	100	100	100	100	Historical
		24.1	22.8	26.7	29.2	25.2	29	Near-future
		5.45	2.5	3.5	7.4	2.1	2.9	Far-future
Change of volume	km^3	-0.0025	-0.0346	-0.6658	-0.0026	-0.0347	-0.6678	Whole period
		-0.002	-0.0281	-0.5402	-0.0019	-0.0279	-0.5376	Historical
		-0.0004	-0.0055	-0.1064	-0.0005	-0.0061	-0.1143	Near-future
		-0.0001	-0.0005	-0.0116	-0.001	-0.0005	-0.0092	Far-future
Rate of change of volume	$km^3\ yr^{-1}$	-2.1 e-05	-0.0003	-0.0056	-2.2 e-05	-0.0003	-0.0056	Whole period
		-4.9 e-05	-0.0007	-0.0135	-4.8 e-05	-0.0007	-0.0134	Historical
		-1.1 e-05	-0.0001	-0.0027	-1.3 e-05	-0.0002	-0.0029	Near-future
		-2.4 e-06	-1.3 e-05	-0.0003	-3.2 e-06	-1.1 e-05	-0.0002	Far-future
Percent change in volume relative to whole period	%	77.8	81.3	81.3	73.8	80.2	80.5	Historical
		17.5	16	15.9	20.1	17.4	17.1	Near-future
		3.9	1.6	1.7	4.9	1.3	1.4	Far-future

Percent change in volume relative to historical period	%	100	100	100	100	100	100	Historical
		22.4	19.7	19.7	27.2	21.7	21.3	Near-future
		4.9	1.9	2.1	6.7	1.6	1.7	Far-future

Comparing glacier behaviour between SSP126 and SSP585, the most notable difference is in the rate of change in both area and volume during the near-future period. For glaciers in all three sizes classes, the rate of change in area and volume during the near-future period under SSP585 is increased compared to that under SSP126. There is a corresponding slight increase in the change in area/volume and percent change in area/volume during this period. While this may be expected for this climate scenario, this phenomenon may also indicate the slightly increased uncertainty under SSP585 as Table 2 is calculated using the M95PPU averaged from the four GCMS and indicated in Figures 4 and 5. As noted earlier, CNRM consistently predicts the highest Upper 95PPU for this study area using this model.

3.4.2 Analysis by glacier elevation

Glaciers were also categorized into three elevation classes ("low", "medium", and "high"), using their initial median elevation from Farinotti et al. (2019). Using this categorization, low elevation glaciers are those with an initial median elevation of 1933-2407 m.a.s.l., medium 2408-2880 m.a.s.l., and high 2881-3356 m.a.s.l. In our study area 53 (20.54%) glaciers fell into the low category, 167 (64.73%) medium, and 38 (14.73%) high. In terms of initial area coverage, low glaciers had an initial area of 28.03 km^2 (which made up 9.29% of initial glacier area coverage), medium glaciers covered 200.53 km^2 (66.43%), and high glaciers 73.32 km^2 (24.28%). Initial volumes were 0.99 km^3 for the low glaciers, 12.74 km^3 for the medium glaciers, and 6.05 km^3 for the high glaciers.

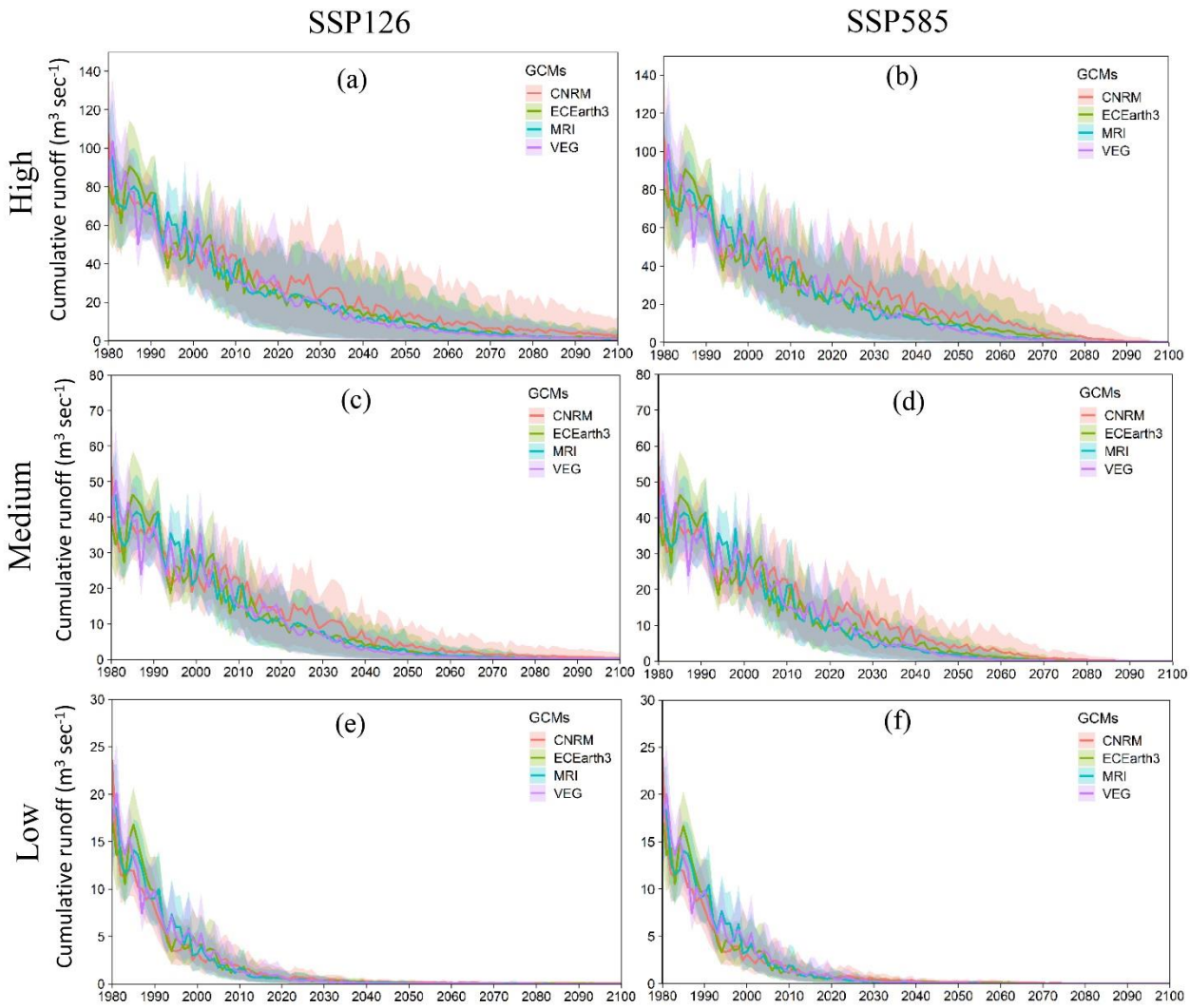

Figure 6. Multimodel ensemble projections of cumulative annual melt runoff for 1980-2100 for glaciers grouped by elevation. The coloured bands indicate the 95 percent prediction uncertainty (95PPU) resulting from CGME simulation under each of the GCM forcing. The single signals within each band represent median of CGME predictions (M95PPU). Figures (a), (c), and (e) show melt runoff under the SSP126 climate scenario, while figures (b), (d), and (f) show melt runoff under the SSP585 climate scenario.

Table 3. Results of cumulative melt runoff predictions from 4 GCMs under 2 SSPs for glaciers grouped by elevation. Results reported below are for the median of the uncertainty range (M95PPU); annual cumulative average (ACA) is the yearly cumulative melt runoff averaged for the 4 GCMs and for the number of years in the sub-period. The historical period is simulated M95PPU for the period 1980-2019; near-future is 2020-2059; and far-future is 2060-2100. The low elevation group had the smallest initial glacier area (9.29%); the medium group had the highest (66.43%); and the high group had in between (24.28%).

		SSP126			SSP585			
	Units	low	medium	high	low	medium	high	Time period
Annual cumulative average (ACA), summed for whole period	$m^3\ sec^{-1}$	236.4	1276.2	2815.5	234.5	1262	2744.8	Whole period (1980-2100)
ACA, summed for sub-period	$m^3\ sec^{-1}$	225.2	1040	2061.5	224.3	1036.2	2057.2	Historical
		9.4	212.7	612.2	9.4	213.8	615.9	Near-future
		1.8	23.3	141.8	0.8	12	71.6	Far-future
%ACA summed for whole period	%	95.3	81.5	73.2	95.6	82.1	74.9	Historical
		3.9	16.7	21.8	4	16.9	22.5	Near-future
		0.8	1.8	5	0.4	1	2.6	Far-future
summed ACA normalized by size class initial area	$m^3\ sec^{-1}$ per km^2	8	5.2	28.1	5.8	5.2	28.1	Historical
		0.3	1.1	8.3	0.2	1.1	8.4	Near-future
		0.1	0.1	1.9	0.02	0.06	1	Far-future
ACA	$m^3\ sec^{-1}\ yr^{-1}$	5.78	26.67	52.86	5.75	26.6	52.7	Historical
		0.24	5.45	16.7	0.24	5.5	15.8	Near-future
		0.05	0.6	3.64	0.05	0.3	1.8	Far-future
ACA normalized by area	$m^3\ sec^{-1}\ yr^{-1}$ per km^2	0.206	0.133	0.721	0.205	0.132	0.719	Historical
		0.009	0.027	0.214	0.009	0.027	0.215	Near-future
		0.002	0.003	0.05	0.001	0.002	0.025	Far-future
%ACA relative to historical	%	100	100	100	100	100	100	Historical
		4.17	20.45	29.7	4.19	20.6	29.94	Near-future
		0.79	2.24	6.88	0.36	1.16	3.48	Far-future

As before, daily melt runoff was accumulated to yearly melt runoff for each group of glaciers for each GCM and ninety-five percent prediction uncertainty (95PPU) was performed on the 100 simulations for the period 1980-2100. Results shown in Figure 6, reported in Table 3, and presented in the following paragraphs are based on the median of the uncertainty range (M95PPU).

The low elevation group had the smallest initial glacier area (9.29%), the medium group had the highest (66.43%), and the high group was in between (24.28%).

Low elevation glaciers are predicted to discharge the least melt runoff (236.4 m^3 sec^{-1} and 234.5 m^3 sec^{-1} under SSP126 and SSP585, respectively) over the full period (1980-2100), which is to be expected as they have the smallest initial area and volume. Of this total, low elevation glaciers are predicted to discharge 95.5% during the historical period, 3.9% (SSP126; 4.0% for SSP 585) during the near-future, and 0.6% (SSP126; 0.4% for SSP585) during the far-future. This indicates that the majority of the glaciers' potential for melt runoff will be discharged during the historical (1980-2019) period; relative to the discharge of the historical period, in the near-future they are predicted to discharge 4.17% (SSP126, 4.19% for SSP585) of the melt runoff discharged during the historical period and in the far-future the prediction is 0.79% for SSP126 (0.36% for SSP585) relative to historical. This is also indicated by the ACA normalized by initial glacier area for each period: 0.206 m^3 sec^{-1} yr^{-1} per km^2 SSP during the historical; 0.009 m^3 sec^{-1} yr^{-1} per km^2 under SSP126 (also 0.009 m^3 sec^{-1} yr^{-1} per km^2 under SSP585) during the near-future; and 0.002 m^3 sec^{-1} yr^{-1} per km^2 under SSP126 (0.001 m^3 sec^{-1} yr^{-1} per km^2 under SSP585) during the far-future.

The results are similar for the medium elevation glaciers, which covered the most initial area and volume. They are predicted to discharge 1276.2 m^3 sec^{-1} and 1262.0 m^3 sec^{-1} of melt runoff under SSP126 and SSP585, respectively, over the full period (1980-2100). Note that results are reported using M95PPU, so while SSP585 appears to predict lower discharge, this value indicates the increased uncertainty range under this climate scenario. Potential decreases in precipitation at higher elevations under SSP585 (Khalili et al., 2021, see section 3.4.1.) may also contribute to melt runoff for medium and high elevation glaciers as indicated in Table 2. Of this

total, medium elevation glaciers are predicted to discharge 81.8% during the historical period, 16.7% during the near-future, and 1.8% during the far-future (under scenario SSP126); it is predicted to be 16.9% and 1.0% respectively under SSP585. Again, this indicates that the majority of the glaciers' potential for melt runoff was discharged during the historical (1980-2019) period; in the near-future, 20.45% under SSP126 and 20.6% under SSP585 of the melt runoff discharged during the historical period; and in the far-future the prediction is 2.24% for SSP126 (1.16% for SSP585) The ACA normalized by initial glacier area for each period reinforces this trend: 0.132 m^3 sec^{-1} yr^{-1} per km^2 during the historical, 0.027 m^3 sec^{-1} yr^{-1} per km^2 for SSP126 (also 0.027 m^3 sec^{-1} yr^{-1} per km^2 for SSP585) during the near-future, and 0.003 m^3 sec^{-1} yr^{-1} per km^2 for SSP 126 (0.002 m^3 sec^{-1} yr^{-1} per km^2 for SSP585) during the far-future.

While the high elevation glaciers exhibit similar trends, the results are slightly different. Despite having the medium amount of initial glacier area and volume, their total ACA for both the whole period and during each sub-period is the highest of the three elevation groups. They are predicted to discharge 2815.5 m^3 sec^{-1} and 2744.8 m^3 sec^{-1} of melt runoff under SSP126 and SSP585, respectively, over the full period (1980-2100). Of this total, high elevation glaciers are predicted to discharge 74.1% during the historical period, 21.8% during the near-future, and 5.0% during the far-future (under scenario SSP126); it is predicted to be 74.9%, 22.5%, and 2.6% respectively under SSP585. While again reflecting the majority of the glaciers' potential for melt runoff will be discharged during the historical (1980-2019) period, it also exhibits the expected resiliency of high elevation glaciers due to their microclimate; their loss rates are slightly lower and they are predicted to persist for slightly longer than similar glaciers at lower elevations in the same basin. This is reinforced by the relative-to-historical period melt runoff; in the near-future they are predicted to discharge 29.70% (SSP126; 29.94% for SSP585) of the melt runoff

discharged during the historical period, and in the far-future the prediction is 6.08% for SSP126 (3.48% for SSP585) relative to historical. This higher-for-longer melt runoff is also shown by the ACA normalized by initial glacier area for each period: 0.720 m^3 sec^{-1} yr^{-1} per during the historical; 0.214 m^3 sec^{-1} yr^{-1} per km^2 SSP 126 (also 0.215 m^3 sec^{-1} yr^{-1} per km^2 for SSP585) during the near-future; and 0.050 m^3 sec^{-1} yr^{-1} per km^2 SSP 126 (0.025 m^3 sec^{-1} yr^{-1} per km^2 for SSP585) during the far-future. While the trends are reflective of the location and expected behaviour of high elevation glaciers, the high values may be due to using M95PPU for analysis of the results. The high elevation glaciers exhibit the highest 95PPU band (Upper 95PPU – Lower 95PPU) of the three groups throughout the whole period, but especially in the far-future (in both SSPs). Thus, these results may indicate increased uncertainty, especially in the far future, in the melt runoff regimes of high elevation glaciers. This may also be a remnant of GCM choice and forcing. Of the 4 GCMs used, CNRM consistently predicts higher melt runoff (especially in the historical period) and greater 95PPU range (under both SSPs) than the other 3 GCMs, which produce relatively similar results. This was especially evident for the high elevation glaciers, where the higher range, and higher M95PPU, notably affected the average M95PPU of all 4 GCMS (under both SSPs). This may reflect on the suitability of CNRM for projections in this region, especially at high elevations.

Comparing results between SSP126 and SSP585, both the percent of ACA for each sub-period relative to the ACA for the whole period and the normalized-by-area ACA for each sub-period are markedly similar (for all elevation groups) in the historical period and the near-future period under both scenarios. For instance, it is 95.5% for low elevation glaciers; 81.8% for medium elevation glaciers; and 74.0% for high elevation glaciers during the historical period. During the near-future, it is 3.9% SSP126/4.0% SSP585 for low elevation glaciers; 16.7% SSP126/16.9%

SSP585 for medium elevation glaciers; and 21.8% SSP126/22.50% SSP585 for high elevation glaciers. However, in the far-future period there is a greater difference between SSPs. For instance, it is 0.8% SSP126/0.4% SSP585 for low elevation glaciers; 1.8% SSP126/1.0% SSP585 for medium elevation glaciers; and 5.0% SSP126/2.6% SSP585 for high elevation glaciers. This is also evident looking at the normalized ACA for the far-future: it is 0.002 SSP126/0.001 SSP585 for low elevation glaciers; 0.003 SSP126/0.002 SSP585 for medium elevation glaciers; and 0.050 SSP126/0.025 SSP585 for high elevation glaciers (all values in m^3 sec^{-1} yr^{-1} per km^2). Both metrics indicate that, while the values of melt runoff in the far future are miniscule compared to those predicted in the historical and near-future periods, the difference between climate scenarios is striking. While both SSPs predict similar behaviour and amounts during 1980-2059, in the far-future (2060-2100) SSP585 consistently predicts melt runoff half that predicted by SSP126. It is expected that by the far-future, glacier volume has decreased substantially, leaving less ice available to melt. This has implications for future water resources in the region and reinforces the need for adaptation and mitigation strategies to be implemented in the coming decades.

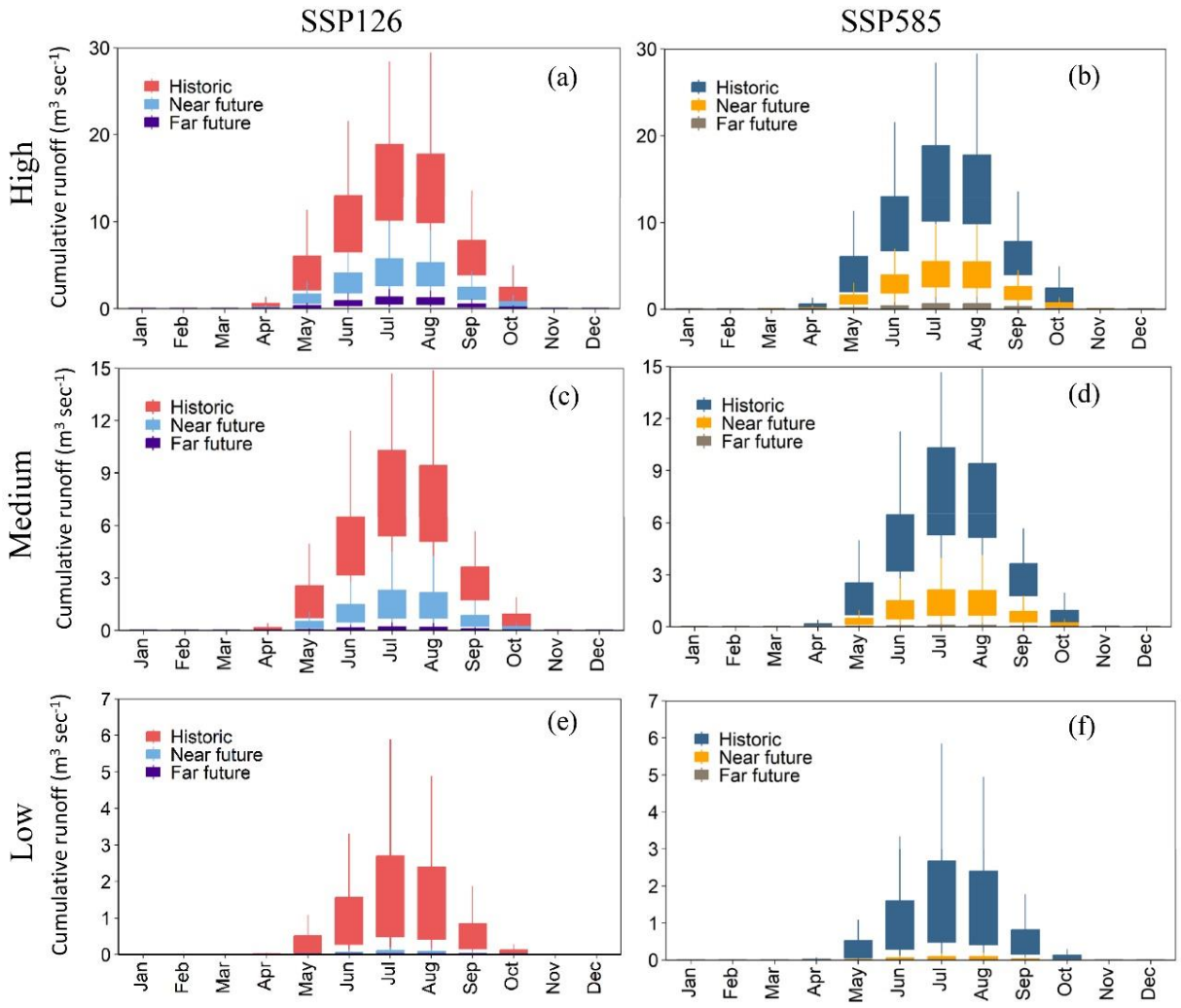

Figure 7. Historical (1980-2019) and multimodel ensemble projections of cumulative monthly runoff for the near future (2020-2059) and far future (2060-2100) periods. The width of the box plot for historical periods is based on simulated runoff values for each month during 1980-2019. The width of the box plot for future periods is based on the monthly values for all years simulated from all GCMs in each period. In these figures only M95PPU were used, therefore the widths are not representing the model parameter uncertainty.

The multimodel ensemble projections of cumulative melt runoff indicate that glaciers in all elevation groups are expected to produce the greatest amount of melt runoff during the historical period (1980-2019) under both climate scenarios. Figure 7 indicates the monthly distribution and variability of cumulative melt runoff for each elevation group across the simulation periods under

both SSPs. The largest amount of melt runoff is again expected during the historical period and runoff being greatly reduced in the far-future (2060-2100) period in both climate scenarios. Low elevation glaciers are predicted to have the majority of their melt during this period. It also shows the predicted evolution of monthly flows, with shoulder-season melt runoff (Apr-May, Sep-Oct) being substantially reduced or non-existent in the far-future period for all glaciers, especially under SSP585. For low elevation glaciers, shoulder-season flows are predicted to disappear after the historical period, with low Jun-Jul-Aug melt runoff in the near-future and indiscernible runoff in the far-future. Medium elevation glaciers are predicted to have indiscernible runoff in the far-future under SSP585, while low melt runoff is indicated to persist under SSP126.

3.5 Conclusions and future directions

In this study, we assess future changes in glacier melt runoff, ice area, and ice volume in mountain glaciers using a coupled glacier mass balance dynamic evolution model (CGME) and a range of input parameters. The potential range of changes for the period 1980-2100 in 258 glaciers in the Canadian Rocky Mountains were simulated by forcing the CGME using four GCMs from CMIP6, two climate scenarios (SSP126 and SSP585), and 100 parameter sets sampled from the maximum physically meaningful range for each parameter. Doing so allowed us to characterize the spectrum of possible glacier responses to future climate and assess the range of uncertainty associated with model output uncertainty due to parameterization. We also assess glacier behaviour based on glacier size and glacier elevation.

The simulations predict dramatic, rapid retreat for all glaciers regardless of the climate scenario. Assessing glacier change by size, all glaciers are predicted to behave similarly across the size classes and SSPs; using ninety-five percent prediction uncertainty (95PPU) and multimodel median averages it was determined that glaciers are predicted to decrease in volume 75-80%,

decrease in area 72-78%, and discharge 70-80% of their potential melt runoff in the first forty years of the simulation period (1980-2019, the historical period). Monthly predicted flow regimes not only indicate greatly reduced melt runoff as the century progresses, but also the loss of late spring and early fall melt runoff, predicting low flows during Jun-Jul-Aug by 2060-2100 (the far-future period). Assessing potential changes by glacier initial elevation indicated similar trends, though low elevation glaciers are predicted to be especially responsive, discharging ~95% of their melt runoff during the historical period. Monthly melt runoff reflects similar trends to those found during size analysis, though low elevation glaciers have the most extreme response, reducing their melt runoff to Jun-July-Aug during the near-future period (2020-2059) and discharging their melt runoff by the end of the near-future. These assessments quantitatively show that recent and imminent glacier retreat will have impacts on the glacio-hydrological regime.

By performing simulations with both an ensemble of CMIP6 GCMs and a range of parameterizations, we are able to characterize the uncertainty due to parameterization while assessing potential changes. Looking at predicted changes both as a result of glacier size and also glacier elevation allows us to characterize more potential glacio-hydrological regimes while constraining model uncertainty using 95PPU. While the results presented here refer to one specific catchment and the relative relevance of the individual components of uncertainty might vary for different climatological settings, the methodologies presented here related to ranges of parameters and characterizing uncertainty using 95PPU are applicable to a wide range of different glacier types and scenarios of future climate change. This approach could also be used to generate predictions of simulated melt runoff to be coupled with other hydrological models to explore the potential range of impacts of glacier melt runoff to a watershed. Future work will focus on translating the range of predictions into projections across several glacierized catchments.

3.6 Acknowledgments

Funding for this study was primarily provided by the Natural Sciences and Engineering Research Council of Canada Discovery Grant (Grant #RES0043463) and Campus Alberta Innovation Program Chair (Grant #RES0034497).

3.7 References

Abbaspour, K. C., Yang, J., Maximov, I., Siber, R., Bogner, K., Mieleitner, J., Zobrist, J., & Srinivasan, R. (2007). Modelling hydrology and water quality in the pre-alpine/alpine Thur watershed using SWAT. *Journal of Hydrology*, *333*(2–4), 413–430. https://doi.org/10.1016/J.JHYDROL.2006.09.014

Ambinakudige, S., & Intsiful, A. (2022). Estimation of area and volume change in the glaciers of the Columbia Icefield, Canada using machine learning algorithms and Landsat images. *Remote Sensing Applications: Society and Environment*, *26*, 100732. https://doi.org/10.1016/J.RSASE.2022.100732

Anderson, S., & Radić, V. (2020). Identification of local water resource vulnerability to rapid deglaciation in Alberta. *Nature Climate Change*, *10*(10), 933–938. https://doi.org/10.1038/s41558-020-0863-4

Bash, E. A., & Marshall, S. J. (2014). Estimation of glacial melt contributions to the Bow River, Alberta, Canada, using a radiation-temperature melt model. Annals of Glaciology, 55(66), 138–152. https://doi.org/10.3189/2014AoG66A226

Baumann, S., Anderson, B., Chinn, T., Mackintosh, A., Collier, C., Lorrey, A., . . . Eaves, S. (2021). Updated inventory of glacier ice in New Zealand based on 2016 satellite imagery. *Journal of Glaciology, 67*(261), 13-26. doi:10.1017/jog.2020.78

Bawden, A. J., Linton, H. C., Burn, D. H., & Prowse, T. D. (2014). A spatiotemporal analysis of hydrological trends and variability in the Athabasca River region, Canada. *Journal of Hydrology*, *509*, 333–342. https://doi.org/10.1016/j.jhydrol.2013.11.051

Bolch, T., Menounos, B., & Wheate, R. (2010). Landsat-based inventory of glaciers in western Canada, 1985-2005. *Remote Sensing of Environment*, *114*(1), 127–137. https://doi.org/10.1016/j.rse.2009.08.015

Bonsal, B., Shrestha, R. R., Dibike, Y., Peters, D. L., Spence, C., Mudryk, L., & Yang, D. (2020). Western Canadian freshwater availability: Current and future vulnerabilities. *Environmental Reviews*, *28*(4), 528–545. https://doi.org/10.1139/ER-2020-0040/ASSET/IMAGES/ER-2020-0040TAB7.GIF

Cannon, A.; Hiebert, J.; Werner, A.; Sobie, S.; Hiebert, M.J. (2016) ClimDown: Climate Downscaling Library for Daily Climate Model Output; Pacific Climate Impacts Consortium (PCIC): Victoria, BC, Canada, 2016.

Chernos, M., MacDonald, R. J., Nemeth, M. W., & Craig, J. R. (2020). Current and future projections of glacier contribution to streamflow in the upper Athabasca River Basin. *Canadian Water Resources Journal,* *45*(4), 324–344. https://doi.org/10.1080/07011784.2020.1815587

Chinn, T. J. (2001). Distribution of the glacial water resources of New Zealand. *Journal of Hydrology (New Zealand)*, *40*(2), 139–187. http://www.jstor.org/stable/43922047

Clarke, G. K. C., Jarosch, A. H., Anslow, F. S., Radić, V., & Menounos, B. (2015). Projected deglaciation of western Canada in the twenty-first century. *Nature Geoscience*, *8*(5), 372–377. https://doi.org/10.1038/ngeo2407

Comeau, L., Pietroniro, A., Demuth, M. et al. (2009) Glacier contribution to the North and South Saskatchewan Rivers. Hydrological Processes. 23, 2640–2653 DOI: 10.1002/hyp.7409

DeBeer, C. M., Wheater, H. S., Carey, S. K., & Chun, K. P. (2016). Recent climatic, cryospheric, and hydrological changes over the interior of western Canada: A review and synthesis. *Hydrology and Earth System Sciences*, *20*(4), 1573–1598. https://doi.org/10.5194/HESS-20-1573-2016

Döscher, R., Acosta, M., Alessandri, A., Anthoni, P., Arneth, A., Arsouze, T., Bergman, T., Bernardello, R., Bousetta, S., Caron, L.-P., Carver, G., Castrillo, M., Catalano, F., Cvijanovic, I., Davini, P., Dekker, E., Doblas-Reyes, F. J., Docquier, D., Echevarria, P., … Zhang, Q. (n.d.). *The EC-Earth3 Earth System Model for the Climate Model Intercomparison Project 6*. https://doi.org/10.5194/gmd-2020-446

Duethmann, D., Menz, C., Jiang, T., & Vorogushyn, S. (2016). Projections for headwater catchments of the Tarim River reveal glacier retreat and decreasing surface water availability but uncertainties are large. *Environmental Research Letters*, *11*(5), 054024. https://doi.org/10.1088/1748-9326/11/5/054024

Eyring, V., Bony, S., Meehl, G. A., Senior, C. A., Stevens, B., Stouffer, R. J., & Taylor, K. E. (2016). Overview of the Coupled Model Intercomparison Project Phase 6 (CMIP6) experimental design and organization. *Geosci. Model Dev*, *9*. https://doi.org/10.5194/gmd-9-1937-2016

Farinotti, D., Huss, M., Bauder, A., Funk, M., & Truffer, M. (2009). A method to estimate the ice volume and ice-thickness distribution of alpine glaciers. *Journal of Glaciology*, *55*(191), 422–430. https://doi.org/10.3189/002214309788816759

Farinotti, D., Huss, M., Fürst, J. J., Landmann, J., Machguth, H., Maussion, F., & Pandit, A. (2019). A consensus estimate for the ice thickness distribution of all glaciers on Earth. *Nature Geoscience 2019 12:3*, *12*(3), 168–173. https://doi.org/10.1038/s41561-019-0300-3

Gan, R., Luo, Y., Zuo, Q., & Sun, L. (2015). Effects of projected climate change on the glacier and runoff generation in the Naryn River Basin, Central Asia. Journal of Hydrology, 523, 240–251. https://doi.org/10.1016/J.JHYDROL.2015.01.057

Gardner, A. S., & Sharp, M. (2009). Sensitivity of net mass-balance estimates to near-surface temperature lapse rates when employing the degree-day method to estimate glacier melt. *Annals of Glaciology*, *50*(50), 80–86. https://doi.org/10.3189/172756409787769663

Hindshaw, R. S., Tipper, E. T., Reynolds, B. C., Lemarchand, E., Wiederhold, J. G., Magnusson, J., Bernasconi, S. M., Kretzschmar, R., & Bourdon, B. (2011). Hydrological control of stream water chemistry in a glacial catchment (Damma Glacier, Switzerland). *Chemical Geology*, *285*(1–4), 215–230. https://doi.org/10.1016/J.CHEMGEO.2011.04.012

Hock, R. (2003). Temperature index melt modelling in mountain areas. *Journal of Hydrology*, *282*(1–4), 104–115. https://doi.org/10.1016/S0022-1694(03)00257-9

Hock, R., Bliss, A., Marzeion, B. E. N., Giesen, R. H., Hirabayashi, Y., Huss, M., Radic, V., & Slangen, A. B. A. (2019). GlacierMIP – A model intercomparison of global-scale glacier mass-balance models and projections. *Journal of Glaciology*, *65*(251), 453–467. https://doi.org/10.1017/JOG.2019.22

Huss, M., Jouvet, G., Farinotti, D., & Bauder, A. (2010). Future high-mountain hydrology: a new parameterization of glacier retreat. Hydrol. Earth Syst. Sci, 14, 815–829. https://doi.org/10.5194/hess-14-815-2010

Huss, M., & Hock, R. (2015). A new model for global glacier change and sea-level rise. Frontiers in Earth Science, 3, 54. https://doi.org/10.3389/feart.2015.00054

Huss, M., Zemp, M., Joerg, P. C., & Salzmann, N. (2014). High uncertainty in 21st century runoff projections from glacierized basins. *Journal of Hydrology*, *510*, 35–48. https://doi.org/10.1016/J.JHYDROL.2013.12.017

Immerzeel, W. W., van Beek, L. P. H., Konz, M., Shrestha, A. B., & Bierkens, M. F. P. (2012). Hydrological response to climate change in a glacierized catchment in the Himalayas. Climatic Change, 110(3–4), 721–736. https://doi.org/10.1007/s10584-011-0143-4

Intergovernmental Panel on Climate (2007) Climate Change 2007: Synthesis Report. Contribution of Working Groups I, II and III to the Fourth Assessment Report of the Intergovernmental Panel on Climate Change [Core Writing Team, Pachauri, R.K and Reisinger, A. (eds.)]. *IPCC, Geneva, Switzerland, 104 pp.*

Intergovernmental Panel on Climate Change (2019) IPCC, 2019: IPCC Special Report on the Ocean and Cryosphere in a Changing Climate [H.-O. Pörtner, D.C. Roberts, V. Masson-Delmotte, P. Zhai, M. Tignor, E. Poloczanska, K. Mintenbeck, A. Alegría, M. Nicolai, A. Okem, J. Petzold, B. Rama, N.M. Weyer (eds.)]. *Cambridge University Press, Cambridge, UK and New York, NY, USA, 755 pp.* https://doi.org/10.1017/9781009157964.

Intsiful, A., & Ambinakudige, S. (2020). Glacier Cover Change Assessment of the Columbia Icefield in the Canadian Rocky Mountains, Canada (1985–2018). *Geosciences*, *11*(1), 19. https://doi.org/10.3390/geosciences11010019

Jarvis, A., Reuter, H. I., Nelson, A., & Guevara, E. (2008). Hole-filled shuttle radar topography mission (SRTM) for the globe Version 4. *Consultative Group on International Agricultural Research-Consortium for Spatial Information (CGIAR-CSI), Washington, DC Available from https://srtm.csi.cgiar.org (accessed Oct 2022)*.

Jiang, R., Gan, T. Y., Xie, J., Wang, N., & Kuo, C. C. (2017). Historical and potential changes of precipitation and temperature of Alberta subjected to climate change impact: 1900–2100. Theoretical and Applied Climatology, 127(3–4), 725–739. https://doi.org/10.1007/s00704-015-1664-y

Jost, G., Moore, R. D., Menounos, B., & Wheate, R. (2012). Hydrology and Earth System Sciences Quantifying the contribution of glacier runoff to streamflow in the upper Columbia River Basin, Canada. Hydrol. Earth Syst. Sci, 16, 849–860. https://doi.org/10.5194/hess-16-849-2012

Khalili, P., Masud, B., Qian, B., Mezbahuddin, S., Dyck, M., & Faramarzi, M. (2021). Non-stationary response of rain-fed spring wheat yield to future climate change in northern latitudes. *Science of the Total Environment*, *772*. https://doi.org/10.1016/J.SCITOTENV.2021.145474

Kotila A., Cui, Q., Silwal, G., Bush, A.B.G., Faramarzi, M. (2022) Uncertainty assessment of empirically-derived parameters and parameter transferability in mountain glacier modeling at the regional scale. *Journal of Hydrology*, In review.

Kraaijenbrink, P. D. A., Bierkens, M. F. P., Lutz, A. F., & Immerzeel, W. W. (2017). Impact of a global temperature rise of 1.5 degrees Celsius on Asia's glaciers. Nature, 549(7671), 257–260. https://doi.org/10.1038/nature23878

Krause, P., Boyle, D. P., & Bäse, F. (2005). Comparison of different efficiency criteria for hydrological model assessment. *Advances in Geosciences*, *5*, 89–97. https://doi.org/10.5194/adgeo-5-89-2005

Litt, M., Shea, J., Wagnon, P., Steiner, J., Koch, I., Stigter, E., & Immerzeel, W. (2019). Glacier ablation and temperature indexed melt models in the Nepalese Himalaya. Scientific Reports 2019 9:1, 9(1), 1–13. https://doi.org/10.1038/s41598-019-41657-5

Liu, J., Long, A., Deng, X., Yin, Z., Deng, M., An, Q., Gu, X., Li, S., & Liu, G. (2022). The Impact of Climate Change on Hydrological Processes of the Glacierized Watershed and Projections. *Remote Sensing 2022, Vol. 14, Page 1314*, *14*(6), 1314. https://doi.org/10.3390/RS14061314

Marshall, S. J., White, E. C., Demuth, M. N., Bolch, T., Wheate, R., Menounos, B., Beedle, M. J., & Shea, J. M. (2011). Glacier Water Resources on the Eastern Slopes of the Canadian Rocky Mountains. Canadian Water Resources Journal, 36(2), 109–134. https://doi.org/10.4296/cwrj3602823

Marzeion, B., Hock, R., Anderson, B., Bliss, A., Champollion, N., Fujita, K., Huss, M., Immerzeel, W. W., Kraaijenbrink, P., Malles, J. H., Maussion, F., Radić, V., Rounce, D. R., Sakai, A., Shannon, S., van de Wal, R., & Zekollari, H. (2020). Partitioning the Uncertainty of Ensemble Projections of Global Glacier Mass Change. *Earth's Future*, *8*(7), e2019EF001470. https://doi.org/10.1029/2019EF001470

Masud, B., Cui, Q., Ammar, M. E., Bonsal, B. R., Islam, Z., & Faramarzi, M. (2021). Means and extremes: Evaluation of a CMIP6 multi-model ensemble in reproducing historical climate characteristics across Alberta, Canada. *Water (Switzerland)*, *13*(5). https://doi.org/10.3390/w13050737

McKay, M. D., Beckman, R. J., Conover, W. J., & Beckman W J Conover, R. J. (1979). Comparison of Three Methods for Selecting Values of Input Variables in the Analysis of Output from a Computer Code. *Technometrics*, *21*(2), 239–245. https://doi.org/10.1080/00401706.1979.10489755

Milner, A. M., Khamis, K., Battin, T. J., Brittain, J. E., Barrand, N. E., Füreder, L., Cauvy-Fraunié, S., Gíslason, G. M., Jacobsen, D., Hannah, D. M., Hodson, A. J., Hood, E., Lencioni, V., Ólafsson, J. S., Robinson, C. T., Tranter, M., & Brown, L. E. (2017). Glacier shrinkage driving global changes in downstream systems. *Proceedings of the National Academy of Sciences of the United States of America*, *114*(37), 9770–9778. https://doi.org/10.1073/PNAS.1619807114/SUPPL_FILE/PNAS.201619807SI.PDF

Moore, R. D., Fleming, S. W., Menounos, B., Wheate, R., Fountain, A., Stahl, K., Holm, K., & Jakob, M. (2009). Glacier change in western North America: influences on hydrology, geomorphic hazards and water quality. Hydrological Processes, 23(1), 42–61. https://doi.org/10.1002/HYP.7162

Mwale, D., Gan, T. Y., Devito, K., Mendoza, C., Silins, U., & Petrone, R. (2009). Precipitation variability and its relationship to hydrologic variability in Alberta. Hydrological Processes, 23(21), 3040–3056. https://doi.org/10.1002/HYP.7415

Ohmura, A. (2001). Physical basis for the temperature-based melt-index method. *Journal of Applied Meteorology, 40(4)*, 753–761. https://doi.org/10.1175/1520-0450(2001)040<0753:PBFTTB>2.0.CO;2

O'Neill, B. C., Kriegler, E., Ebi, K. L., Kemp-Benedict, E., Riahi, K., Rothman, D. S., van Ruijven, B. J., van Vuuren, D. P., Birkmann, J., Kok, K., Levy, M., & Solecki, W. (2017). The roads ahead: Narratives for shared socioeconomic pathways describing world futures in the 21st century. *Global Environmental Change*, *42*, 169–180. https://doi.org/10.1016/J.GLOENVCHA.2015.01.004

Paul, F., & Mölg, N. (2014). Hasty retreat of glaciers in northern Patagonia from 1985 to 2011. *Journal of Glaciology*, *60*(224), 1033–1043. https://doi.org/10.3189/2014JOG14J104

Payne, J.T., Wood, A.W., Hamlet, A.F. et al. (2004) Mitigating the Effects of Climate Change on the Water Resources of the Columbia River Basin. Climatic Change 62, 233–256. https://doi.org/10.1023/B:CLIM.0000013694.18154.d6

Pellicciotti, F., Brock, B., Strasser, U., Burlando, P., Funk, M., & Corripio, J. (2005). An enhanced temperature-index glacier melt model including the shortwave radiation balance: development and testing for Haut Glacier d'Arolla, Switzerland. *Journal of Glaciology*, *51*(175), 573–587. https://doi.org/10.3189/172756505781829124

Perroud, M., Fasel, M., & Marshall, S. J. (2019). Development and testing of a subgrid glacier mass balance model for nesting in the Canadian Regional Climate Model. *Climate Dynamics*, *53*(3–4), 1453–1476. https://doi.org/10.1007/s00382-019-04676-6

Pfeffer, W. T., Arendt, A. A., Bliss, A., Bolch, T., Graham, J., Gardner, A. S., Hagen, J.-O., Hock, R., Kaser, G., Kienholz, C., Miles, E. S., Moholdt, G., Mo¨lg, N., Mo¨lg, M., Paul, F., Radic´, V., Radic´, R., Rastner, P., Raup, B. H., … Consortium, R. (2017). The Randolph Glacier Inventory: a globally complete inventory of glaciers. https://doi.org/10.3189/2014JoG13J176

Radić, V., & Hock, R. (2010). Regional and global volumes of glaciers derived from statistical upscaling of glacier inventory data. *Journal of Geophysical Research: Earth Surface*, *115*(1). https://doi.org/10.1029/2009JF001373

Radić, V., Hock, R., & Oerlemans, J. (2007). Volume-area scaling vs flowline modelling in glacier volume projections. Annals of Glaciology, 46, 234–240. https://doi.org/10.3189/172756407782871288

Radić, V., Bliss, A., Beedlow, A. C., Hock, R., Miles, E., & Cogley, J. G. (2014). Regional and global projections of twenty-first century glacier mass changes in response to climate scenarios from global climate models. *Climate Dynamics*, *42*(1–2), 37–58. https://doi.org/10.1007/S00382-013-1719-7/TABLES/5

Rokaya, P., Peters, D. L., Elshamy, M., Budhathoki, S., & Lindenschmidt, K. (2020). Impacts of future climate on the hydrology of a northern headwaters basin and its implications for a downstream deltaic ecosystem. *Hydrological Processes*, *34*(7), 1630–1646. https://doi.org/10.1002/hyp.13687

Rounce, D. R., Hock, R., & Shean, D. E. (2020). Glacier Mass Change in High Mountain Asia Through 2100 Using the Open-Source Python Glacier Evolution Model (PyGEM). Frontiers in Earth Science, 7, 331. https://doi.org/10.3389/FEART.2019.00331/BIBTEX

Shea, J. M., Moore, R. D., & Stahl, K. (2009). Derivation of melt factors from glacier mass-balance records in western Canada. *Journal of Glaciology*, *55*(189), 123–130. https://doi.org/10.3189/002214309788608886

Shea, J. M., Immerzeel, W. W., Wagnon, P., Vincent, C., & Bajracharya, S. (2015). Modelling glacier change in the Everest region, Nepal Himalaya. *Cryosphere, 9(3),* 1105–1128. https://doi.org/10.5194/tc-9-1105-2015 0

Silwal G., Ammar M., Thapa A., Bonsal B., Faramarzi M. (2022). Response of glacier melt modelling parameters to time, space, and model complexity: examples from eastern slopes of Canadian Rocky Mountains. *Science of the Total Environment*, In review.

Singh, V., Jain, S. K., & Goyal, M. K. (2021). An assessment of snow-glacier melt runoff under climate change scenarios in the Himalayan basin. Stochastic Environmental Research and Risk Assessment, 1–26. https://doi.org/10.1007/s00477-021-01987-1

Stahl, K., Moore, R. D., Shea, J. M., Hutchinson, D., and Cannon, A. J. (2008). Coupled modelling of glacier and streamflow response to future climate scenarios, Water Resour. Res., 44, W06201, doi:10.1029/2006WR005022

Strong, W.L., & Leggat, K.R. (1992.) Ecoregions of Alberta (ISBN 0 -86499-840-6). Alberta Forestry, Lands and Wildlife. https://open.alberta.ca/dataset/9dae82c1-7fda-47d3-b8eb-269d6ffc2451/resource/3453233f-7295-4104-9601-8d1978d1fda5/download/enr-t-4-ecoregions-of-alberta.pdf

Tennant, C., Menounos, B., Wheate, R., & Clague, J. J. (2012). Area change of glaciers in the Canadian rocky mountains, 1919 to 2006. Cryosphere, 6(6), 1541–1552. https://doi.org/10.5194/tc-6-1541-2012

Tolotti, M., Cerasino, L., Donati, C., Pindo, M., Rogora, M., Seppi, R., & Albanese, D. (2020). Alpine headwaters emerging from glaciers and rock glaciers host different bacterial communities: Ecological implications for the future. *Science of The Total Environment*, *717*, 137101. https://doi.org/10.1016/J.SCITOTENV.2020.137101

Voldoire, A., Saint-Martin, D., Sénési, S., Decharme, B., Alias, A., Chevallier, M., Colin, J., Guérémy, J. F., Michou, M., Moine, M. P., Nabat, P., Roehrig, R., Salas y Mélia, D., Séférian, R., Valcke, S., Beau, I., Belamari, S., Berthet, S., Cassou, C., … Waldman, R. (2019). Evaluation of CMIP6 DECK Experiments With CNRM-CM6-1. *Journal of Advances in Modeling Earth Systems*, *11*(7), 2177–2213. https://doi.org/10.1029/2019MS001683

Wheater, H. S., Pomeroy, J. W., Pietroniro, A., Davison, B., Elshamy, M., Yassin, F., Rokaya, P., Fayad, A., Tesemma, Z., Princz, D., Loukili, Y., DeBeer, C. M., Ireson, A. M., Razavi, S., Lindenschmidt, K. E., Elshorbagy, A., MacDonald, M., Abdelhamed, M., Haghnegahdar, A., & Bahrami, A. (2022). Advances in modelling large river basins in cold regions with Modélisation Environmentale Communautaire—Surface and Hydrology (MESH), the Canadian hydrological land surface scheme. *Hydrological Processes*, *36*(4), e14557. https://doi.org/10.1002/HYP.14557

Yukimoto, S., Kawai, H., Koshiro, T., Oshima, N., Yoshida, K., Urakawa, S., Tsujino, H., Deushi, M., Tanaka, T., Hosaka, M., Yabu, S., Yoshimura, H., Shindo, E., Mizuta, R., Obata, A., Adachi, Y., & Ishii, M. (2019). The Meteorological Research Institute Earth System Model Version 2.0, MRI-ESM2.0: Description and Basic Evaluation of the Physical Component. *Journal of the Meteorological Society of Japan. Ser. II*, *97*(5), 931–965. https://doi.org/10.2151/JMSJ.2019-051

CHAPTER IV – CONCLUSION

4.1 Research Summary

The primary goals of this study are to validate and optimize a parameterization for a coupled glacier mass balance dynamic evolution model (CGME) using a range of values for each parameter and then to apply this parameterization to projections of glacier response under various future climate scenarios. The study area is the Athabasca River Basin, which is selected as it is glacierized with a highly heterogeneous variety of glaciers including a portion of the Columbia Icefield, which has been consistently monitored and had data available which is used for calibration and validation. This catchment is also a key source of water for both natural ecosystems and downstream human consumption. To meet the first study objective, we select a maximum meaningful range for each parameter used by the CGME, calibrate, validate, and perform sensitivity analyses to create an optimized range for each parameter. We assess model performance, and compare two melt model frameworks within the CGME and develop and optimize parameter ranges for both versions of the model. Selecting the model framework that was performing better with the input data available to us, we proceed to apply the parametrization at the regional scale, assessing its performance during the historical period 1984-2007.

For each of the 258 glaciers we perform 100 simulations using the optimum parameter ranges that were obtained through calibration iterations for the Athabasca glacier. The simulations are based on 100 sets of new sampled parameters from the optimum range using the Latin Hypercube Sampling approach (Mckay et al., 1979). This approach quantifies model output uncertainty using the 95 Percent Prediction Uncertainty (95PPU). 95PPU predicts an uncertainty

band calculated at the 2.5% and 97.5% levels of the cumulative distribution of model output in response to parameter uncertainty (Abbaspour et al., 2007), instead of a single modelled value response to a single parameter. The predicted uncertainty range, which is calculated as the difference between L95PPU (mm) and U95PPU (mm) for each glacier (Δ95PPU (mm)), varies from 0.04 mm to ~ 134 mm across glaciers. In these glaciers different sets of input parameter values in the model result in different runoff accumulations, with the largest differences being up to 134 mm above their predicted L95PPU (mm). The results indicate that the largest values of Δ95PPU are observed only in large glaciers which count for < 3% of the total number of glaciers in the region. To mask the effect of error propagation issues in the interpretation of our results, we normalize the predicted uncertainty ranges. The normalized uncertainty prediction (Rn) varies from 0.37 to 1 across glaciers (cf. Fig. 6d), which show ~ 63% of the glaciers in the region have an Rn value of greater than 0.5. This indicates that in more than 63% of the glaciers in the region, the input parameters for melt-mass balance-evolution modeling (such the one developed in this study) cannot be accurately driven from empirical measurements from other adjacent glaciers. By using a range of parameter values, calibrated from the maximum physically meaningful range for each parameter from an adjacent glacier (e.g., Athabasca glacier in this study), we demonstrate different levels of uncertainty arising from the parameter transferability in each glacier.

Using this parameterization approach, we then assess glacier responses to future climate scenarios. We explore regional changes in Albertan glacier runoff, area, and volume in response to climate model results and forcings for the future as presented in CMIP6. We utilized 4 CMIP6 GCMs and 2 SSPs to project the ranges of potential glacier behaviour based on the latest climate scenarios and models, which will be useful for adaptive planning and mitigation. By applying the previously explored methodology, we seek to keep the uncertainty band due to model

parameterization narrow while still exploring the maximum possible range of predictions in glacier behaviour by avoiding use of just a single value for each input parameter. We use LHS to sample 100 parameter sets and use them with our chosen climate forcings to simulate the changes in melt runoff, area, and volume for the 258 glaciers in the Athabascan River Basin for the period 1980-2100. We also assess predicted glacier change based on glacier initial size and glacier initial median elevation.

The multimodel ensemble projections of cumulative melt runoff indicates that glaciers in all size classes are expected to produce the greatest amount of melt runoff during the historical period (1980-2019), under both climate scenarios. It also shows the predicted evolution of monthly flows, with shoulder-season melt runoff (Apr-May, Sep-Oct) being substantially reduced or non-existent in the far-future period, especially under SSP585. The multimodel ensemble projections of cumulative melt runoff indicate that glaciers in all elevation groups are expected to produce the greatest amount of melt runoff during the historical period (1980-2019), under both climate scenarios. The monthly distribution and variability of cumulative melt runoff for each elevation group evolves across the simulation periods under both SSPs. The largest amount of melt runoff is again expected during the historical period and runoff being greatly reduced in the far-future (2060-2100) period in both climate scenarios. Low elevation glaciers are predicted to have the majority of their melt during this period. It also shows the predicted evolution of monthly flows, with shoulder-season melt runoff (Apr-May, Sep-Oct) being substantially reduced or non-existent in the far-future period for all glaciers, especially under SSP585. For low elevation glaciers, shoulder-season flows are predicted to disappear after the historical period, with low Jun-Jul-Aug melt runoff in the near-future and indiscernible runoff in the far-future. Medium elevation glaciers

are predicted to have indiscernible runoff in the far-future under SSP585, while low melt runoff is indicated to persist under SSP126.

By performing simulations with both an ensemble of CMIP6 GCMs and a range of parameterizations, we are able to characterize the uncertainty due to parameterization while assessing potential changes. Looking at predicted changes both as a result of glacier size and also glacier elevation allows us to characterize more potential glacio-hydological regimes while constraining model uncertainty using 95PPU.

4.2 Study Conclusions

Calibration and validation determined that while both versions of the CGME with different melt models (CTIM or PTIM) gave similar ranges of uncertainty for melt runoff from 1000 simulations forced by the maximum meaningful parameter range for each model, representation of observed data by the simulated predictions were vastly different. Using 95 percent prediction uncertainty (95PPU), high uncertainty associated with both overestimation and underestimation of melt runoff in the PTIM-based model was found. While model performance may be improved by using a range of parameter values compared to a singular value, prediction uncertainty may still be high due to model selection and quality of input data.

One-at-a-time (OAT) sensitivity analysis of each parameter for both model types showed the sensitivity of simulated melt runoff to each parameter. Both were found to be highly sensitive to similar parameters associated with temperature and melt runoff, with even small changes in parameter values leading to large changes in runoff. This highlights the importance and associated uncertainty of parameter selection and parameter transferability both spatially and temporally.

Assessment of 95PPU of melt runoff at a larger spatiotemporal scale reinforced this idea. The normalized uncertainty prediction (Rn), which accounts for differences in glacier area, demonstrated that approximately two-thirds of glaciers in the study area higher sensitivity of the predicted melt runoff to their underlying input parameters and that these glaciers ought not to be driven with parameters from empirical measurements from other adjacent glaciers. Assessment of cumulative melt runoff differences and % difference of cumulative melt runoff based on glacier size determined that small glaciers have a greater cumulative melt runoff difference arising from the input parameter variability and larger parameter dependence at a regional scale. From this, we conclude that small glaciers have a wide range of potential cumulative melt runoff values that are regionally significant and ought not to be overlooked in examinations and discussions of regional projections.

With this in mind, we used the GCME and optimized parameter ranges to characterize uncertainty in future regional projections. These simulations predict dramatic, rapid retreat for all glaciers regardless of the climate scenario. Assessing glacier change by size, all glaciers are predicted to behave similarly across the size classes and SSPs; using ninety-five percent prediction uncertainty (95PPU) and multimodel median averages it was determined that glaciers are predicted to decrease in volume in the first forty years of the simulation period (1980-2019, the historical period). Monthly predicted flow regimes not only indicate greatly reduced melt runoff as the century progresses, but also the loss of late spring and early fall melt runoff, predicting low flows during Jun-Jul-Aug by 2060-2100 (the far-future period). Assessing potential changes by glacier initial elevation indicated similar trends, though low elevation glaciers are predicted to be especially responsive, discharging the majority of their melt runoff during the historical period. Monthly melt runoff reflects similar trends to those found during size analysis, though low

elevation glaciers have the most extreme response, reducing their melt runoff to Jun-July-Aug during the near-future period (2020-2059) and discharging their melt runoff by the end of the near-future. These assessments show that recent and imminent glacier retreat will have impacts on the glacio-hydrological regime.

To conclude, we explored different levels of uncertainty in using ranges of parameter values in CGME modeling approaches. We determined that ranges of model predictions compared to observed data can be improved (and we developed optimized ranges for each parameter and modeling approach), but overall model performance is dependent on available input data and associated melt model selection. Both melt model versions of the CGME are more sensitive to changes in the range of some parameters and not responsive to others, which can help identify sources of uncertainty. We also assessed uncertainty at the regional scale, determining the appropriateness of parameter range transferability and that small glaciers are especially sensitive to input parameter variability.

We also assessed future changes in glacier melt runoff, ice area, and ice volume in mountain glaciers, assessing projected changes based on glacier size and elevation. All sizes and elevation groups of glaciers exhibit similar trends, with glaciers losing most of their volume and discharging it as runoff during the 1980-2019 period and making greatly reduced contributions to streamflow later in the century (2060-2100). Low-elevation glaciers were found to be especially sensitive. All glaciers also exhibited changes in their monthly melt runoff, losing early- and late-season flows by the 2020-2059 period. The combined changes to glacier volume/area, streamflow contributions, and the timing of melt runoff foretell lasting and irreversible impacts to the surrounding and downstream hydrological regime and the ecosystems and users that rely on it. These trends are indicated by all climate projection scenarios and the range of uncertainty from

both future climate and model parametrization, highlighting the imminent need for preparing and implementing adaptation and mitigation strategies.

4.3 Study Limitations and Future Directions

The complex physics of glaciers and their dynamics that can change even on an hourly basis mean that any glacier model is a simplification, which is certainly true of the CGME. It utilizes empirically-derived parameters to simulate processes at the daily or annual timescale. It uses a mass balance framework, with accumulation being precipitation falling as snow and ablation being glacier ice melt runoff. It cannot account for processes like blowing snow or sublimation. It is limited by data availability, both for initial glacier geometry such as ice thickness and for climatic forcing data such as daily temperature and precipitation. For the historical observations, data from the single closest climate station is interpolated using lapse rates and precipitation gradients to approximate conditions on the individual glaciers in the region. Calibration and validation are also limited by data availability; there are temporal interruptions in both the climate station record and the streamflow record used to calibrate and validate melt runoff, meaning the most continuous period of matching records is 2006-2018. Regarding future projections, initial glacier geometry has to be assumed from approximate ice thickness and glacier surface area products, which are based on observations 10+ years old. We also utilize General Circulation Models downscaled to our study area to force the future projections, rather than Regional Climate Models. This was based on the availability of models to form a coherent multimodel ensemble. Our research characterizes the differing levels of uncertainty associated with parameter transferability.

Glaciers are a precious natural resource, which benefit the watershed and ecosystems far beyond their mountainous reaches. The glaciers of the Canadian Rocky Mountains are known to be vulnerable and responsive to changes in climates, while being remote and difficult to observe directly. By using models to simulate their dynamics, we can gain a better picture of the current and potential future changes these glaciers may undergo, and their potential interaction and impact on the larger hydrological system. It is my hope that this and similar studies can lend some insight into the future demise of glaciers and assist in wise stewardship of our water resources.

5. BIBLIOGRAPHY

Abbaspour, K. C., Johnson, C. A., & Genuchten, M. T. van. (2004). Estimating Uncertain Flow and Transport Parameters Using a Sequential Uncertainty Fitting Procedure. *Vadose Zone Journal*, *3*(4), 1340–1352. https://doi.org/10.2136/VZJ2004.1340

Abbaspour, K. C., Yang, J., Maximov, I., Siber, R., Bogner, K., Mieleitner, J., Zobrist, J., & Srinivasan, R. (2007). Modeling hydrology and water quality in the pre-alpine/alpine Thur watershed using SWAT. *Journal of Hydrology*, *333*(2–4), 413–430. https://doi.org/10.1016/J.JHYDROL.2006.09.014

Adhikari, S., & Marshall, S. J. (2013). The Cryosphere Influence of high-order mechanics on simulation of glacier response to climate change: insights from Haig Glacier, Canadian Rocky Mountains. *The Cryosphere*, *7*, 1527–1541. https://doi.org/10.5194/tc-7-1527-2013

Ambinakudige, S., & Intsiful, A. (2022). Estimation of area and volume change in the glaciers of the Columbia Icefield, Canada using machine learning algorithms and Landsat images. *Remote Sensing Applications: Society and Environment*, *26*, 100732. https://doi.org/10.1016/J.RSASE.2022.100732

Anderson, S., & Radić, V. (2020). Identification of local water resource vulnerability to rapid deglaciation in Alberta. *Nature Climate Change*, *10*(10), 933–938. https://doi.org/10.1038/s41558-020-0863-4

Arendt, A., & Sharp, M. (1999). Energy balance measurements on a Canadian high Arctic glacier and their implications for mass-balance modeling. (*Symposium at Birmingham, 1 July 1999 – Interactions between the Cryosphere, Climate and Greenhouse Gases, 165–172, 1999). International Association of Hydrological Sciences Publications, Issue 256.*

Bash, E. A., & Marshall, S. J. (2014). Estimation of glacial melt contributions to the Bow River, Alberta, Canada, using a radiation-temperature melt model. *Annals of Glaciology*, *55*(66), 138–152. https://doi.org/10.3189/2014AoG66A226

Baumann, S., Anderson, B., Chinn, T., Mackintosh, A., Collier, C., Lorrey, A., . . . Eaves, S. (2021). Updated inventory of glacier ice in New Zealand based on 2016 satellite imagery. *Journal of Glaciology, 67*(261), 13-26. doi:10.1017/jog.2020.78

Bawden, A. J., Linton, H. C., Burn, D. H., & Prowse, T. D. (2014). A spatiotemporal analysis of hydrological trends and variability in the Athabasca River region, Canada. *Journal of Hydrology*, *509*, 333–342. https://doi.org/10.1016/j.jhydrol.2013.11.051

Bolch, T., Menounos, B., & Wheate, R. (2010). Landsat-based inventory of glaciers in western Canada, 1985-2005. *Remote Sensing of Environment, 114(1)*, 127–137. https://doi.org/10.1016/j.rse.2009.08.015

Bonsal, B., Shrestha, R. R., Dibike, Y., Peters, D. L., Spence, C., Mudryk, L., & Yang, D. (2020). Western Canadian freshwater availability: Current and future vulnerabilities. *Environmental Reviews*, *28*(4), 528–545. https://doi.org/10.1139/ER-2020-0040/ASSET/IMAGES/ER-2020-0040TAB7.GIF

Braithwaite, R. J. (1995). Positive degree-day factors for ablation on the Greenland ice sheet studied by energy-balance modeling. *Journal of Glaciology, 41(137),* 153–160. https://doi.org/10.3189/s0022143000017846

Braithwaite, R. J. and Olesen, O. B. (1985.) Ice ablation in West Greenland in relation to air temperature and global radiation. *Zeitschrift für Gletscherkunde und Glazialgeologie, 20,* 155–168. Retrieved February 23, 2021, from https://www.research.manchester.ac.uk/portal/files/24283613/POST-PEER-REVIEW-PUBLISHERS.PDF

Braun, L.N., Grabs, W., & Rana, B. (1993) Application of a Conceptual Precipitation Runoff Model in the Langtang Kfaola Basin, Nepal Himalaya. *Snow and Glacier Hydrology (Proceedings of the Kathmandu Symposium, November 1992). International Association of Hydrological Sciences Publications no. 218.* Retrieved February 23, 2021, from https://www.researchgate.net/publication/242567643

Brock, B. W., & Arnold, N. S. (2000). A spreadsheet-based (microsoft excel) point surface energy balance model for glacier and snow melt studies. *Earth Surface Processes and Landforms, 25(6)*, 649–658. https://doi.org/10.1002/1096-9837(200006)25:6<649::AID-ESP97>3.0.CO;2-U

Brown, L. E., Hannah, D. M., & Milner, A. M. (2007). Vulnerability of alpine stream biodiversity to shrinking glaciers and snowpacks. *Global Change Biology*, *13*(5), 958–966. https://doi.org/10.1111/J.1365-2486.2007.01341.X

Cannon, A.; Hiebert, J.; Werner, A.; Sobie, S.; Hiebert, M.J. (2016) ClimDown: Climate Downscaling Library for Daily Climate Model Output; Pacific Climate Impacts Consortium (PCIC): Victoria, BC, Canada, 2016.

Cannone, N., Diolaiuti, G., Guglielmin, M., & Smiraglia, C. (2008). ACCELERATING CLIMATE CHANGE IMPACTS ON ALPINE GLACIER FOREFIELD ECOSYSTEMS IN THE EUROPEAN ALPS. *Ecological Applications*, *18*(3), 637–648. https://doi.org/10.1890/07-1188.1

Cauvy-Fraunié, S., Andino, P., Espinosa, R., Calvez, R., Jacobsen, D., & Dangles, O. (2016). Ecological responses to experimental glacier-runoff reduction in alpine rivers. *Nature Communications 2016 7:1*, *7*(1), 1–7. https://doi.org/10.1038/ncomms12025

Chernos, M., MacDonald, R. J., Nemeth, M. W., & Craig, J. R. (2020). Current and future projections of glacier contribution to streamflow in the upper Athabasca River Basin.

Canadian Water Resources Journal, 45(4), 324–344. https://doi.org/10.1080/07011784.2020.1815587

Chinn, T. J. (2001). Distribution of the glacial water resources of New Zealand. *Journal of Hydrology (New Zealand)*, *40*(2), 139–187. http://www.jstor.org/stable/43922047

Clarke, G. K. C., Anslow, F. S., Jarosch, A. H., Radić, V., Menounos, B., Bolch, T., & Berthier, E. (2013). Ice volume and subglacial topography for western Canadian glaciers from mass-balance fields, thinning rates, and a bed stress model. *Journal of Climate*, *26*(12), 4282–4303. https://doi.org/10.1175/JCLI-D-12-00513.1

Clarke, G. K. C., Jarosch, A. H., Anslow, F. S., Radić, V., & Menounos, B. (2015). Projected deglaciation of western Canada in the twenty-first century. *Nature Geoscience, 8(5),* 372–377. https://doi.org/10.1038/ngeo2407

Comeau, L., Pietroniro, A., Demuth, M. *et al.* (2009) Glacier contribution to the North and South Saskatchewan Rivers. *Hydrological Processes.* 23, 2640–2653 DOI: 10.1002/hyp.7409

DeBeer, C. M., Wheater, H. S., Carey, S. K., & Chun, K. P. (2016). Recent climatic, cryospheric, and hydrological changes over the interior of western Canada: A review and synthesis. *Hydrology and Earth System Sciences*, *20*(4), 1573–1598. https://doi.org/10.5194/HESS-20-1573-2016

Döscher, R., Acosta, M., Alessandri, A., Anthoni, P., Arneth, A., Arsouze, T., Bergman, T., Bernardello, R., Bousetta, S., Caron, L.-P., Carver, G., Castrillo, M., Catalano, F., Cvijanovic, I., Davini, P., Dekker, E., Doblas-Reyes, F. J., Docquier, D., Echevarria, P., … Zhang, Q. (n.d.). *The EC-Earth3 Earth System Model for the Climate Model Intercomparison Project 6*. https://doi.org/10.5194/gmd-2020-446

Duethmann, D., Menz, C., Jiang, T., & Vorogushyn, S. (2016). Projections for headwater catchments of the Tarim River reveal glacier retreat and decreasing surface water availability but uncertainties are large. *Environmental Research Letters*, *11*(5), 054024. https://doi.org/10.1088/1748-9326/11/5/054024

Engelhardt, M., Schuler, T. V., & Andreassen, L. M. (2013). Glacier mass-balance of Norway 1961-2010 calculated by a temperature-index model. *Annals of Glaciology*, *54*(63), 32–40. https://doi.org/10.3189/2013AoG63A245

Eyring, V., Bony, S., Meehl, G. A., Senior, C. A., Stevens, B., Stouffer, R. J., & Taylor, K. E. (2016). Overview of the Coupled Model Intercomparison Project Phase 6 (CMIP6) experimental design and organization. *Geoscientific Model Development*, *9*(5), 1937–1958. https://doi.org/10.5194/gmd-9-1937-2016

Farinotti, D., Huss, M., Bauder, A., Funk, M., & Truffer, M. (2009). A method to estimate the ice volume and ice-thickness distribution of alpine glaciers. *Journal of Glaciology, 55(191),* 422–430. https://doi.org/10.3189/002214309788816759

Farinotti, D., Huss, M., Fürst, J. J., Landmann, J., Machguth, H., Maussion, F., & Pandit, A. (2019). A consensus estimate for the ice thickness distribution of all glaciers on Earth. *Nature Geoscience 2019 12:3*, *12*(3), 168–173. https://doi.org/10.1038/s41561-019-0300-3

Faramarzi, M., Abbaspour, K. C., Adamowicz, V., Lu, W., Fennell, J., Zehnder, A. J. B., & Goss, G. G. (2017). Uncertainty based assessment of dynamic freshwater scarcity in semi-arid watersheds of Alberta, Canada. *Journal of Hydrology: Regional Studies*, *9*, 48–68. https://doi.org/10.1016/j.ejrh.2016.11.003

Finsterwalder, S., Schunk, H., 1887. Der Suldenferner. *Zeitschrift des Deutschen und Oesterreichischen Alpenvereins 18,* 72–89

Follum, M. L., Downer, C. W., Niemann, J. D., Roylance, S. M., & Vuyovich, C. M. (2015). A radiation-derived temperature-index snow routine for the GSSHA hydrologic model. Journal of Hydrology, 529(P3), 723–736. https://doi.org/10.1016/j.jhydrol.2015.08.044

Frey, H., Machguth, H., Huss, M., Huggel, C., Bajracharya, S., Bolch, T., Kulkarni, A., Linsbauer, A., Salzmann, N., & Stoffel, M. (2014). Estimating the volume of glaciers in the Himalayan-Karakoram region using different methods. *Cryosphere, 8(6),* 2313–2333. https://doi.org/10.5194/tc-8-2313-2014

Gan, R., Luo, Y., Zuo, Q., & Sun, L. (2015). Effects of projected climate change on the glacier and runoff generation in the Naryn River Basin, Central Asia. Journal of Hydrology, 523, 240–251. https://doi.org/10.1016/J.JHYDROL.2015.01.057

Gardner, A. S., & Sharp, M. (2009). Sensitivity of net mass-balance estimates to near-surface temperature lapse rates when employing the degree-day method to estimate glacier melt. *Annals of Glaciology*, *50*(50), 80–86. https://doi.org/10.3189/172756409787769663

Gardner, A. S., Sharp, M. J., Koerner, R. M., Labine, C., Boon, S., Marshall, S. J., Burgess, D. O., & Lewis, D. (2009). Near-surface temperature lapse rates over arctic glaciers and their implications for temperature downscaling. *Journal of Climate, 22(16),* 4281–4298. https://doi.org/10.1175/2009JCLI2845.1

Gleick, P. H., & Palaniappan, M. (2010). Peak water limits to freshwater withdrawal and use. *Proceedings of the National Academy of Sciences of the United States of America*, *107*(25), 11155–11162. https://doi.org/10.1073/pnas.1004812107

Haslinger, K., Koffler, D., Schöner, W., & Laaha, G. (2014). Exploring the link between meteorological drought and streamflow: Effects of climate-catchment interaction. *Water Resources Research*, *50*(3), 2468–2487. https://doi.org/10.1002/2013WR015051

Heynen, M., Pellicciotti, F., & Carenzo, M. (2013). Parameter sensitivity of a distributed enhanced temperature-index melt model. *Annals of Glaciology*, *54*(63), 311–321. https://doi.org/10.3189/2013AOG63A537

Hindshaw, R. S., Tipper, E. T., Reynolds, B. C., Lemarchand, E., Wiederhold, J. G., Magnusson, J., Bernasconi, S. M., Kretzschmar, R., & Bourdon, B. (2011). Hydrological control of stream water chemistry in a glacial catchment (Damma Glacier, Switzerland). *Chemical Geology*, *285*(1–4), 215–230. https://doi.org/10.1016/J.CHEMGEO.2011.04.012

Hock, R. (1999). A distributed temperature-index ice- and snowmelt model including potential direct solar radiation. *Journal of Glaciology, 45(149),* 101–111. https://doi.org/10.3189/s0022143000003087

Hock, R. (2003). Temperature index melt modeling in mountain areas. *Journal of Hydrology*, *282*(1–4), 104–115. https://doi.org/10.1016/S0022-1694(03)00257-9

Hock, R., Bliss, A., Marzeion, B. E. N., Giesen, R. H., Hirabayashi, Y., Huss, M., Radic, V., & Slangen, A. B. A. (2019). GlacierMIP – A model intercomparison of global-scale glacier mass-balance models and projections. *Journal of Glaciology*, *65*(251), 453–467. https://doi.org/10.1017/JOG.2019.22

Huss, M., & Farinotti, D. (2012). Distributed ice thickness and volume of all glaciers around the globe. *Journal of Geophysical Research: Earth Surface*, *117*(F4), 4010. https://doi.org/10.1029/2012JF002523

Huss, M., & Hock, R. (2015). A new model for global glacier change and sea-level rise. *Frontiers in Earth Science, 3*, 54. https://doi.org/10.3389/feart.2015.00054

Huss, M., Jouvet, G., Farinotti, D., & Bauder, A. (2010). Future high-mountain hydrology: a new parameterization of glacier retreat. Hydrol. Earth Syst. Sci, 14, 815–829. https://doi.org/10.5194/hess-14-815-2010

Huss, M., Zemp, M., Joerg, P. C., & Salzmann, N. (2014). High uncertainty in 21st century runoff projections from glacierized basins. *Journal of Hydrology*, *510*, 35–48. https://doi.org/10.1016/J.JHYDROL.2013.12.017

Immerzeel, W. W., van Beek, L. P. H., Konz, M., Shrestha, A. B., & Bierkens, M. F. P. (2012). Hydrological response to climate change in a glacierized catchment in the Himalayas. *Climatic Change*, *110*(3–4), 721–736. https://doi.org/10.1007/s10584-011-0143-4

Immerzeel, W.W., Lutz, A.F., Andrade, M. et al. (2019) Importance and vulnerability of the world's water towers. *Nature 577*, 364–369 https://doi.org/10.1038/s41586-019-1822-y

Intergovernmental Panel on Climate (2007) Climate Change 2007: Synthesis Report. Contribution of Working Groups I, II and III to the Fourth Assessment Report of the Intergovernmental Panel on Climate Change [Core Writing Team, Pachauri, R.K and Reisinger, A. (eds.)]. *IPCC, Geneva, Switzerland, 104 pp.*

Intergovernmental Panel on Climate Change (2019) IPCC, 2019: IPCC Special Report on the Ocean and Cryosphere in a Changing Climate [H.-O. Pörtner, D.C. Roberts, V. Masson-

Delmotte, P. Zhai, M. Tignor, E. Poloczanska, K. Mintenbeck, A. Alegría, M. Nicolai, A. Okem, J. Petzold, B. Rama, N.M. Weyer (eds.)]. *Cambridge University Press, Cambridge, UK and New York, NY, USA, 755 pp.* https://doi.org/10.1017/9781009157964.

Intsiful, A., & Ambinakudige, S. (2020). Glacier Cover Change Assessment of the Columbia Icefield in the Canadian Rocky Mountains, Canada (1985–2018). *Geosciences*, *11*(1), 19. https://doi.org/10.3390/geosciences11010019

Jarvis, A., Reuter, H. I., Nelson, A., & Guevara, E. (2008). Hole-filled shuttle radar topography mission (SRTM) for the globe Version 4. *Consultative Group on International Agricultural Research-Consortium for Spatial Information (CGIAR-CSI), Washington, DC Available from https://srtm.csi.cgiar.org (accessed Oct 2022)*.

Jiang, R., Gan, T. Y., Xie, J., Wang, N., & Kuo, C. C. (2017). Historical and potential changes of precipitation and temperature of Alberta subjected to climate change impact: 1900–2100. Theoretical and Applied Climatology, 127(3–4), 725–739. https://doi.org/10.1007/s00704-015-1664-y

Jóhannesson, T. (1997). The response of two Icelandic glaciers to climatic warming computed with a degree-day glacier mass-balance model coupled to a dynamic glacier model. *Journal of Glaciology, 43(144)*, 321–327. https://doi.org/10.3189/s0022143000003270

Jóhannesson, T., Sigurdsson, O., Laumann, T., & Kennett, M. (1995). Degree-day glacier mass-balance modeling with applications to glaciers in Iceland, Norway and Greenland. *Journal of Glaciology, 41(138)*, 345–358. https://doi.org/10.3189/s0022143000016221

Jost, G., Moore, R. D., Menounos, B., & Wheate, R. (2012). Hydrology and Earth System Sciences Quantifying the contribution of glacier runoff to streamflow in the upper Columbia River Basin, Canada. Hydrol. Earth Syst. Sci, 16, 849–860. https://doi.org/10.5194/hess-16-849-2012

Khadka, M., Kayastha, R. B., & Kayastha, R. (2020). Future projection of cryospheric and hydrologic regimes in Koshi River basin, Central Himalaya, using coupled glacier dynamics and glacio-hydrological models. *Journal of Glaciology*, *66*(259), 831–845. https://doi.org/10.1017/jog.2020.51

Khalili, P., Masud, B., Qian, B., Mezbahuddin, S., Dyck, M., & Faramarzi, M. (2021). Non-stationary response of rain-fed spring wheat yield to future climate change in northern latitudes. *Science of the Total Environment*, *772*. https://doi.org/10.1016/J.SCITOTENV.2021.145474

Klein Goldewijk, K., Beusen, A., Van Drecht, G., & De Vos, M. (2011). The HYDE 3.1 spatially explicit database of human-induced global land-use change over the past 12,000 years. *Global Ecology and Biogeography*, *20*(1), 73–86. https://doi.org/10.1111/j.1466-8238.2010.00587.x

Kotila A., Cui, Q., Silwal, G., Bush, A.B.G., Faramarzi, M. (2022) Uncertainty assessment of empirically-derived parameters and parameter transferability in mountain glacier modeling at the regional scale. *Journal of Hydrology*, In review.

Kraaijenbrink, P. D. A., Bierkens, M. F. P., Lutz, A. F., & Immerzeel, W. W. (2017). Impact of a global temperature rise of 1.5 degrees Celsius on Asia's glaciers. *Nature, 549(7671),* 257–260. https://doi.org/10.1038/nature23878

Krause, P., Boyle, D. P., & Bäse, F. (2005). Comparison of different efficiency criteria for hydrological model assessment. *Advances in Geosciences*, *5*, 89–97. https://doi.org/10.5194/adgeo-5-89-2005

Li, Z., Yang, Y., Kan, G., & Hong, Y. (2018). Study on the applicability of the Hargreaves potential evapotranspiration estimation method in CREST distributed hydrological model (version 3.0) applications. *Water (Switzerland)*, *10*(12), 1–15. https://doi.org/10.3390/w10121882

Litt, M., Shea, J., Wagnon, P., Steiner, J., Koch, I., Stigter, E., & Immerzeel, W. (2019). Glacier ablation and temperature indexed melt models in the Nepalese Himalaya. Scientific Reports 2019 9:1, 9(1), 1–13. https://doi.org/10.1038/s41598-019-41657-5

Liu, J., Long, A., Deng, X., Yin, Z., Deng, M., An, Q., Gu, X., Li, S., & Liu, G. (2022). The Impact of Climate Change on Hydrological Processes of the Glacierized Watershed and Projections. *Remote Sensing 2022, Vol. 14, Page 1314*, *14*(6), 1314. https://doi.org/10.3390/RS14061314

Lute, A. C., & Abatzoglou, J. T. (2021). Best practices for estimating near-surface air temperature lapse rates. *International Journal of Climatology*, *41*(S1), E110–E125. https://doi.org/10.1002/JOC.6668

Marshall, S. J., & Miller, K. (2020). *Seasonal and Interannual Variability of Melt-Season Albedo at Haig Glacier, Canadian Rocky Mountains*. https://doi.org/10.5194/tc-2020-87

Marshall, S., & White, E. (2010). *Alberta Glacier Inventory and Ice Volume Estimation*. Report for the Alberta Water Research Institute, 55 pp. https://albertawater.com/dmdocuments/01_2010_12_Alberta_Glacier_Inventory_and_Ice_Volume_Estimation_Marshall_et_al%20(15).pdf

Marshall, S. J., White, E. C., Demuth, M. N., Bolch, T., Wheate, R., Menounos, B., Beedle, M. J., & Shea, J. M. (2011). Glacier Water Resources on the Eastern Slopes of the Canadian Rocky Mountains. *Canadian Water Resources Journal, 36(2),* 109–134. https://doi.org/10.4296/cwrj3602823

Martinec, J., Rango, A., & Roberts, R. (2008). Snowmelt runoff model (SRM) user's manual. *Agricultural Experiment Station Special Report 100*, 180. https://doi.org/10.3882/j.issn.1674-2370.2010.03.003

Marzeion, B., Hock, R., Anderson, B., Bliss, A., Champollion, N., Fujita, K., Huss, M., Immerzeel, W. W., Kraaijenbrink, P., Malles, J. H., Maussion, F., Radić, V., Rounce, D. R., Sakai, A., Shannon, S., van de Wal, R., & Zekollari, H. (2020). Partitioning the Uncertainty of Ensemble Projections of Global Glacier Mass Change. *Earth's Future*, *8*(7), e2019EF001470. https://doi.org/10.1029/2019EF001470

Masud, B., Cui, Q., Ammar, M. E., Bonsal, B. R., Islam, Z., & Faramarzi, M. (2021). Means and Extremes: Evaluation of a CMIP6 Multi-Model Ensemble in Reproducing Historical Climate Characteristics across Alberta, Canada. *Water 2021, Vol. 13, Page 737*, *13*(5), 737. https://doi.org/10.3390/W13050737

McKay, M. D., Beckman, R. J., & . Conover, W. J (1979) Comparison of Three Methods for Selecting Values of Input Variables in the Analysis of Output from a Computer Code, *Technometrics*, 21:2, 239-245https://doi.org/10.1080/00401706.1979.10489755

Milner, A. M., Brown, L. E., & Hannah, D. M. (2009). Hydroecological response of river systems to shrinking glaciers. *Process*, *23*, 62–77. https://doi.org/10.1002/hyp.7197

Milner, A. M., Khamis, K., Battin, T. J., Brittain, J. E., Barrand, N. E., Füreder, L., Cauvy-Fraunié, S., Gíslason, G. M., Jacobsen, D., Hannah, D. M., Hodson, A. J., Hood, E., Lencioni, V., Ólafsson, J. S., Robinson, C. T., Tranter, M., & Brown, L. E. (2017). Glacier shrinkage driving global changes in downstream systems. *Proceedings of the National Academy of Sciences of the United States of America*, *114*(37), 9770–9778. https://doi.org/10.1073/PNAS.1619807114/SUPPL_FILE/PNAS.201619807SI.PDF

Moore, R. D., Fleming, S. W., Menounos, B., Wheate, R., Fountain, A., Stahl, K., Holm, K., & Jakob, M. (2009). Glacier change in western North America: influences on hydrology, geomorphic hazards and water quality. Hydrological Processes, 23(1), 42–61. https://doi.org/10.1002/HYP.7162

Mwale, D., Gan, T. Y., Devito, K., Mendoza, C., Silins, U., & Petrone, R. (2009). Precipitation variability and its relationship to hydrologic variability in Alberta. Hydrological Processes, 23(21), 3040–3056. https://doi.org/10.1002/HYP.7415

Ohmura, A. (2001). Physical basis for the temperature-based melt-index method. *Journal of Applied Meteorology, 40(4)*, 753–761. https://doi.org/10.1175/1520-0450(2001)040<0753:PBFTTB>2.0.CO;2

Omani, N., Srinivasan, R., Smith, P.K. & Karthikeyan, R. (2017) Glacier mass-balance simulation using SWAT distributed snow algorithm, Hydrological Sciences Journal, 62:4, 546-560, https://doi.org/10.1080/02626667.2016.1162907

O'Neill, B. C., Kriegler, E., Ebi, K. L., Kemp-Benedict, E., Riahi, K., Rothman, D. S., van Ruijven, B. J., van Vuuren, D. P., Birkmann, J., Kok, K., Levy, M., & Solecki, W. (2017). The roads ahead: Narratives for shared socioeconomic pathways describing world futures in the 21st

century. *Global Environmental Change*, *42*, 169–180. https://doi.org/10.1016/J.GLOENVCHA.2015.01.004

Paul, F., & Mölg, N. (2014). Hasty retreat of glaciers in northern Patagonia from 1985 to 2011. *Journal of Glaciology*, *60*(224), 1033–1043. https://doi.org/10.3189/2014JOG14J104

Payne, J.T., Wood, A.W., Hamlet, A.F. et al. (2004) Mitigating the Effects of Climate Change on the Water Resources of the Columbia River Basin. *Climatic Change 62,* 233–256. https://doi.org/10.1023/B:CLIM.0000013694.18154.d6

Pellicciotti, F., Brock, B., Strasser, U., Burlando, P., Funk, M., & Corripio, J. (2005). An enhanced temperature-index glacier melt model including the shortwave radiation balance: development and testing for Haut Glacier d'Arolla, Switzerland. *Journal of Glaciology, 51(175)*, 573–587. https://doi.org/10.3189/172756505781829124

Perroud, M., Fasel, M., & Marshall, S. J. (2019). Development and testing of a subgrid glacier mass balance model for nesting in the Canadian Regional Climate Model. *Climate Dynamics*, *53*(3–4), 1453–1476. https://doi.org/10.1007/s00382-019-04676-6

Peters, D. L., Atkinson, D., Monk, W. A., Tenenbaum, D. E., & Baird, D. J. (2013). A multi- scale hydroclimatic analysis of runoff generation in the Athabasca River, western Canada. *Hydrological Processes, 27(13)*, 1915–1934. https://doi.org/10.1002/hyp.9699

Pfeffer, W. T., Arendt, A. A., Bliss, A., Bolch, T., Graham, J., Gardner, A. S., Hagen, J.-O., Hock, R., Kaser, G., Kienholz, C., Miles, E. S., Moholdt, G., Mo¨lg, N., Mo¨lg, M., Paul, F., Radic´, V., Radic´, R., Rastner, P., Raup, B. H., … Consortium, R. (2017). *The Randolph Glacier Inventory: a globally complete inventory of glaciers*. https://doi.org/10.3189/2014JoG13J176

Quick, M. C., & Pipes, A. (1977). U.b.c. watershed model. *Hydrological Sciences Bulletin*, *22*(1), 153–161. https://doi.org/10.1080/02626667709491701

Radić, V., & Hock, R. (2010). Regional and global volumes of glaciers derived from statistical upscaling of glacier inventory data. *Journal of Geophysical Research: Earth Surface*, *115*(1). https://doi.org/10.1029/2009JF001373

Radić, V., Hock, R., & Oerlemans, J. (2007). Volume-area scaling vs flowline modeling in glacier volume projections. *Annals of Glaciology*, *46*, 234–240. https://doi.org/10.3189/172756407782871288

Radić, V., Bliss, A., Beedlow, A. C., Hock, R., Miles, E., & Cogley, J. G. (2014). Regional and global projections of twenty-first century glacier mass changes in response to climate scenarios from global climate models. *Climate Dynamics*, *42*(1–2), 37–58. https://doi.org/10.1007/S00382-013-1719-7/TABLES/5

Ragettli, S., & Pellicciotti, F. (2012). Calibration of a physically based, spatially distributed hydrological model in a glacierized basin: On the use of knowledge from

glaciometeorological processes to constrain model parameters. *Water Resources Research*, *48*(3). https://doi.org/10.1029/2011WR010559

Rokaya, P., Peters, D. L., Elshamy, M., Budhathoki, S., & Lindenschmidt, K. (2020). Impacts of future climate on the hydrology of a northern headwaters basin and its implications for a downstream deltaic ecosystem. *Hydrological Processes*, *34*(7), 1630–1646. https://doi.org/10.1002/hyp.13687

Rounce, D. R., Hock, R., & Shean, D. E. (2020). Glacier Mass Change in High Mountain Asia Through 2100 Using the Open-Source Python Glacier Evolution Model (PyGEM). Frontiers in Earth Science, 7, 331. https://doi.org/10.3389/FEART.2019.00331/BIBTEX

Sao, D., Kato, T., Tu, L. H., Thouk, P., Fitriyah, A., & Oeurng, C. (2020). Evaluation of different objective functions used in the sufi-2 calibration process of swat-cup on water balance analysis: A case study of the pursat river basin, cambodia. *Water (Switzerland)*, *12*(10), 1–22. https://doi.org/10.3390/w12102901

Schaefli, B., & Huss, M. (2011). Integrating point glacier mass-balance observations into hydrologic model identification. *Hydrology and Earth System Sciences*, *15*(4), 1227–1241. https://doi.org/10.5194/HESS-15-1227-2011

Shea, J. M., Immerzeel, W. W., Wagnon, P., Vincent, C., & Bajracharya, S. (2015). Modeling glacier change in the Everest region, Nepal Himalaya. *Cryosphere, 9(3),* 1105–1128. https://doi.org/10.5194/tc-9-1105-2015

Shea, Joseph M., Moore, R. D., & Stahl, K. (2009). Derivation of melt factors from glacier mass-balance records in western Canada. *Journal of Glaciology*, *55*(189), 123–130. https://doi.org/10.3189/002214309788608886

Silwal G., Ammar M., Thapa A., Bonsal B., Faramarzi M. (2023). Response of glacier melt modelling parameters to time, space, and model complexity: examples from eastern slopes of Canadian Rocky Mountains. *Science of the Total Environment*, In review.

Singh, V., Jain, S. K., & Goyal, M. K. (2021). An assessment of snow-glacier melt runoff under climate change scenarios in the Himalayan basin. Stochastic Environmental Research and Risk Assessment, 1–26. https://doi.org/10.1007/s00477-021-01987-1

Stahl, K., Moore, R. D., Shea, J. M., Hutchinson, D., & Cannon, A. J. (2008). Coupled modeling of glacier and streamflow response to future climate scenarios. *Water Resources Research, 44(2).* https://doi.org/10.1029/2007WR005956

Strong, W.L., & Leggat, K.R. (1992.) Ecoregions of Alberta (ISBN 0 -86499-840-6). Alberta Forestry, Lands and Wildlife. https://open.alberta.ca/dataset/9dae82c1-7fda-47d3-b8eb-269d6ffc2451/resource/3453233f-7295-4104-9601-8d1978d1fda5/download/enr-t-4-ecoregions-of-alberta.pdf

Tennant, C., Menounos, B., Wheate, R., & Clague, J. J. (2012). Area change of glaciers in the Canadian rocky mountains, 1919 to 2006. Cryosphere, 6(6), 1541–1552. https://doi.org/10.5194/tc-6-1541-2012

Todd Walter, M., Brooks, E. S., McCool, D. K., King, L. G., Molnau, M., & Boll, J. (2005). Process-based snowmelt modeling: does it require more input data than temperature-index modeling? *Journal of Hydrology*, *300*(1–4), 65–75. https://doi.org/10.1016/J.JHYDROL.2004.05.002

Tolotti, M., Cerasino, L., Donati, C., Pindo, M., Rogora, M., Seppi, R., & Albanese, D. (2020). Alpine headwaters emerging from glaciers and rock glaciers host different bacterial communities: Ecological implications for the future. *Science of The Total Environment*, *717*, 137101. https://doi.org/10.1016/J.SCITOTENV.2020.137101

Tsai, V. C., & Ruan, X. (2018). A simple physics-based improvement to the positive degree day model. Journal of Glaciology, 64(246), 661–668. https://doi.org/10.1017/jog.2018.55

Viviroli, D., Dürr, H. H., Messerli, B., Meybeck, M. & Weingartner, R. (2007). Mountains of the world, water towers for humanity: typology, mapping, and global significance. *Water Resources Research 43*, 1–13

Voldoire, A., Saint-Martin, D., Sénési, S., Decharme, B., Alias, A., Chevallier, M., Colin, J., Guérémy, J. F., Michou, M., Moine, M. P., Nabat, P., Roehrig, R., Salas y Mélia, D., Séférian, R., Valcke, S., Beau, I., Belamari, S., Berthet, S., Cassou, C., … Waldman, R. (2019). Evaluation of CMIP6 DECK Experiments With CNRM-CM6-1. *Journal of Advances in Modeling Earth Systems*, *11*(7), 2177–2213. https://doi.org/10.1029/2019MS001683

Walter, M. T., Brooks, E. S., Mccool, D. K., King, L. G., Molnau, M., & Boll, J. (n.d.). Process-based snowmelt modeling: does it require more input data than temperature-index modeling? https://doi.org/10.1016/j.jhydrol.2004.05.002

Wheater, H. S., Pomeroy, J. W., Pietroniro, A., Davison, B., Elshamy, M., Yassin, F., Rokaya, P., Fayad, A., Tesemma, Z., Princz, D., Loukili, Y., DeBeer, C. M., Ireson, A. M., Razavi, S., Lindenschmidt, K. E., Elshorbagy, A., MacDonald, M., Abdelhamed, M., Haghnegahdar, A., & Bahrami, A. (2022). Advances in modelling large river basins in cold regions with Modélisation Environmentale Communautaire—Surface and Hydrology (MESH), the Canadian hydrological land surface scheme. *Hydrological Processes*, *36*(4), e14557. https://doi.org/10.1002/HYP.14557

Wortmann, M., Bolch, T., Su, B., & Krysanova, V. (2019). An efficient representation of glacier dynamics in a semi-distributed hydrological model to bridge glacier and river catchment scales. *Journal of Hydrology*, *573*, 136–152. https://doi.org/10.1016/J.JHYDROL.2019.03.006

Yukimoto, S., Kawai, H., Koshiro, T., Oshima, N., Yoshida, K., Urakawa, S., Tsujino, H., Deushi, M., Tanaka, T., Hosaka, M., Yabu, S., Yoshimura, H., Shindo, E., Mizuta, R., Obata, A.,

Adachi, Y., & Ishii, M. (2019). The Meteorological Research Institute Earth System Model Version 2.0, MRI-ESM2.0: Description and Basic Evaluation of the Physical Component. *Journal of the Meteorological Society of Japan. Ser. II*, *97*(5), 931–965. https://doi.org/10.2151/JMSJ.2019-051

APPENDICES

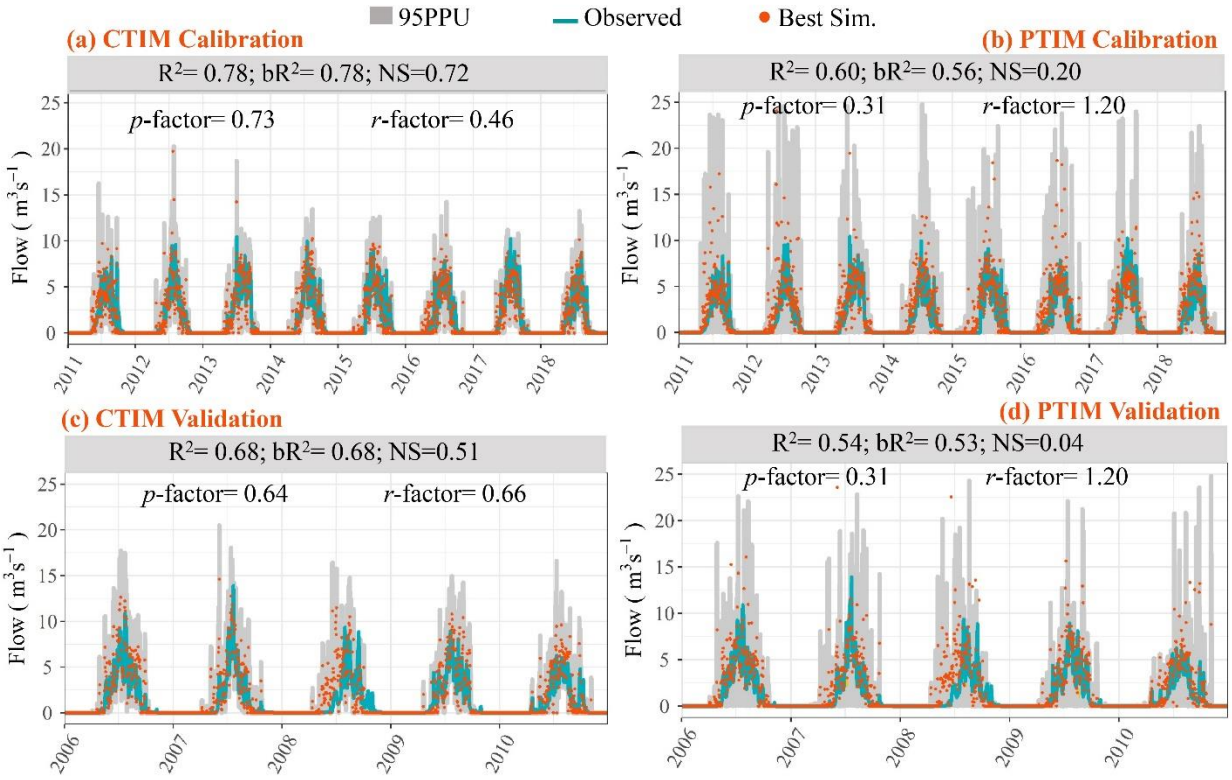

Figure A1. Comparison of the simulated daily melt runoff with observed data for the Athabasca Glacier based on (a, c) CTIM-based CGMEM, (b,d) PTIM-based CGMEM for the 2011-2018 calibration and 2006-2010 validation periods. Simulated daily runoff based on the best parameter sets are indicated by orange dots, while observed flow data is indicated by the blue line. The 95 percent prediction uncertainty (95PPU) for 1000 simulations based on the optimal parameter ranges is indicated by the grey band.

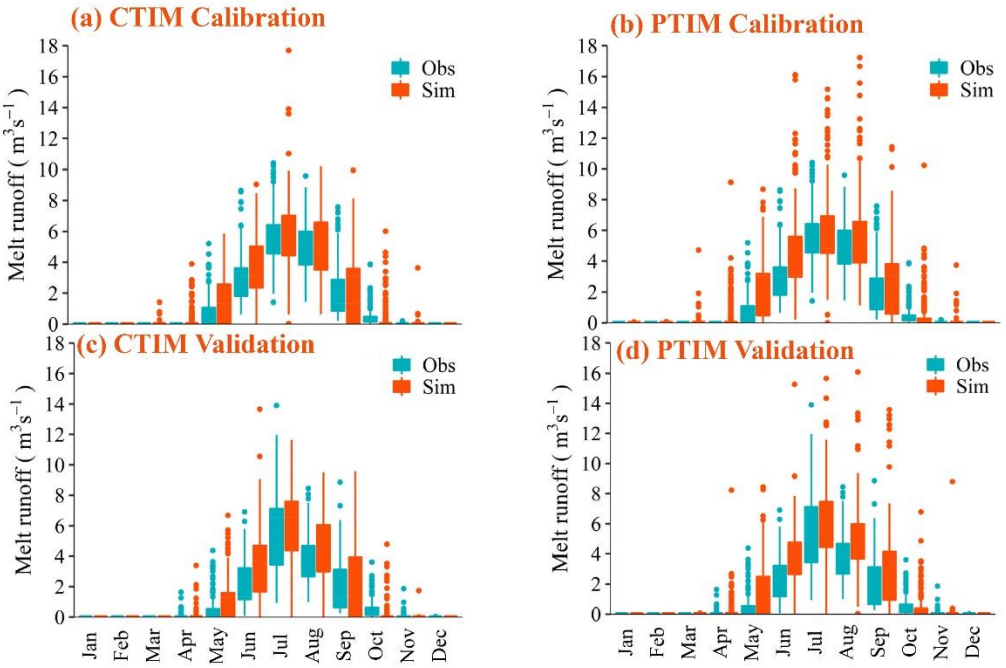

Figure A2. Long-term average data for different months based on (a) CTIM-based CGMEM, (b) PTIM-based CGMEM for the 2011-2018 calibration period and (c) CTIM-based CGMEM, (d) PTIM-based CGMBDEM for the 2006-2018 validation period.

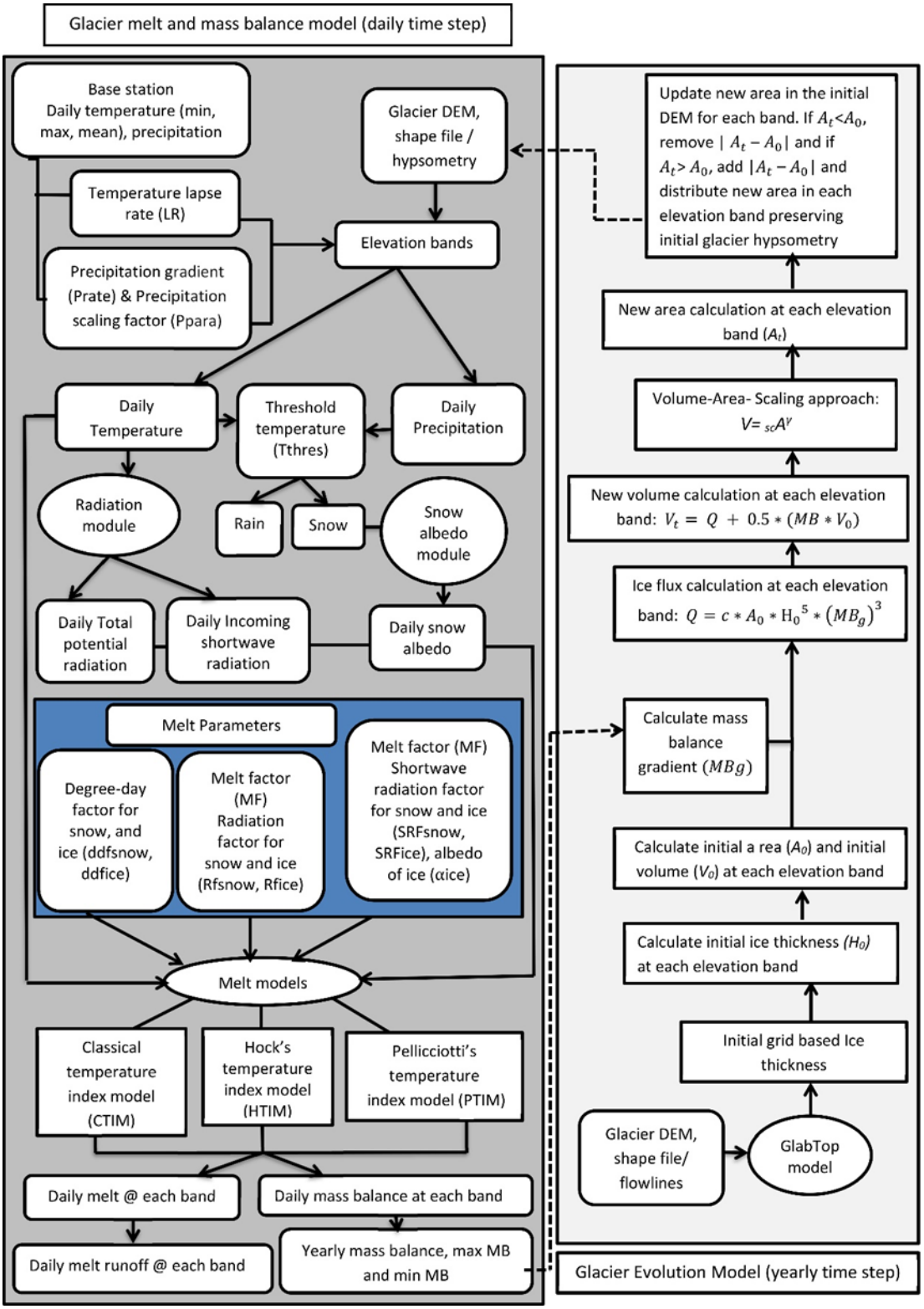

Figure A3. Flowchart showing the workflow involved in coupled glacier melt, mass balance, and evolution model adapted in this study. Courtesy of Silwal et al. (in review). It is to be noted that the volume-area scaling approach used in this thesis work is spline-based (as opposed to that

presented in this figure. Also in this thesis work, instead of using the GlabTop model to initialize the ice thickness of each glacier, ice thickness approximations from Farinotti et al. (2019) were used, as was noted in section 2.3.4.1.

Table A1. Objective functions used in calibration and validation (after Abbaspour et al., 2007; Omani et al., 2017; and Sao et al., 2020).

Index	**bR^2**	**R^2**	**NS**	***p*-factor**	***r*-factor**
Range	0 to 1	0 to 1	$-\infty$ to 1	0 to 1	$-\infty$ to 1
Optimal Value	1	1	1	1	0
Satisfactory Value	>0.5	>0.5	>0.5	0.6-0.8	~1
Calibrated Value (CTIM)	0.78	0.78	0.72	0.73	0.46
Validated Value (CTIM)	0.68	0.68	0.51	0.64	0.66
Calibrated Value (PTIM)	0.60	0.56	0.2	0.31	1.2
Validated Value (PTIM)	0.54	0.53	0.04	0.31	1.2

Table A2. Data accessed or obtained for the purpose of this study.

Data type, description	**Source**	**Units**
Glacier Outlines, Randolph Glacier Inventory-RGI v6.0, 2017	Global Land Ice Measurements from Space (GLIMS) Randolph Glacier Inventory http://www.glims.org/RGI/randolph.html	50m×50m
Digital elevation model of glacier hypsometry, 2017	Government of Canada https://maps.canada.ca/czs/index-en.html	10m×10m
Digital elevation model of glacier ice thickness, 2018	Farinotti et al., 2019. https://doi.org/10.3929/ethz-b-000315707	10m×10m
Daily simulated max, min, mean temperature, precipitation, 1980-	World Climate Research Programme Coupled Model Intercomparison Project Phase 6	daily ◦C, mm

2100 (CMIP6)	https://esgf-node.llnl.gov/search/cmip6/ Downscaled by Watershed Science and Modeling Laboratory, University of Alberta, Canada https://cms.eas.ualberta.ca/faramarzilab/contact/	